

GLOBAL JOURNAL

OF RESEARCHES IN ENGINEERING: A

Mechanical & Mechanics Engineering

A Study of Automated Optical

Self-Designed 3-D Printed Mask

Highlights

Abrasive Waterjet from Macro

Machines and Mechanical Gears

Discovering Thoughts, Inventing Future

VOLUME 20

ISSUE 1

VERSION 1.0



GLOBAL JOURNAL OF RESEARCHES IN ENGINEERING: A
MECHANICAL AND MECHANICS ENGINEERING



GLOBAL JOURNAL OF RESEARCHES IN ENGINEERING: A
MECHANICAL AND MECHANICS ENGINEERING

VOLUME 20 ISSUE 1 (VER. 1.0)

OPEN ASSOCIATION OF RESEARCH SOCIETY

© Global Journal of
Researches in Engineering.
2020.

All rights reserved.

This is a special issue published in version 1.0
of "Global Journal of Researches in
Engineering." By Global Journals Inc.

All articles are open access articles distributed
under "Global Journal of Researches in
Engineering"

Reading License, which permits restricted use.
Entire contents are copyright by of "Global
Journal of Researches in Engineering" unless
otherwise noted on specific articles.

No part of this publication may be reproduced
or transmitted in any form or by any means,
electronic or mechanical, including
photocopy, recording, or any information
storage and retrieval system, without written
permission.

The opinions and statements made in this
book are those of the authors concerned.
Ultrapublishing has not verified and neither
confirms nor denies any of the foregoing and
no warranty or fitness is implied.

Engage with the contents herein at your own
risk.

The use of this journal, and the terms and
conditions for our providing information, is
governed by our Disclaimer, Terms and
Conditions and Privacy Policy given on our
website [http://globaljournals.us/terms-and-condition/
menu-id-1463/](http://globaljournals.us/terms-and-condition/menu-id-1463/).

By referring / using / reading / any type of
association / referencing this journal, this
signifies and you acknowledge that you have
read them and that you accept and will be
bound by the terms thereof.

All information, journals, this journal,
activities undertaken, materials, services and
our website, terms and conditions, privacy
policy, and this journal is subject to change
anytime without any prior notice.

Incorporation No.: 0423089
License No.: 42125/022010/1186
Registration No.: 430374
Import-Export Code: 1109007027
Employer Identification Number (EIN):
USA Tax ID: 98-0673427

Global Journals Inc.

(A Delaware USA Incorporation with "Good Standing"; Reg. Number: 0423089)

Sponsors: Open Association of Research Society

Open Scientific Standards

Publisher's Headquarters office

Global Journals® Headquarters
945th Concord Streets,
Framingham Massachusetts Pin: 01701,
United States of America

USA Toll Free: +001-888-839-7392

USA Toll Free Fax: +001-888-839-7392

Offset Typesetting

Global Journals Incorporated
2nd, Lansdowne, Lansdowne Rd., Croydon-Surrey,
Pin: CR9 2ER, United Kingdom

Packaging & Continental Dispatching

Global Journals Pvt Ltd
E-3130 Sudama Nagar, Near Gopur Square,
Indore, M.P., Pin:452009, India

Find a correspondence nodal officer near you

To find nodal officer of your country, please
email us at local@globaljournals.org

eContacts

Press Inquiries: press@globaljournals.org

Investor Inquiries: investors@globaljournals.org

Technical Support: technology@globaljournals.org

Media & Releases: media@globaljournals.org

Pricing (Excluding Air Parcel Charges):

Yearly Subscription (Personal & Institutional)
250 USD (B/W) & 350 USD (Color)

EDITORIAL BOARD

GLOBAL JOURNAL OF RESEARCH IN ENGINEERING

Dr. Ren-Jye Dzung

Professor Civil Engineering, National Chiao-Tung University, Taiwan Dean of General Affairs, Ph.D., Civil & Environmental Engineering, University of Michigan United States

Dr. Iman Hajirasouliha

Ph.D. in Structural Engineering, Associate Professor, Department of Civil and Structural Engineering, University of Sheffield, United Kingdom

Dr. Ye Tian

Ph.D. Electrical Engineering The Pennsylvania State University 121 Electrical, Engineering East University Park, PA 16802, United States

Dr. Eric M. Lui

Ph.D., Structural Engineering, Department of Civil & Environmental Engineering, Syracuse University United States

Dr. Zi Chen

Ph.D. Department of Mechanical & Aerospace Engineering, Princeton University, US Assistant Professor, Thayer School of Engineering, Dartmouth College, Hanover, United States

Dr. T.S. Jang

Ph.D. Naval Architecture and Ocean Engineering, Seoul National University, Korea Director, Arctic Engineering Research Center, The Korea Ship and Offshore Research Institute, Pusan National University, South Korea

Dr. Ephraim Suhir

Ph.D., Dept. of Mechanics and Mathematics, Moscow University Moscow, Russia Bell Laboratories Physical Sciences and Engineering Research Division United States

Dr. Pangil Choi

Ph.D. Department of Civil, Environmental, and Construction Engineering, Texas Tech University, United States

Dr. Xianbo Zhao

Ph.D. Department of Building, National University of Singapore, Singapore, Senior Lecturer, Central Queensland University, Australia

Dr. Zhou Yufeng

Ph.D. Mechanical Engineering & Materials Science, Duke University, US Assistant Professor College of Engineering, Nanyang Technological University, Singapore

Dr. Pallav Purohit

Ph.D. Energy Policy and Planning, Indian Institute of Technology (IIT), Delhi Research Scientist, International Institute for Applied Systems Analysis (IIASA), Austria

Dr. Balasubramani R

Ph.D., (IT) in Faculty of Engg. & Tech. Professor & Head, Dept. of ISE at NMAM Institute of Technology

Dr. Sofoklis S. Makridis

B.Sc(Hons), M.Eng, Ph.D. Professor Department of Mechanical Engineering University of Western Macedonia, Greece

Dr. Steffen Lehmann

Faculty of Creative and Cultural Industries Ph.D., AA Dip University of Portsmouth United Kingdom

Dr. Wenfang Xie

Ph.D., Department of Electrical Engineering, Hong Kong Polytechnic University, Department of Automatic Control, Beijing University of Aeronautics and Astronautics China

Dr. Hai-Wen Li

Ph.D., Materials Engineering, Kyushu University, Fukuoka, Guest Professor at Aarhus University, Japan

Dr. Saeed Chehreh Chelgani

Ph.D. in Mineral Processing University of Western Ontario, Adjunct professor, Mining engineering and Mineral processing, University of Michigan United States

Belen Riveiro

Ph.D., School of Industrial Engineering, University of Vigo Spain

Dr. Adel Al Jumaily

Ph.D. Electrical Engineering (AI), Faculty of Engineering and IT, University of Technology, Sydney

Dr. Maciej Gućma

Assistant Professor, Maritime University of Szczecin Szczecin, Ph.D.. Eng. Master Mariner, Poland

Dr. M. Meguellati

Department of Electronics, University of Batna, Batna 05000, Algeria

Dr. Haijian Shi

Ph.D. Civil Engineering Structural Engineering Oakland, CA, United States

Dr. Chao Wang

Ph.D. in Computational Mechanics Rosharon, TX, United States

Dr. Joaquim Carneiro

Ph.D. in Mechanical Engineering, Faculty of Engineering, University of Porto (FEUP), University of Minho, Department of Physics Portugal

Dr. Wei-Hsin Chen

Ph.D., National Cheng Kung University, Department of Aeronautics, and Astronautics, Taiwan

Dr. Bin Chen

B.Sc., M.Sc., Ph.D., Xian Jiaotong University, China. State Key Laboratory of Multiphase Flow in Power Engineering Xi'an Jiaotong University, China

Dr. Charles-Darwin Annan

Ph.D., Professor Civil and Water Engineering University Laval, Canada

Dr. Jalal Kafashan

Mechanical Engineering Division of Mechatronics KU Leuven, Belgium

Dr. Alex W. Dawotola

Hydraulic Engineering Section, Delft University of Technology, Stevinweg, Delft, Netherlands

Dr. Shun-Chung Lee

Department of Resources Engineering, National Cheng Kung University, Taiwan

Dr. Gordana Colovic

B.Sc Textile Technology, M.Sc. Technical Science Ph.D. in Industrial Management. The College of Textile? Design, Technology and Management, Belgrade, Serbia

Dr. Giacomo Risitano

Ph.D., Industrial Engineering at University of Perugia (Italy) "Automotive Design" at Engineering Department of Messina University (Messina) Italy

Dr. Maurizio Palesi

Ph.D. in Computer Engineering, University of Catania, Faculty of Engineering and Architecture Italy

Dr. Salvatore Brischetto

Ph.D. in Aerospace Engineering, Polytechnic University of Turin and in Mechanics, Paris West University Nanterre La Defense Department of Mechanical and Aerospace Engineering, Polytechnic University of Turin, Italy

Dr. Wesam S. Alaloul

B.Sc., M.Sc., Ph.D. in Civil and Environmental Engineering, University Technology Petronas, Malaysia

Dr. Ananda Kumar Palaniappan

B.Sc., MBA, MED, Ph.D. in Civil and Environmental Engineering, Ph.D. University of Malaya, Malaysia, University of Malaya, Malaysia

Dr. Hugo Silva

Associate Professor, University of Minho, Department of Civil Engineering, Ph.D., Civil Engineering, University of Minho Portugal

Dr. Fausto Gallucci

Associate Professor, Chemical Process Intensification (SPI), Faculty of Chemical Engineering and Chemistry Assistant Editor, International J. Hydrogen Energy, Netherlands

Dr. Philip T Moore

Ph.D., Graduate Master Supervisor School of Information Science and engineering Lanzhou University China

Dr. Cesar M. A. Vasques

Ph.D., Mechanical Engineering, Department of Mechanical Engineering, School of Engineering, Polytechnic of Porto Porto, Portugal

Dr. Jun Wang

Ph.D. in Architecture, University of Hong Kong, China Urban Studies City University of Hong Kong, China

Dr. Stefano Invernizzi

Ph.D. in Structural Engineering Technical University of Turin, Department of Structural, Geotechnical and Building Engineering, Italy

Dr. Togay Ozbakkaloglu

B.Sc. in Civil Engineering, Ph.D. in Structural Engineering, University of Ottawa, Canada Senior Lecturer University of Adelaide, Australia

Dr. Zhen Yuan

B.E., Ph.D. in Mechanical Engineering University of Sciences and Technology of China, China Professor, Faculty of Health Sciences, University of Macau, China

Dr. Jui-Sheng Chou

Ph.D. University of Texas at Austin, U.S.A. Department of Civil and Construction Engineering National Taiwan University of Science and Technology (Taiwan Tech)

Dr. Houfa Shen

Ph.D. Manufacturing Engineering, Mechanical Engineering, Structural Engineering, Department of Mechanical Engineering, Tsinghua University, China

Prof. (LU), (UoS) Dr. Miklas Scholz

Cand Ing, BEng (equiv), PgC, MSc, Ph.D., CWEM, CEnv, CSci, CEng, FHEA, FIEMA, FCIWEM, FICE, Fellow of IWA, VINNOVA Fellow, Marie Curie Senior, Fellow, Chair in Civil Engineering (UoS) Wetland Systems, Sustainable Drainage, and Water Quality

Dr. Yudong Zhang

B.S., M.S., Ph.D. Signal and Information Processing, Southeast University Professor School of Information Science and Technology at Nanjing Normal University, China

Dr. Minghua He

Department of Civil Engineering Tsinghua University Beijing, 100084, China

Dr. Philip G. Moscoso

Technology and Operations Management IESE Business School, University of Navarra Ph.D. in Industrial Engineering and Management, ETH Zurich M.Sc. in Chemical Engineering, ETH Zurich, Spain

Dr. Stefano Mariani

Associate Professor, Structural Mechanics, Department of Civil and Environmental Engineering, Ph.D., in Structural Engineering Polytechnic University of Milan Italy

Dr. Ciprian Lapusan

Ph. D in Mechanical Engineering Technical University of Cluj-Napoca Cluj-Napoca (Romania)

Dr. Francesco Tornabene

Ph.D. in Structural Mechanics, University of Bologna Professor Department of Civil, Chemical, Environmental and Materials Engineering University of Bologna, Italy

Dr. Kitipong Jaojaruek

B. Eng, M. Eng, D. Eng (Energy Technology, Asian Institute of Technology). Kasetsart University Kamphaeng Saen (KPS) Campus Energy Research Laboratory of Mechanical Engineering

Dr. Burcin Becerik-Gerber

University of Southern California Ph.D. in Civil Engineering Ddes, from Harvard University M.S. from University of California, Berkeley M.S. from Istanbul, Technical University

Hiroshi Sekimoto

Professor Emeritus Tokyo Institute of Technology Japan Ph.D., University of California Berkeley

Dr. Shaoping Xiao

BS, MS Ph.D. Mechanical Engineering, Northwestern University The University of Iowa, Department of Mechanical and Industrial Engineering Center for Computer-Aided Design

Dr. A. Stegou-Sagia

Ph.D., Mechanical Engineering, Environmental Engineering School of Mechanical Engineering, National Technical University of Athens, Greece

Diego Gonzalez-Aguilera

Ph.D. Dep. Cartographic and Land Engineering, University of Salamanca, Avilla, Spain

Dr. Maria Daniela

Ph.D in Aerospace Science and Technologies Second University of Naples, Research Fellow University of Naples Federico II, Italy

Dr. Omid Gohardani

Ph.D. Senior Aerospace/Mechanical/ Aeronautical,
Engineering professional M.Sc. Mechanical Engineering,
M.Sc. Aeronautical Engineering B.Sc. Vehicle
Engineering Orange County, California, US

Dr. Paolo Veronesi

Ph.D., Materials Engineering, Institute of Electronics,
Italy President of the master Degree in Materials
Engineering Dept. of Engineering, Italy

CONTENTS OF THE ISSUE

- i. Copyright Notice
 - ii. Editorial Board Members
 - iii. Chief Author and Dean
 - iv. Contents of the Issue
-
1. Review of Accomplishments in Abrasive-Waterjet from Macro to Micro Machining – Part 1. ***1-16***
 2. The Load Distribution with Modification and Misalignment and Thermal Elastohydrodynamic Lubrication Simulation of Helical Gears. ***17-34***
 3. Wheel Tooth Profiles of Hydraulic Machines and Mechanical Gears: Traditions and Innovations. ***35-44***
 4. Mathematical Modeling for Optimization of Periodicity in the Preventive Maintenance Plans. ***45-56***
 5. Self-Designed 3-D Printed Mask to Tackle COVID-19. ***57-65***
 6. A Study of Automated Optical Inspection of Rapid Influenza Diagnostic Tests. ***67-72***
-
- v. Fellows
 - vi. Auxiliary Memberships
 - vii. Preferred Author Guidelines
 - viii. Index



GLOBAL JOURNAL OF RESEARCHES IN ENGINEERING: A
MECHANICAL AND MECHANICS ENGINEERING
Volume 20 Issue 1 Version 1.0 Year 2020
Type: Double Blind Peer Reviewed International Research Journal
Publisher: Global Journals
Online ISSN: 2249-4596 & Print ISSN: 0975-5861

Review of Accomplishments in Abrasive-Waterjet from Macro to Micro Machining – Part 1

By H.T. Peter Liu

Abstract- Abrasive-waterjet (AWJ) technology possesses inherent characteristics unmatched by most machine tools. The initial commercialization of AWJ in the mid 1980s was to take advantage of its superior cutting power for raw cutting of thick and difficult-to-machine materials. Subsequently, considerable R&D was devoted to take full advantage of the above characteristics while refining machining processes toward precision machining and automation. This two-part paper presents the accomplishments that advance AWJ technology in terms of improving the cutting accuracy and efficiency, broadening applications for machining delicate materials from macro to micro scales, and enabling 3D capability for multimode machining. In Part 1 of the paper, six topical areas are presented to demonstrate some of the important achievements in advancing AWJ technology. The areas include: - control software, meso-micro and stack machining, macro to micro machining, cold cutting, hole drilling, and gear making. Additional topical areas will be presented in Part 2 of the paper to fully explore the technological and manufacturing merits of AWJ technology. Such merits had elevated AWJ technology as one of the most versatile machine tools competing on equal footing, and with advantage in some cases, among subtractive and additive manufacturing tools. The accomplishments presented in this paper had clearly demonstrated that AWJ technology was capable of multi-mode machining for most materials from macro to micro scales, the “7M” advantage. The versatility of AWJ technology has clearly demonstrated its “7M” advantage.

GJRE-A Classification: FOR Code: 290501p



REVIEW OF ACCOMPLISHMENTS IN ABRASIVE WATERJET FROM MACRO TO MICRO MACHINING PART 1

Strictly as per the compliance and regulations of:



© 2020. H.T. Peter Liu. This is a research/review paper, distributed under the terms of the Creative Commons Attribution-Noncommercial 3.0 Unported License <http://creativecommons.org/licenses/by-nc/3.0/>, permitting all non commercial use, distribution, and reproduction in any medium, provided the original work is properly cited.

Review of Accomplishments in Abrasive-Waterjet from Macro to Micro Machining – Part 1

H.T. Peter Liu

Abstract- Abrasive-waterjet (AWJ) technology possesses inherent characteristics unmatched by most machine tools. The initial commercialization of AWJ in the mid1980s was to take advantage of its superior cutting power for raw cutting of thick and difficult-to-machine materials. Subsequently, considerable R&D was devoted to take full advantage of the above characteristics while refining machining processes toward precision machining and automation. This two-part paper presents the accomplishments that advance AWJ technology in terms of improving the cutting accuracy and efficiency, broadening applications for machining delicate materials from macro to micro scales, and enabling 3D capability for multimode machining. In Part 1 of the paper, six topical areas are presented to demonstrate some of the important achievements in advancing AWJ technology. The areas include: - control software, meso-micro and stack machining, macro to micro machining, cold cutting, hole drilling, and gear making. Additional topical areas will be presented in Part 2 of the paper to fully explore the technological and manufacturing merits of AWJ technology. Such merits had elevated AWJ technology as one of the most versatile machine tools competing on equal footing, and with advantage in some cases, among subtractive and additive manufacturing tools. The accomplishments presented in this paper had clearly demonstrated that AWJ technology was capable of multi-mode machining for most materials from macro to micro scales, the “7M” advantage. The versatility of AWJ technology has clearly demonstrated its “7M” advantage.

I. INTRODUCTION

In 1973, after joining Flow Research, Inc., where the waterjet technology was developed and commercialized, the author had the privilege of participating in R&D activities to advance the technology.¹ He subsequently joined OMAX Corporation in 2005 and continued his pursue in advancing waterjet technology. He was involved in the commercialization of the technology while witnessing its maturing and growth in the adaptation by the manufacturing community. In the early stage, when the abrasive waterjet (AWJ) was commercialized in the mid1980s, a reasonable controller to maneuver the operation had yet to be developed. It merely served as a raw cutting tool for difficult-to-cut

Author: Senior Scientist, OMAX Corporation. e-mail: www.omax.com

¹ The author had the honor to be supervised by the late Dr. John Olsen who enabled the commercialization of waterjet technology by perfecting the ultra-high pressure intensifier pump.

and thick materials to take advantage of its superior cutting power. As the technology advanced, additional technological and manufacturing merits were discovered and progressively verified. Among the merits in addition to the superior cutting power are green machining process, material independence, cold cutting, adaptability to automation, amenability to micromachining, low loading on work pieces, and 3D capability (Liu and Schubert, 2012; Liu, 2017a). Most of the development efforts in the last three decades, in addition to hardware improvement for cutting performance, were to develop controller and smart software for operating the machine toward precision machining. In modern times, AWJ possesses technological and manufacturing merits that are superior to most other tools. It has been elevated as a modern machine tool competing on equal footing among lasers, electrical discharged machining (EDM), and precision milling tools.

Since AWJ carries out machining by means of a high-speed and thin beam of water-only-jet (WJ) and AWJ, it is amenable to micromachining. Recent success in commercialization of micro abrasive-waterjet (μ AWJ) technology has broadened the range from macro to micro machining. The diameter of the WJ was defined by the diameter of the orifice, the single phase WJ with diameters smaller than 100 μm has been used to cut relatively soft materials such as fabrics, rubber, foam, thin plastics, and various food products (Yadav and Singh, 2016). With the entrainment of abrasives and air together with the incorporation of the mixing tube, the diameter of the three-phase AWJ is about three to four times that of the WJ. At present, the smallest kerf width achievable with commercially available AWJ systems is around 300 to 400 μm . Preliminary tests using a research μ AWJ nozzle, with a $\phi 76 \mu\text{m}$ orifice and a $\phi 175 \mu\text{m}$ mixing tube, showed that a kerf width of 200 μm was achievable (Liu and Gershenfeld, 2020). Very thin materials that are too delicate to machine otherwise can be machined by stacking multiple layers of materials with the powerful AWJ. The increase in the thickness of the stack not only stiffens the individual layers for ease of fixturing but also allows utilization of the Tilt-A-Jet for machining nearly taper free edges of individual thin materials within the stack.²

² For very thin materials, the Tilt-A-Jet is deactivated as the cutting speeds are too fast such that the Tilt-A-Jet is too slow

AWJ is capable of machining most materials from metal, nonmetal, to anything in between, whether they are conductive or nonconductive and reflective or non reflective. In particular, AWJ will meet the challenge of machining nanomaterials integrated with various material types possessing nonlinear material properties (Liu, 2017b). Such nanomaterials would present considerable challenge to conventional tools. As a cold cutting tool without the introduction of a heat-affected zone (HAZ), AWJ often is capable of cutting one order of magnitude faster than solid state lasers (pulsed at high frequency) and wire EDM (cut with multiple passes) (Liu, 2019a). For extremely high precision parts made of difficult-to-cut materials, end mills and spindles are often subject to severe tool wear resulting in high retooling costs. AWJ could preferably apply as a near-net shaping tool to remove the bulk of the materials. Near-net shaped parts can then be finished via light trimming with precision CNC tools. Such a hybrid process, particularly for delicate and difficult-to-machine materials, would speed up the turnaround time while minimizing the retooling costs.

The unconventional AWJ differs from most machine tools as its cutting tool is a flexible beam of abrasive slurry. One of the emphases to achieve superior precision is to develop smart control software to mitigate anomalies induced by the flexibility of the AWJ. Continued advancements in AWJ technology would unleash its potential to be one of the all-in-one and one-in-all process to machine a wide range of advanced materials that present considerable challenge to most machine tools. The benefits would include the preservation of structural and chemical properties of parent materials, extension of tool lives, and expediting turnaround time leading to significant overall cost saving.

Future advancement in AWJ technology is expected to develop an all-in-one and one-in-all tool for precision machining from macro to micro scales. Continued efforts are underway to improve the cutting accuracy and to further downsize μ AWJ nozzles. In this two-part paper, recent advancements in AWJ technology to take advantage of its technological and manufacturing merits are described. In particular, emphasis will be made to present several established and new trends in applying AWJ for precision machining.

II. R&D AND DEMONSTRATION FACILITIES

OMAX is equipped with two laboratories for R&D and demonstration. The R&D Lab is dedicated to engineering research and development from components and processes, cutting model, to nozzle

performance testing. The Demo Lab is mainly for demonstrating AWJ machining for prospective and existing clients. There are several Jet Machining® Center (JMC) from the four product lines installed in the two laboratories (<https://www.omax.com/products>). The OMAX 2652 and MicroMAX were used most often for general and meso-micro machining. A number of accessories are installed on these machines to enhance AWJ machining (<https://www.omax.com/accessories>). Key accessories include but are not limited to:

- Tilt-A-Jet (TAJ) for compensating edge.
- Rotary Axis (RA) for axisymmetric machining.
- A-Jet or articulated jet for beveling and countersinking.
- Precision Optical Locator (POL) for facilitating alignment and orientation of pre-machined components for precision machining.
- Vacuum Assist (VA) for low-pressure piercing and machining to mitigate nozzle clogging.

These accessories were used in machining the sample parts presented in the paper. A combination of multiple accessories were often used to machine certain features. For example, the combined operations of the A-Jet and Rotary Axis can be used to machine rather complicated 3D features such as the “fish mouth” saddle weld joints on pipes and features on curved surfaces.

There are R&D and manufacturing machine shops equipped with CNC machines for fabricating components used in R&D activities and assembling the four product lines of waterjet systems. Various instruments and devices are available in the laboratories and Quality Control Department for measuring parameters to quantify the part geometries such as edge taper, surface roughness, part accuracy, and others. Several sample parts presented herein were made by academic and industrial collaborators. Their tools will be described briefly where these parts are presented.

III. ADVANCES IN AWJ TECHNOLOGY

a) Controller software

Based on the fact that AWJ process is adaptable to digital machining, considerable efforts were placed to develop PC-based computer numeric control (CNC) software toward automation. The Intelli-MAX Software Suite was developed to take abrasive waterjet cutting to the industry’s highest levels of speed and performance. The Suite contains a collection of a number of PC-based software modules related to AWJ machining. Two of the most used modules are the Layout (CAD) and MAKE (CAM). LAYOUT is used to transform the design intent into a continuous tool path by adding Lead-In and Lead-Out (the entry and exit of the AWJ stream to cut paths) to different parts of the tool path. LAYOUT uses colors to represent five different

to respond for taper compensation, The lag in the response could lead unacceptable anomalies.

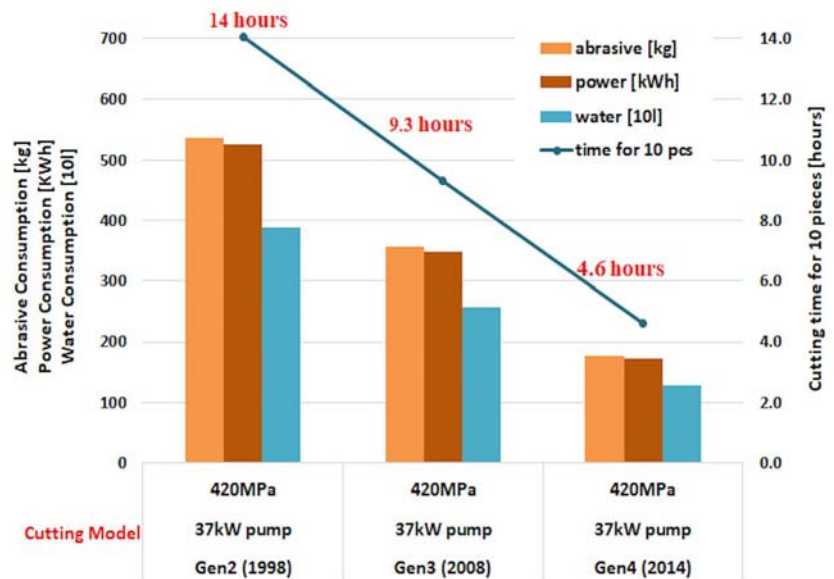
edge qualities from rough (Q1) to precision (Q5) cutting. The colors of a LAYOUT drawing indicate the edge quality that will be used to make it. The tool path is saved in an ORD (OMAX Routed Data) file and contains a series of commands for moving the AWJ machining head. The ORD file is then loaded to MAKE to assign cutting parameters based on the cutting model, the brain of the controller software.

Since AWJ is not a rigid tool, it must simply be guided along a particular path to make a part with the controller software. In particular, the controller must be designed to correct for several errors induced by the AWJ moving at high speeds, including jet lag, edge striation pattern, edge taper, kerf width, and kickback. For common engineering materials, the cutting model assigns a machinability index, M , that was defined based on the results of extensive cutting tests (Zeng, 2007, Zeng et al., 1992, Liu, 2019b). The value of M is proportional to the cutting speed for a given material. For example, The M indices equal 215, 108, and 81 for aluminum, stainless steel, and titanium, respectively. In other words, waterjet cuts aluminum 215/81 or 2.65 times faster than it cuts stainless steel for the same setup. Since erosion by the impact of high-speed abrasives is the primary mode of material removal, it

behaves differently from cutting with CNC hard tools. As such, waterjet cuts titanium 34% faster than it cuts steel.; It also cuts hardened steel nearly as fast as it cuts the annealed counterpart thus saving the need to shape the part in the annealed condition and mitigate the distortion of thermal treatment after shaping. The incorporation of the machinability index into the cutting model enabled waterjet as an automation machining process. In particular, the cutting model has been upgraded through the optimization of cutting processes and strategies to increase the cutting speed without degrading the cutting accuracy. There were three upgrades of the cutting model since it was incorporated into the IntelliMAX Software Suite, each upgrade had led to significant enhancement in the cutting efficiency (Liu et al., 2018a). Figure 1a illustrates three 12.7 mm thick stainless-steel gears cut with three different generation of cutting models. The gears were cut at a quality of Q5 for all three.³ The lengths of cut for the three gears are 0.28, 0.15, and 0.13 m. The ratio of the lengths of cut, therefore represented the performance of the three cutting models: G4 versus G2 215% and G4 versus G3 187%. Figure 1b shows the cutting times for 10 pieces of identical parts. The ratios of the cutting times are consistent with those of the cutting length.



a. Cutting stainless steel



b. Cutting speeds of three cutting models (Henning and Miles, 2016)

Figure 1: Performance of latest three cutting models, G2 through G4 (Liu et al., 2018a)

³ There are five edge qualities defined for AWJ machining, Q1, Q2, Q3, Q4, and Q5. Q1 and Q5 correspond to the edge qualities of rough and precision cuts, respectively.

b) *Meso-micro and stack machining*

The diameter of the AWJ is controlled by those of the orifice and mixing tube; it is amenable to micro-machining (Miller, 2003; 2005). Micro abrasive-waterjet (μ AWJ) technology was successfully developed under the support of an NSF SBIR grant (Liu and Schubert, 2012). The μ AWJ technology was commercialized in 2013, culminating in a new product - the award-winning MicroMAX® JetMachining® Center. It was equipped with a production 7/15 nozzle with a $\phi 0.007$ " ($\phi 0.18$ mm) orifice and $\phi 0.015$ " ($\phi 0.38$ mm) mixing tube is capable of machining features around 0.018 " (0.5 mm).⁴ A 5/10 nozzle capable of machining features around 0.3 mm has been under beta testing. The μ AWJ technology was enhanced through upgrading the MicroMAX by incorporating a Rotary Axis for machining axisymmetric parts and by further downsizing the μ AWJ nozzle toward micromachining. Subsequently, experimental nozzles as small as a 2/6 nozzle combination was investigated with good promise.

In parallel to downsizing of the μ AWJ nozzle, the size of the garnet abrasives must be reduced accordingly. As a rule of thumb, the average size of the abrasives should be smaller than 1/3 of the internal diameter (ID) of the mixing tube in order to mitigate clogging the mixing tube due to the bridging of two

large particles. For the 5/10 and 4/8 nozzles, 240 mesh garnet with an average particle size of $60 \mu\text{m}$ meets the above criterion as the ID of the 4/8 nozzle is $203 \mu\text{m}$. For the 3/6 nozzle with the ID of the mixing tube equal to $152 \mu\text{m}$, the 240-mesh garnet no longer meets the above criterion. The next smaller size 320 mesh garnet with an average particle size of $30 \mu\text{m}$ was used instead. Unfortunately, the powdery 320 garnet ceases to flow consistently under gravity feed, as the flow ability of abrasive is known to deteriorate with the reduction in particle size (Xu et al., 2018). One of the common problems is that the flow of fine abrasive is interrupted with the development of "worm hole" inside the hopper. A solution to overcome the poor flow ability of fine abrasives was through the development of patented novel processes and devices. This allowed the successful operation of the downsized μ AWJ nozzles. With the 5/10 nozzle, the kerf width is $\leq 300 \mu\text{m}$. However, it is capable of machining certain features with size near $100 \mu\text{m}$ to take advantage of the cold cutting and low exertion of side force on the work piece (Liu and Gershenfeld, 2020). Figure 2 shows a set of tweezers machined with several nozzles to demonstrate the progress in the development of μ AWJ technology toward micromachining (Liu, 2015).

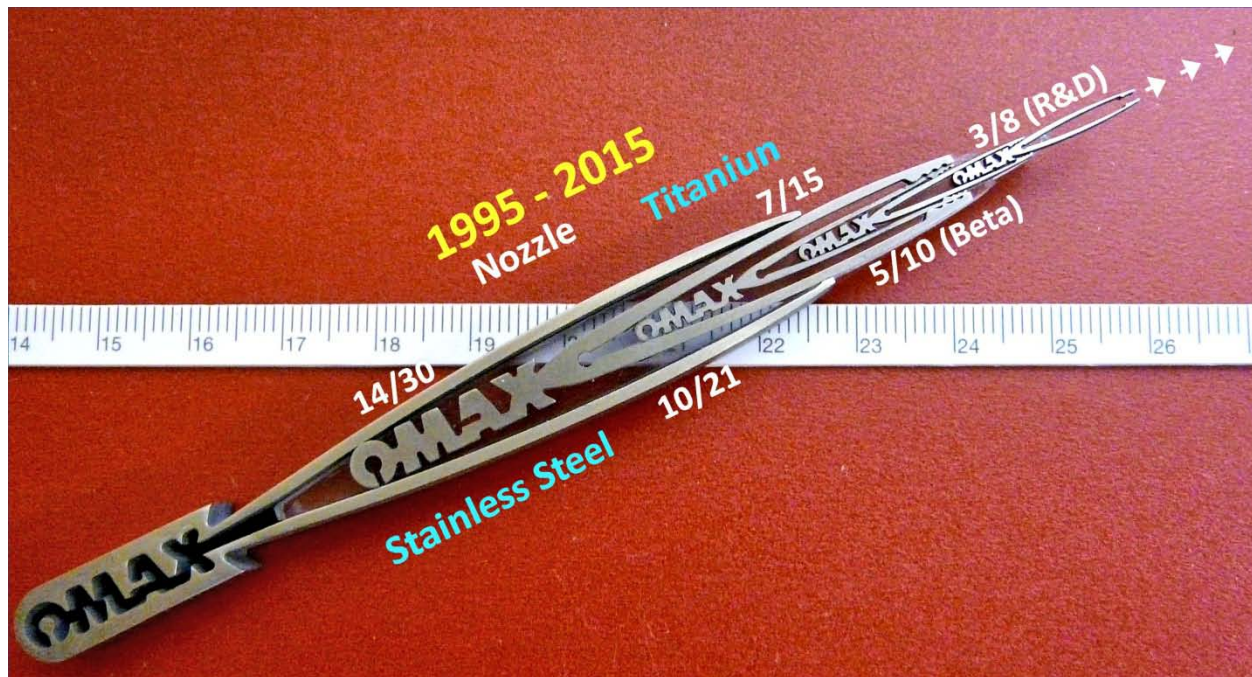


Figure 2: Progress in AWJ meso-micro machining (Liu, 2015)

⁴ The naming convention of nozzle is the orifice diameter versus the mixing tube diameter in thousandth of an inch.

In collaborating with JPL/NASA, cutting tests were conducted using the μ AWJ nozzles to machine several miniature flexures used in prototype microsplines for asteroid grippers developed under the Asteroid Redirect Mission at NASA (Tate, 2013). Comparison of the performance of the μ AWJ and wire EDM conducted at JPL, the cost ratio between waterjet and wire EDM was 1:14, leading to a cost reduction to 7% of that of the EDM process (Liu, 2019a). During AWJ machining, only very low loading was exerted onto the workpiece. This simplifies fixturing to secure the even relatively thin workpieces. The low side force exerted onto the workpiece together with cold cutting enables AWJ cutting very thin walls with large aspect ratios (length-to-width and length-to-thickness) even on delicate materials such as thin glass without deforming them thermally and mechanically (Liu et al., 2018a).

A MicroCutting Project was initiated at the MIT Center for Bits and Atoms (CBA – www.cba.mit.edu) (Liu and Gershenfeld, 2020). The performances of μ AWJ and several subtractive and additive tools were compared by machining one of the above flexures. Subtractive tools included waterjets, lasers, micro-milling systems, and additive tools such as laser powder bed fusion and 3D printers using metal and non-metal media. For this particular flexure, it should be pointed out that the geometry and/or materials of the flexure were not necessarily optimized for some of the machine tools.

The results of MicroCutting Project are partly summarized in Figure 3 in which aluminum flexures machined with both subtractive and additive tools are shown. The nominal size of the full-scale flexure was 60.7 mm (L) x 32.5 mm (W). The flexures were fabricated in different material thicknesses around 0.5 mm. Two additional flexures with 1/2 and 1/3 scales were also

fabricated with several tools. The performance of the machine tools were evaluated by inspecting the geometries of the flexures under the microscope and observing the match/mismatch between the flexures and the tool path. Based on the test results, the performances of the μ AWJ on the MicroMAX platform and the CNC micro milling conducted on the Zund G-3 L2500 stood out among all the tools investigated in the MicroCutting Project. For machining a single piece of flexure, the Zund took 2.5 min to machine part. The Zund performed slightly better than the MicroMAX in terms of part accuracy (element width and the uniformity along its axis) and edge quality (roughness and taper) (Liu and Gershenfeld, 2020).

For very thin materials, the OMAX PC-based CAM, MAKE, includes an optimum stack height calculator to estimate iteratively the optimum stack height that achieves the shortest cut time for the single sheet. As shown in Table 1, the AWJ using the 7/15 nozzle took 2.25 minutes to machine the flexure on a single sheet of 0.51 mm thick aluminum. The optimum number of sheets from the iteration to achieve the minimum time for one layer of 0.806 min was 11. The corresponding total stack thickness was 5.59 mm. As a result, there was a 2.79 times reduction in the cut time. In addition, there are two other benefits associated with of AWJ stack machining. First, the increase in the material thickness would effectively enable the activation of the TAJ for taper compensation. As a result, the taper for the individual sheets was minimized. Second, single sheets could be too delicate to be fixtured securely and firmly, degrading the cutting accuracy. The single sheets might be deformed under the load exerted onto the workpieces or distorted by the induced heat during machining.

Table 1: Optimum stack height estimate

Number of Sheets in Stack	Time for Stack (min)	Time For one Layer (min)	Total Thickness
1	2.2455	2.2455	0.02/0.51
2	2.5879	1.2939	0.04/1.02
3	3.0557	1.0186	0.06/1.52
4	3.6441	0.9110	0.08/2.03
5	4.2408	0.8482	0.10/2.54
6	4.9268	0.8211	0.12/3.05
7	5.6523	0.8075	0.14/3.56
8	6.4519	0.8065	0.16/4.06
9	7.2732	0.8081	0.18/4.57
10	8.0696	0.8070	0.20/5.08
11	8.8651	0.8059	0.22/5.59
12	9.7329	0.8111	0.24/6.10

When stacking together with taper compensation using the TAJ was adopted for the μ AWJ, the above advantages of the Zund over the μ AWJ disappeared or the trend even reversed. The combined stack machining and taper compensation not only improved the part accuracy and edge quality but also enhanced the productivity of the μ AWJ. Comparing to

single-sheet machining, AWJ stack cutting cut the aluminum flexure above three times faster than the Zund did. As μ AWJ is further downsized toward micromachining of very thin and delicate materials, stack machining would serve as an enhancer to fixture such materials.


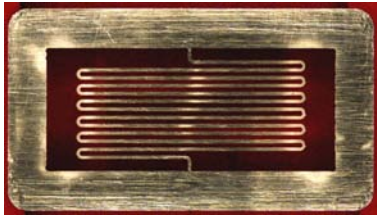
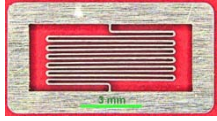
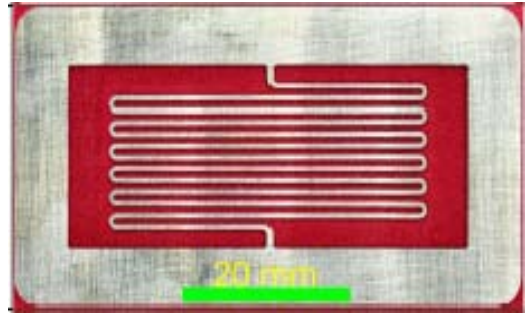

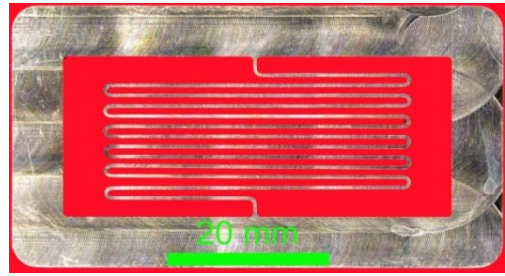
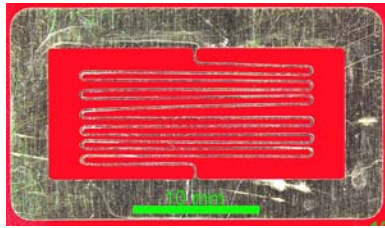
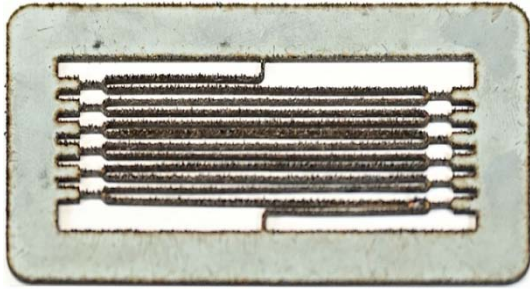
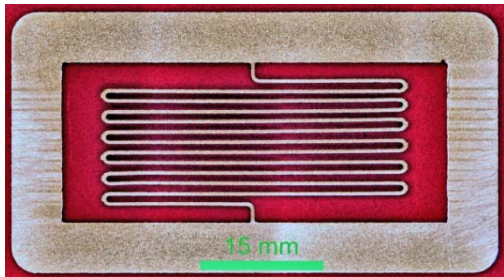
	Full scale (58.2 mm (L) x 30.0 mm (w))	1/2 scale	1/3 scale
MicroMAX (OMAX)			
Zund (MIT/CBA)			Not attempted
Neo (Datron)			Milling head too coarse
Fablght 3000 Laser (MIT/CAB)		Required process optimization (such as lower power with reduced cutting speed) or cutting with solid state lasers	Required process optimization (such as lower power with reduced cutting speed) or cutting with solid state lasers
Laser Powder Bed Fusion – LPBF (Moog)		Not attempted	Not attempted

Figure 3: Aluminum flexures machined with subtractive and additive tools (Liu and Gershenfeld, 2020)

On the other hand, stack machining would not be an option for most CNC micromachining as the miniature spindles and end mills are too delicate to handle the increased load of the stack and the thickness-limited microlasers. For a detailed description of the above, refer to Liu and Gershenfeld (2020).

c) Macro to Micro Machining

In the early stage after the AWJ was commercialized, most R&D was focused on improving its performance in machining thick and difficult-to-cut materials to take advantage of its superior cutting power. Emphasis was made to engage in macro machining using relatively large nozzles and coarse abrasives at high feed rates. Metal parts such as aluminum and steel (annealed and/or hardened) around 0.20 m thick were routinely cut with AWJ (Liu and McNiel, 2010). An example is an AWJ-cut segment of a $\phi 1.52$ m and 100 mm thick Bisalloy gear of a wind turbine to replace a damaged counterpart below it, as shown in Figure 4. Also shown in the lower left of the figure is a portion of the damaged and AWJ-cut segments.

As the AWJ technology was maturing, R&D effort was subsequently shifted to improve the performance of AWJ for precision machining. Since AWJ is largely material independent, AWJ had progressively broadened the applications for machining most

materials from metals, to nonmetals, and anything in between (Liu, 2017a). One of the important demonstrations was the success to apply AWJ to machine a simulated nanomaterial with large gradients of nonlinear material properties (Liu 2017b). The stack consisted of eight thin sheets of different materials including titanium, float glass, G-10 (black), aluminum, polycarbonate, stainless steel, carbon fiber, and copper. Based on the diverse properties of the individual materials, the stack possessed a wide range of properties from metallic to nonmetallic, conductive to non conductive, reflective to non reflective, and ductile to brittle. There would be few conventional tools, if any, capable of machining such a stack. Meanwhile, smart digital control software was developed to streamline machining processes toward automation.

As described in Section 3.2, parallel effort was devoted to develop μ AWJ technology for meso-micro machining with good success. In Figure 4 a μ AWJ-cut miniature $\phi 3.5$ mm planetary gear machined with the 5/10 μ AWJ nozzle was superimposed onto one of the teeth of the wind turbine gear; the miniature gear was merely shown as a speckle on the photograph. The striking size contrast in the two gears had demonstrated the capability of AWJ for machining features from macro to micro scales.



Figure 4: Macro to micro machining with AWJ (Liu, 2017a)

Note that the cutting power of AWJ diminishes with the nozzle size. Table 2 compares the typical parameters used with the 5/10 and 10/21 nozzles. First of all, at the same pressure the hydraulic power and the water flow rate are proportional to the square of the orifice ID. In addition, the abrasive size ($<1/3$ mixing tube ID) and abrasive feed rate ($\sim 12\%$ of water by weight) must reduce according to the mixing tube ID. As a result, the typical mean abrasive particle size and feed

rate reduce $1/3$ and $1/4$, respectively. It is the combination of the reduction in the above parameters that leads to the diminishing of the cutting power. As such, the optimum material thickness reduces noticeably as the nozzle size decreases. For cutting thick materials, large nozzles with 10/21, 14/30, and 22/48 combination were preferably used for high productivity.

Table 2: Typical parameters for the 5/10 and 10/21 nozzles

Orifice ID (in/mm)	Pressure (ksi/MPa)	Hydraulic Power (hp/kW)	Flow Rate (gpm/l/min)	Abrasive Feed Rate (lb/min/g/min)	Abrasive and Mean Size (Mesh/ μm)	Standoff Distance (in/mm)
0.005/0.127	55/379	3.7/2.7	0.11/0.53	0.10/26	240/60	0.03/0.76
0.010/0.254	55/379	15/11	0.44/2.1	0.35/92	80/250	0.06/1.52

d) Cold Cutting

The high-speed water not only accelerates the abrasive particles but also serves as the coolant. During AWJ cutting, the heat generated by the erosive mechanism of the abrasive is carried away by the spent water. As a result, the temperature at the cut edges only raised moderately to around 80°C or less particularly when a chiller is used (Jerman, et al., 2011). On the other hand, the induced heat by lasers cutting and EDM was so high that they must slow down the cutting speed significantly to minimize the heat-affected zone (HAZ). The remedies were to pulse Lasers at high frequencies (e.g. solid-state lasers) and apply thin wire EDM to cut with multiple passes. For heat sensitive materials, therefore, AWJ is capable of cutting at speeds about one order of magnitude faster than lasers and EDM (Liu, 2019a; Liu and Gershenfeld, 2020). Other thermal-based machine tools such as plasma and oxyfuel cutters induced so much HAZ for cutting stainless steel and hardened steel that results in surface hardening and reduces the weld integrity of the workpiece. The HAZ must be removed by secondary processes such as grinding (Wright, 2016). The secondary process of grinding is often time consuming and labor intensive, particularly for very large structure such as shells of spherical pressure vessels made from stainless steel or hardened steel.

For thermal or mechanical-based machine tools, the high heat or large side force distorts the parts during machining. Such distortions may lead to permanent blemishes on the parts. In collaboration with the Center of Bits and Atoms at Massachusetts Institutes of Technology, the performances of a CO₂ and a solid-state lasers with the 5/10 μAWJ nozzle were compared by machining a miniature butterfly on 0.5 mm thick stainless steel.⁵ Figure 5 shows three photographs of the laser- and μAWJ -cut parts. It is evident that the heat generated by the CO₂ laser led to evaporate most of the material. The μAWJ -cut butterfly shows that the kerf width of about 280 μm was slightly too large to negotiate the narrow slots that are wider than the designed width of these slots. As a result, the walls between the slots are thinner than their designed width.

The cold cutting and low side force exertion onto the work-piece by the μAWJ induced minimum mechanical and thermal distortion to the thin walls, preserving their designed shapes with no breakage. The average power of the solid-state laser pulsed at 5 kHz was about 6W. It induced no HAZ on the cut edges and no observed distortion on the walls. With a spot size of 50 μm , it was able to cut the slots and walls accurately according to the designed dimensions. As such, the slots and walls were narrower and wider, respectively, for the solid-state laser cut butterfly than for the μAWJ and solid-state laser-cut counterparts. Pulsing the solid-state laser to minimize the HAZ resulted in slowing down the cut speed considerably. The cut time for the solid-state laser was about 60 minutes while that for the AWJ 5/10 nozzle was 2.2 min. In other words, the 5/10 nozzle cut 27 times faster than the solid-state laser did.

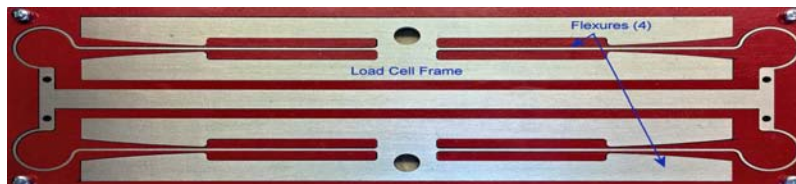


Figure 5: Miniature butterflies machined with lasers and μAWJ (Liu, 2017c, 2019a)

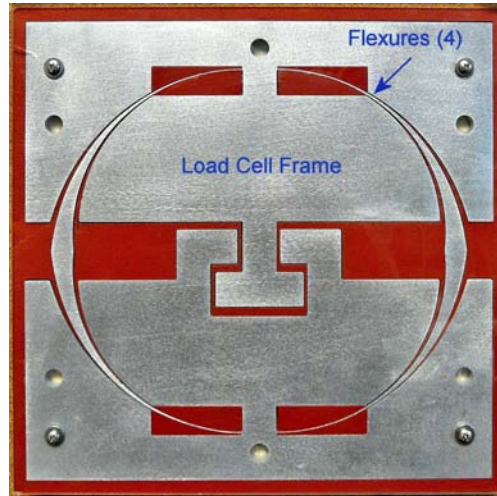
⁵ Beam Dynamics Model LMC10000 CO₂ laser system (500W) and Oxford Solid State Micro Machining Laser - 532nm diodepumped solid-state laser (6W at 10 kHz).

The MIT Precision Engineering Research Group (www.perg.com) has developed flexure-based nonlinear load cells, with 1% change in the force and five orders of magnitude in the force range (MIT US Patent #20150233440). There were two designs of the load cells consisted of large-aspect-ratio thin flexures with constant and variable width, respectively (Kluger et al., 2016, 2017). The constant taper load cell consisted of four 1 mm wide flexure straight elements with an aspect ratio (length to width) of 98.3. The tapered load cell consisted of four tapered ring-shaped flexures with a diameter of 19.1 mm. The taper began and ended with widths of 10 mm and 0.5 mm. The narrow gaps between the flexures and the frames of the load cells were 1.06 mm and 0.42 mm, respectively. There was considerable challenge in machining the load cells made from 6.35 mm thick 6061T6 aluminum because of their geometries and tight tolerances. Note that lasers were not efficient in cutting the aluminum with high thermal conductivity; EDM was expected to be too slow because it must cut via multiple passes to minimize the

HAZ; and CNC milling must cut slowly to avoid the mechanical distortion of the high aspect ratio thin flexures. The flexures were subsequently machined with the μ AWJ to take advantage of its capability of cold cutting and low side force exertion to the workpiece. Machining was successfully conducted using the 7/15 nozzle with 240 mesh garnet. The Tilt A-Jet was activated to minimize the edge taper. Figure 6 shows photographs of the two μ AWJ machined nonlinear load cells. Their performances were verified through laboratory tests conducted at MIT (Kluger et al., 2016, 2017). One of the essential criteria for the success in the verification of their performances was that the edge taper on the flexure element must be minimized. The software's IntelliTaper process was utilized to minimize the edge taper. Machined aluminum coupons that were 51 mm long x 12.7 mm width x 6.35 mm thick, the same thickness as the load cells, showed that the average edge taper of the two sides on the coupon was reduced to 0.03 degree. (Liu, 2016).



a. Constant-width flexures

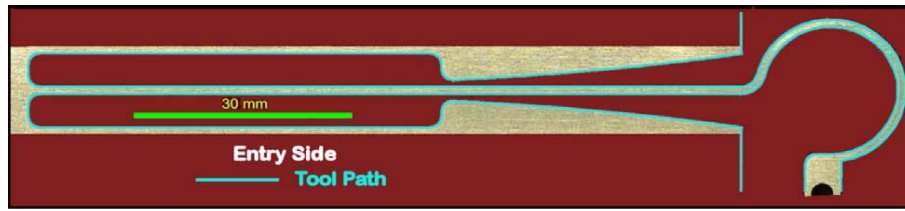
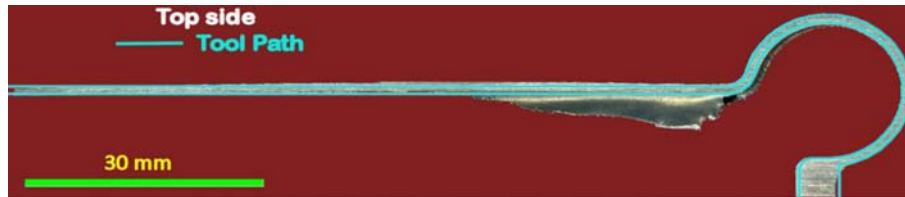


b. Tapered flexures

Figure 6: Two μ AWJ-machined nonlinear load cells (Liu, 2019a)

Figure 7a is a micrograph of one of the four flexures shown in Figure 6a with the superimposition of the corresponding tool path. Excellent match between the μ AWJ-machined part and the tool path is observed. The constant-width and tapered flexures were also machined with CNC milling on a Haas UMC750 with a 6.35 mm end mill, as shown in Figure 7b. Since the diameter of the end mill is larger than the gaps between the flexures and the frame of the load cells, the above setup would be unable to machine the load cells. Modifications of the flexures by enlarging the gaps were

made to accommodate the large end mill. The CNC-milled constant-width flexure shown in Figure 7b was bent slightly either due to the side force exerted by the end mill on the flexure or the excessive heat induced during milling (Liu, 2019a). Besides, a part of the flexure did not cut through its full depth. The above findings demonstrated that the cold cutting and low side force exertion of the AWJ are important factors in achieving the part accuracy and structural integrity for meso-micro machining.


 a. μ AWJ-cut flexure with tool path


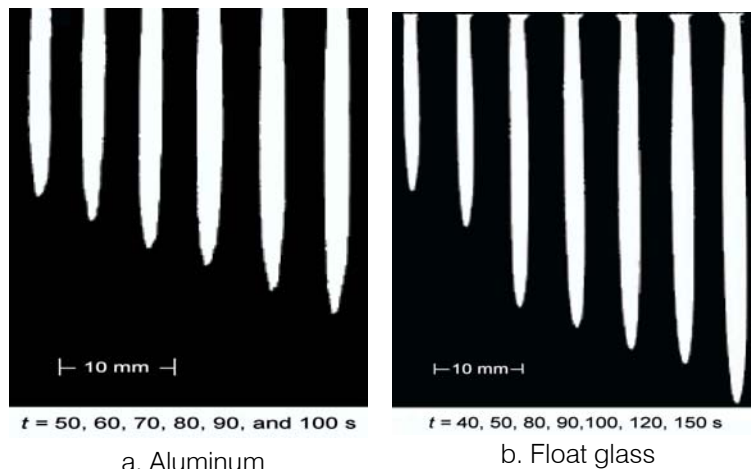
b. CNC-milled flexure with tool path

 Figure 7: Comparison of flexure elements machined with μ AWJ and CNC mill (Liu, 2019a)

e) Hole Drilling

As a material independent tool, AWJ has been applied to drill holes on most materials (Liu, 2016a, 2016b). Since the AWJ cuts with erosive mechanism, it is largely material independent. Note that lasers and EDM are material restrictive because they are incapable of cutting reflective material with high conductivity and conductive materials, respectively. As a flexible cutting/drilling tool, AWJ does not drill straight walled holes but with specific geometries that vary with the materials (Liu, 2006b). Figures 8a and 8b show photo-

graphs of two sets of holes drilled with the AWJ at $p = 241$ MPa on aluminum and float glass, respectively. The overall geometries of these holes are similar except at the hole entry. The difference in geometries, as can be observed in the profiles of the holes shown in Figures 8a and 8b is attributed to the difference in the material properties and the wear resistance. Note that the float glass and aluminum are brittle and ductile materials with machinability numbers of $M = 350$ and 215, respectively. During drilling blind holes, the return slurry



a. Aluminum

b. Float glass

Figure 8: AWJ-drilled holes (Liu, 2006b)

flow when exiting the entry holes wears the glass more than the aluminum. As a result, the glass hole entry was rounded to form a funnel shape. Figure 9a presents the profiles of the holes measured from the photographs shown in Figure 8. By scaling the hole depth, l , with the maximum depth, l_{max} , and the hole diameter, d , with, the logarithm of the drill time, t , as given in the equation

$$\frac{d(l)}{\ln(t)} = f\left(\frac{l}{l_{max}}\right),$$

The profiles shown in Figure 9a were reasonably collapsed as demonstrated in Figure 9b. As a

result, the dependency on drill time was minimized. Note that the left-hand-side of the equation would become non dimensional provided the drill time is multiplied by the drill speed. However, the drill time was not monitored at that time. For an in-depth study of AWJ drilling in ductile materials such as aluminum and mild steel, empirical modeling by means of nonlinear regression methods was conducted to include a wide range of relevant parameters including pump pressure abrasive flow rate, material thickness, dwell time, and nozzle combination (Liu, 2006c).

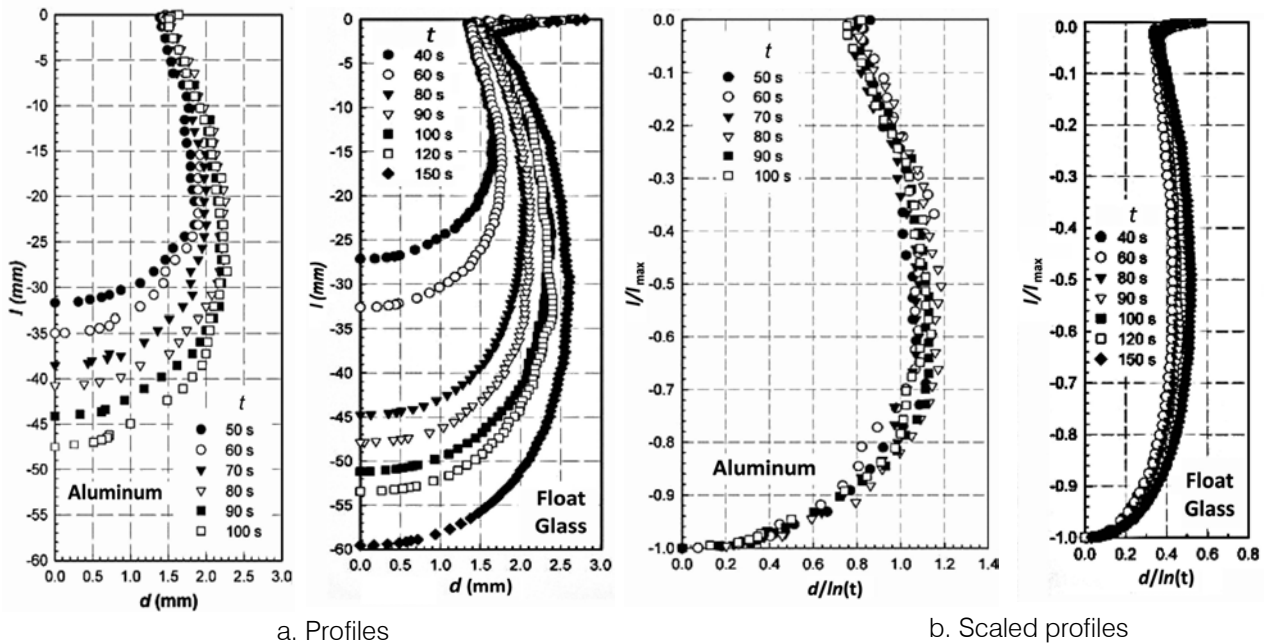


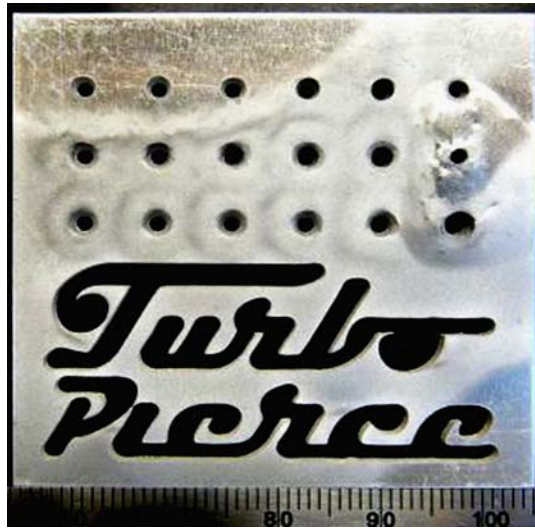
Figure 9: Profiles of AWJ-drilled holes in aluminum and float glass (Liu, 2006b)

Early attempts to pierce delicate materials such as composites and laminates with AWJ had failed due to cracking, delamination, and chipping. Considerable R&D was devoted to investigate the causes of the phenomenon. Based on a CFD simulation in drilling holes with AWJ, it was determined that the damage was attributed to the buildup of stagnation pressure during the initial piercing stage before breakthrough (Liu et al., 1998; Liu, 2006a). As the high-speed waterjet jet enters the blind hole, it decelerates, stops, and reverses its course. At the stagnation point near the bottom of the blind hole, the kinetic energy of the waterjet largely converts into the potential energy in the form of the stagnation pressure (Bachelor, 1967). Damage takes place when the stagnation pressure exceeds the tensile strength of the delicate materials.

One of the remedies was to minimize the buildup of the stagnation pressure inside the blind hole. Subsequently, abrasive cryogenic jet (ACJ) and the patented flash abrasive waterjet (FAWJ) were developed by using liquefied nitrogen and super-heated water as working fluids to accelerate the abrasives (Liu, 2006b; Liu and Schubert, 2009). Most of the liquefied nitrogen of the ACJ and the superheated water of the FAWJ evaporated upon exiting the nozzles leaving mainly the accelerated abrasives entering into the blind holes. As such the buildup of the stagnation pressure was minimized and piercing damage of delicate materials was mitigated. However, both the ACJ and the FAWJ were not practical tools for industrial applications as the working fluids were too aggressive for the components of the high-pressure pump and accessories. Based on the understanding derived from the test results of the ACJ and the FAWJ, proprietary processes were

successfully developed to modify the AWJ through pressure control during piercing (Liu, 2015). Two proprietary processes, a TurboPierce and a MiniPierce, were developed and applied to pierce large and small holes, respectively.

Figure 10 illustrates photographs of aluminum-laminate samples (BAC1534-63F) pierced with the TurboPierce process. The laminate consisted of 19 aluminum sheets 0.076 mm thick with an overall thickness of 1.6 mm. The laminate was formed by stacking the sheets together with adhesive between sheets. Most adhesives do not have very strong adhesive strength. If the stagnation pressure developed inside the blind hole during piercing exceeds the adhesive strength, delamination would result. The 14/42 nozzle with 80 mesh garnet were used in cutting the internal features on the samples. Piercing was carried out by slightly pressurizing the abrasive hopper. Cutting was performed at $p = 380$ MPa. The photographs shown in Figures 10a and 10b correspond to the samples machined before and after the TurboPiercer was optimized, respectively. The left photograph showed delamination around most of the holes. The most serious damage was observed on the right most three holes with a large delamination bubble covered all three holes. There is however no sign of any delamination on the right photograph. The effectiveness in mitigating delamination of the optimized Turbo Piercer was evident.



a. Before optimized



b. After optimized

Figure 10: AWJ-machined internal features on aluminum laminate with TurboPiercer (Liu, 2015)

For cutting small internal features on the aluminum laminate described above, the Mini Piercer with a 5/10 nozzle was used. In this case, pressures of 41 MPa and lower were required to mitigate delamination. For such low pressures, the Venturi vacuum developed after the waterjet exits the orifice was too weak to entrain all the abrasives fed from the hopper. Vacuum assist was required to enhance the

vacuum level while removing excessive abrasives accumulated in the mixing chamber. Otherwise, the mixing tube would be clogged by the excessive abrasives. As soon as breakthrough took place, normal high-pressure cutting at 380 MPa resumes to cut the features at high speeds. Figure 11a shows the top view of the aluminum laminate machined with the Mini Piercer. No delamination was observed.



a. Stack



b. Individual sheets

Figure 11: AWJ-machined miniature holes on aluminum laminate with MiniPiercer (Liu, 2015c)

For thin workpieces such as the 0.076 mm individual shims of the aluminum laminate, as discussed in Section 3.2, the optimum way to machine them with AWJ was through stack cutting. The top and bottom shims of the stack would serve as the sacrificial covers to protect the interior ones from frosting (top shim) and burring (bottom shim). After the stack is cut, the internal

shims would be nearly identical with no frosting and burr, as illustrated in Figure 11b.

For modern aircraft engines operating at a very high temperature, there is need for drilling inclined and shaped air breathing holes to achieve efficient and maximum cooling. The current practice requires a two-step process to drill inclined and shaped holes on TBC

coated metal. First, the nonconductive TBC is removed with a laser and the hole in the substrate is drilled with an EDM process. The versatile AWJ was one of the suitable tools to drill such holes on refractory metals with and without a thermal barrier coating Liu et al., 2018b). By mounting the workpiece on the Rotary Axis, any inclined angle of the holes can be drilled. The geometries of the holes were drilled by controlling the tilting of the A-Jet. Within a certain limitation, the inclined angle and the shape can vary simultaneously along the hole axis. The process involved drilling through the thermal barrier coating at low pressures and then followed by drilling into the refractory metal at high pressures. As such, delamination in the delicate thermal barrier coating was mitigated while accelerating the drilling in the difficult substrate without the HAZ (Liu, 2017a).

f) Gear Making

AWJ has been used extensively for machining gears, racks, and sprockets. Examples of gear from macro to micro scale are shown in Figures 1 and 4. The OMAX PC-based CAD program, LAYOUT, has a gear command for creating a variety of gears and racks. A gear command creates a drawing exchange format (dxf) file by choosing the options of the gear (external or internal), rack, or sprocket, and defining the number of teeth, pitch, and pressure angle. For special gears, an option is to import a CAD drawing to the PC-based LAYOUT to create the tool paths to run in MAKE. Additional examples are shown in this section to demonstrate the versatility of AWJ for machining gears made from several materials for various applications.

One of the interesting projects was to machine a wood clock with the AWJ and then assembled the parts into a working one. There were many choices of design available from a number of websites. The Genesis that was simple but elegant was selected (Boyer, 2018). The complete plan in the dxf file was available online. All the components of the Genesis clock mostly made of high-density plywood with thicknesses ranging from 3.2 mm to 19.1 mm were then cut on a MAXIEM waterjet system in the OMAX Demo Lab. It took just hours to cut all the components with high accuracy as opposed to days using a scroll saw. Figure 12 shows the assembled wood clock. The faces of the hour (lower left), minute (middle), and second (right) gears were cut from a thin stainless-steel sheet rather than cutting the individual numbers from wood or engraving them onto the wheels. The clock was controlled by the adjustable length of the pendulum; it was calibrated with an electric clock. The clock was driven by a 3.2 kg stainless steel round bar that turned a click wheel attached to the back of the minute gear via a fish line. A small aluminum round bar serves as the counter balance to straighten the fish line as the clock

runs. The assembled clock ran well with a pleasant clicking sound as designed (Boyer, 2018).

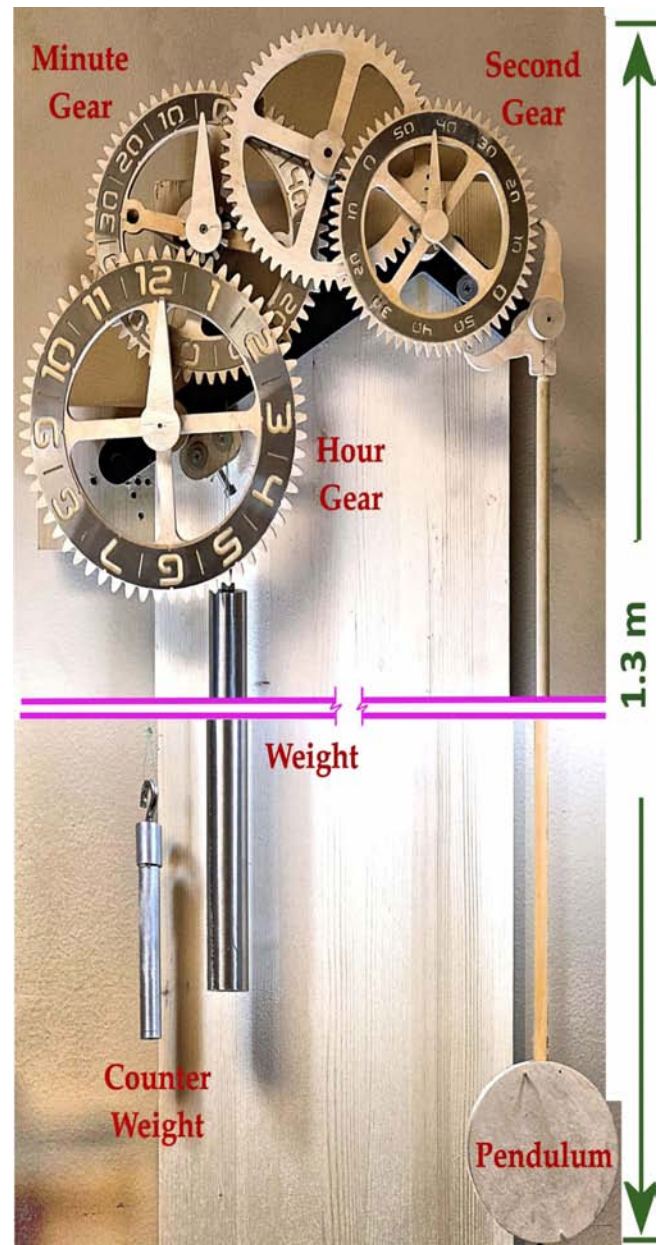
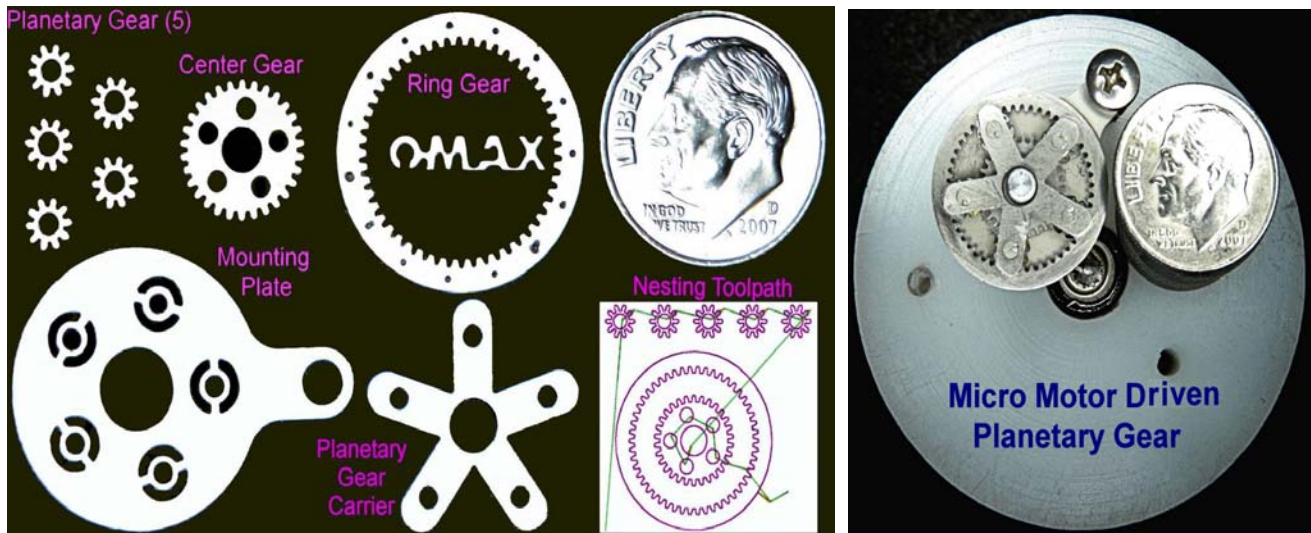


Figure 12: Genesis wood clock (Liu et al., 2018)

A miniature planetary gear set made of titanium sheet 0.25 mm thick was machined on the MicroMAX using the 5/10 nozzle with the 320 mesh garnet. Figure 13 shows the photographs of the nested components and the assembled planetary gear. Also shown in Figure 13a is a part of the nested tool paths; the tool paths of the center and ring gears were cut coaxially on the material. The same set of gears were machined on stainless steel, and Polyether Ether Ketone (PEEK) without and with reinforced fibers to demonstrate the material independence of AWJ machining.



a. Components and tool paths

b. Assembled

Figure 13: AWJ-cut miniature planetary gear set (Liu, 2015)

IV. SUMMARY

In this paper, AWJ-machined samples were presented to demonstrate the versatility of waterjet technology for macro to micro machining for a wide range of materials. Part 1 of the paper emphasizes six particular areas to take advantage of the technological and manufacturing merits of waterjet technology:

- Smart controller software that is smart and intuitive but powerful.
- Meso-micro and stack machining through the development of μ AWJ technology and downsizing of AWJ nozzle.
- Macro to micro machining that is carried out with a single tool using several sizes of nozzle and abrasives on JetMachining Center with a wide range of work envelopes.
- Cold cutting together with exertion of low side force on workpieces that induces no heat-affected zone while preserving the structural integrity of parent materials.
- Hole drilling on both difficult and delicate materials.
- Gear making for a wide range of geometries and sizes on various materials.

Based on the above applications, the versatile AWJ/ μ AWJ technology has established and will set new trends in advanced manufacturing. One of the established trends that has the most impacts on the manufacturing industry is its “7M” advantage, that is, multimode machining of most materials from macro to micro scales (Liu, 2017a). Specifically, all it takes is a single tool using different sizes of nozzles, abrasives, and JetMachining platforms to achieve the above. The “7M” advantage can be applied to a wide range of precision machining:

- AWJ relies on erosion by high-speed abrasives. It is largely material independent and is capable of machining both delicate and difficult-to-machine materials from metals to nonmetals and anything in between. It is even capable of machining nanomaterials with large gradients of nonlinear material properties that present considerable challenge to conventional machine tool (Liu, 2017b)
- Macro machining using large nozzles and coarse abrasives with high feed rates on JMCs with large work envelopes to machining both delicate and difficult materials
 - Delicate materials include glass (except highly tempered ones), composites, laminates, and others
 - Difficult materials include refractory metals, various alloys (such as Inconel, tungsten, and Titanium), tool/hardened steel, and others
 - Cut stainless steel 0.2 m and thicker
- Meso-micro machining of most materials Although the current production and experimental μ AWJ nozzles are capable of machining feature as fine as 200 μ m, cold cutting with low side force exertion on workpieces enables machining very thin wall (<100 μ m) between features
 - For relatively soft materials, water-only jets are capable of machining features <100 μ m.
 - Stack machining is expected to be most advantageous for micromachining as it
 - Serves as “self fixturing” through stiffening individual shims that are difficult to fixture and machine otherwise
 - Increases productivity through machine multiple nearly identical parts at optimum cut time for individual shims

- Increases overall thickness enabling activation the TAJ to achieve minimum taper of individual shims

In Part 2 of the paper, additional examples of AWJ/ μ AWJ machining will be presented to complete the description of recent advancements in the technology. The paper in its entirety will enable to describe the established and new trends of AWJ technology in advanced manufacturing.

REFERENCES RÉFÉRENCES REFERENCIAS

- Bachelor, G. K. (1967) "An Introduction to Fluid Dynamics," Cambridge University Press, London, p. 285.
- Boyer, C. Genesis (2018), Available from: <http://lisaboyer.com/Claytonsite/Genesispage1.htm>
- Henning, A. and Miles, P. (2016) "Conservation of Energy Drives Cutting Performance," *Proc. of the 23rd Int Conf on Water Jetting*, Seattle, WA November 16 – 18.
- Jerman, M., Orbanic, H., Etxeberria, I., Suarez, A., Junkar, M., and Lebar, A. (2011) "Measuring the Water Temperature Changes throughout the Abrasive Waterjet Cutting System," *Proc 2011 WJTA-ICMA Conference and Expo*, September 19-21, Houston, Texas
- Liu, H.-T. (2006a) "Collateral Damage by Stagnation Pressure Buildup during Abrasive-Fluidjet Piercing," *Proc. 18th Int. Conf. On Water Jetting*, Gdansk, Poland, September 13-15.
- Liu, H.-T. (2006b) "Hole Drilling with Abrasive Fluidjets," *Int. J. of Adv. Manuf. Tech.*, Vol. 32, pp. 942-957. (DOI 10.1007/s00170-005-0398-x).
- Liu, H.-T. (2006c) "Empirical Modeling of Hole Drilling with Abrasive Waterjets," *Proc. 18th Int. Conf. On Water Jetting*, Gdansk, Poland, September 13-15.
- Liu, (Peter) H.-T. (2015) "Novel Processes for Improving Precision of Abrasive-Waterjet Machining," *Proc 2015 WJTA-ICMA Conference and Expo*, New Orleans, Louisiana, November 2-4.
- Liu, (Peter) H.-T. (2016) "Roles of taper compensation in AWJ precision machining," *Proc. 23rd Int. Conf. on Water Jetting*, Seattle, WA, Nov. 16-18.
- Liu, H.-T. (2017a) "'7M' Advantage of Abrasive Waterjet for Machining Advanced Materials," *J. Manuf. Mater. Process.*, 1 (1), 11, MDPI, Basel, Switzerland (<http://www.mdpi.com/2504-4494/1/1/11/pdf>). (URL:<https://www.mdpi.com/2504-4494/1/1/11>).
- Liu, H.-T. (2017b) "Versatility of micro abrasive waterjet technology for machining nanomaterials," *Dekker Encyclopedia of Nanoscience and Nanotechnology*, Third Edition DOI: 10.1081/E-ENN3-120054064, pp. 1-18.
- Liu, H.-T. (2017c) "Precision machining of advanced materials with abrasive waterjets." *IOP Conf. Series: Materials Science and Engineering*, 164. 012008. (<http://iopscience.iop.org/article/10.1088/1757-899X/164/1/012008/pdf>).
- Liu, H.-T. (Peter) (2019a) "Performance Comparison on Meso-Micro Machining of Waterjet, Lasers, EDM, and CNC Milling," *International Journal of Emerging Engineering Research and Technology*, 7 (6), 2019, 31-46. ISSN 2349-4395(print) & ISSN 2349-4409 (Online) DOI: i6 (<http://ijeert.org/papers/v7-i6/4.pdf>)
- Liu, H.-T. (Peter) (2019b) "Advanced Waterjet Technology for Machining Curved and Layered Structures," *Curled and Layer Structure Journal*, 6 (1): 41-56, ISSN (Online) 2353-7396, DOI: <https://www.degruyter.com/downloadpdf/j/cls.2019.6.issue-1/cls-2019-0004/cls-2019-0004.pdf>
- Liu, H.-T. and Schubert, E. (2009) "Piercing in Delicate Materials with Abrasive-Waterjets," *Int. J. of Adv. Manuf. Tech*, Vol. 42: No. 3-4, pp. 263 - 279. (DOI: 10.1007/s00170-008-1583-5).
- Liu, H.-T. and McNeil, D. (2010) "Versatility of waterjet technology: from macro and micro machining for most materials" *Proc. 20th Int. Conf. on Water Jetting*, October 20–22, Graz, Austria.
- Liu, H.-T. and Schubert, E. (2012) "Micro Abrasive-Waterjet Technology (Chapter Title)", *Micromachining Techniques for Fabrication of Micro and Nano Structures*, Ed. Mojtaba Kahrizi, INTECH Open Access Publisher, ISBN 978-953-307-906-6, January, pp. 205-34 (<http://cdn.intechweb.org/pdfs/27087.pdf>).
- Liu, (Peter) H.-T. (2015) "Novel Processes for Improving Precision of Abrasive-Waterjet Machining," *Proc. 2015 WJTA-ICMA Conference and Expo*, New Orleans, Louisiana, November 2-4.
- Liu, (Peter) H.-T. and Neil Gershenfeld (2020) "Performance comparison of subtractive and additive machine tools for meso-micro machining," *J. Manuf. Mater. Process. (JMMP)*, 4 (1), 19, MDPI, Basel, Switzerland, <https://www.mdpi.com/2504-4494/4/1/19/pdf>.
- Liu, H.-T., Miles, P., and Veenhuizen, S. D. (1998) "CFD and Physical Modeling of UHP AWJ Drilling" *Proc. 14th Int. Conf. on Jetting Technology*, Brugge, Belgium, September 21 – 23, pp. 15-24.
- Liu, (Peter) H.-T., Cutler, V., and Webers, N. (2018a) "Recent Advancement in Abrasive Waterjet for Precision Multimode Machining," *Proc. 24th Int. Conf. on Water Jetting*, Manchester, UK, September 5-7. Liu, (Peter) H.-T., Cutler, V., Raghavan, C., Miles, P., and Webers, N. (2018b) "Advanced Abrasive Waterjet for Precision Multimode Machining," *Abrasive Technology - Characteristics and Applications*, Ed. Anna Rudawska, Intech Open Publisher, ISBN 978 953-307-906-6, October, pp. 39-64. (<https://www.intechopen.com/books/abrasive-technology-chara>)

cteristics-and-applications/advanced-abrasive-water-jet-for-multimode-machining).

22. Miller, D. S. (2003) "Developments in Abrasive Waterjets for Micromachining," Proc. 2003 WJTA Amer. Waterjet Conf., Houston, Texas, Paper 5-F. 17-19 August 2003.
23. Miller, D. S. (2005) "New Abrasive Waterjet Systems to Complete with Lasers," *Proc. 2005 WTJA Amer. Waterjet Conf.*, Houston, Texas, August 21-23, Paper 1A-1.
24. Tate, K. (2013) "How to Catch an Asteroid: NASA Mission Explained (Infographic)," April; <https://www.space.com/20610-nasa-asteroid-capture-mission-infographic.html>.
25. Wright, I. (2016) "An Engineer's Guide to Waterjet Cutting," *Manufacturing*, July (https://www.engineering.com/AdvancedManufacturing/ArticleID/12716/An-Engineers-Guide-to-Waterjet-Cutting.aspx#disqus_thread)
26. Xu, G., Lu, P., Li, M., Liang, C., Xu, P. Liu, D., and Chen, Xi. (2018) "Investigation on characterization of powder flowability using different testing methods," *Experimental Thermal and Fluid Science*, 92, pp. 390-401.
27. Yadav, G. S. and Singh, B. K. (2016) "Study on water jet machining and Its future trends," *International Journal of Recent Research Aspects*, ISSN: 2349-7688, 3 (2) June, pp. 50-54.
28. Zeng, J. (2007) "Determination of machinability and abrasive cutting properties in AWJ cutting," 2007 *Proc. Amer. WJTA Conf. and Expo*, August 19-21, 2007, Houston, Texas.
29. Zeng, J., Kim, T. J., and Wallace, R. J., (1992) "Quantitative fvaluation of machinability in abrasive waterjet machining," Proc. of 1992 *Winter Annual Meeting of ASME*, Precision Machining: Technology and Machine Development and Improvement, PEDVol.58, Anaheim, 1992, pp. 169-179.



GLOBAL JOURNAL OF RESEARCHES IN ENGINEERING: A
MECHANICAL AND MECHANICS ENGINEERING
Volume 20 Issue 1 Version 1.0 Year 2020
Type: Double Blind Peer Reviewed International Research Journal
Publisher: Global Journals
Online ISSN: 2249-4596 & Print ISSN: 0975-5861

The Load Distribution with Modification and Misalignment and Thermal Elastohydrodynamic Lubrication Simulation of Helical Gears

By Jian-hua Xue, Zhen-hua Zhang & Huan-rui Wang

Abstract- A non-uniform model of the load per unit of length distribution of helical gear with modification and misalignment was proposed based on the meshing stiffness, transmission error, and load-balanced equation. The distribution of unit-line load, transmission error (TE), and contact press of any point on the contact plane were calculated by the numerical method. The feature coordinate system was put forward to implement the helical preliminary design and strength rating. The thermal elastohydrodynamic lubrication (EHL) model of helical gear was established, and the pressure, film, and temperature fields were obtained from the thermal EHL model. The maximum contact temperature and minimum film thickness solved by thermal EHL were applied to check the scuffing load capacity. The highest flash temperature and thinnest film occur in the dedendum of the pinion. The thermal EHL method to evaluate the scuffing load capacity is effective.

Keywords: helical gear; meshing stiffness; load distribution; scuffing load capacity.

GJRE-A Classification: FOR Code: 290501



Strictly as per the compliance and regulations of:



© 2020. Jian-hua Xue, Zhen-hua Zhang & Huan-rui Wang. This is a research/review paper, distributed under the terms of the Creative Commons Attribution-Noncommercial 3.0 Unported License (<http://creativecommons.org/licenses/by-nc/3.0/>), permitting all non commercial use, distribution, and reproduction in any medium, provided the original work is properly cited.

The Load Distribution with Modification and Misalignment and Thermal Elastohydrodynamic Lubrication Simulation of Helical Gears

Jian-hua Xue^α, Zhen-hua Zhang^ο & Huan-rui Wang^ρ

Abstract- A non-uniform model of the load per unit of length distribution of helical gear with modification and misalignment was proposed based on the meshing stiffness, transmission error, and load-balanced equation. The distribution of unit-line load, transmission error (TE), and contact press of any point on the contact plane were calculated by the numerical method. The feature coordinate system was put forward to implement the helical preliminary design and strength rating. The thermal elastohydrodynamic lubrication (EHL) model of helical gear was established, and the pressure, film, and temperature fields were obtained from the thermal EHL model. The maximum contact temperature and minimum film thickness solved by thermal EHL were applied to check the scuffing load capacity. The highest flash temperature and thinnest film occur in the dedendum of the pinion. The thermal EHL method to evaluate the scuffing load capacity is effective.

Keywords: helical gear; meshing stiffness; load distribution; scuffing load capacity.

I. INTRODUCTION

A helical gear is a common transmission device and has been widely used in all the fields, especially the machine under high speeds and heavy loads. The load distribution is the foundation of the gear preliminary design and strength rating process. It is known that the load distribution depends on the meshing stiffness of the tooth pair, and the load per unit of length is different at any point in the contact plane. The simple equations in standard ISO [1,2] to describe the load distribution, which is not in good agreement with experimental results. The contact lines of a helical gear are not parallel with the axial line, and the length of contact lines is dynamic changing in the meshing process.

Some studies on the meshing stiffness and load distribution of involute gears can be found in technical literature. Z. Chen et al. [3-6] studied the tooth mesh stiffness and transmission error via the finite element method (FEM). However, this method is feasible but has the problem no generality of the obtained results. Afterward, J.I.Pedrero et al. [7-9] proposed a method to calculate non-uniform load distribution along the line of contact from the minimum elastic criterion potential, which depends on the transverse contact ratio. Through

this method, the author analyzed the bending strength and pitting load capacity of helical gears. But the balanced load equation was not considered in this method. Thus it can't provide the load distribution of any point on the contact plane, and it is hard to locate the maximum value of the load.

The heavy load and high-speed gear generate a lot of heat and temperature rise. High contact temperature of lubricant and tooth surfaces at the instantaneous contact position may lead to the breakdown of the lubricant film at the contact interface. The scuffing failure is unpredictable and fatal for the gear system. Therefore the scuffing load capacity is of great importance in the process of helical gear system preliminary design and strength rating, especially for the heavy load and high-speed gear system. ISO [10,11] provides two methods, namely the flash temperature method and integral temperature method, to evaluate the scuffing load capacity of the gear system, nevertheless the load distribution uses the simplified form and the flash temperature calculated based on the Blok flash temperature equation [12], which can't get the accurate flash temperature and need to attach a large safety factor to amend it.

The thermal elastohydrodynamic lubrication (EHL) is also a hot research topic. So far, most studies focused on the thermal EHL of spur gears. Wang and Cheng obtained a comprehensive research on a numerical simulation of the contact conditions of straight spur gear pairs [13,14]. L.M. Li proposed an inverse approach to establish the pressure, temperature rise, and apparent viscosity distribution in an EHL line contact [15]. Some methods and beneficial work to study on the EHL of spur gear, and a mass of cases were obtained, but these researches mostly stay in the theoretical and ignore the practical application [16-19]. Besides the spur gears, the EHL research of helical gears is rare, no matter under the isothermal or thermal conditions. Recently, P. Yang and P.R. Yang used the multilevel multi-integration method to study the thermal elastohydrodynamic lubrication of tapered rollers in the opposite orientation; this model can be applied to the helical gear system [20]. These technical literatures mentioned above mostly focus on the calculation method and directly offer the load; they can express the thermal EHL characteristic in theory but can't apply to

Author α ρ : Shaaxi Hande Axle Co., Ltd., Xi'an Shaanxi, China.
e-mail: xjh1986818@163.com

the actual conditions. The scuffing load capacity can be evaluated by the maximum contact temperature and minimum film thickness, which can be solved by the thermal EHL method. The literature of thermal EHL mostly focus on the temperature and film thickness of some single points [16-20]. The literature which makes the thermal EHL theory to design and check gear is absent.

This paper proposes a method to study the load per unit of length distribution of all the points on

contact plane of helical gears accurately based on the balanced Load equation, transmission error, and meshing stiffness. The feature coordinate to simplify the preliminary design and strength check process of helical gears is established. Based on the load distribution, the thermal EHL model, which corresponds more to actual conditions, is put forward. The hydrodynamic pressure, film thickness, and contact temperature, as well as the flash temperature, to check the scuffing load capacity are calculated via the numerical method.

Nomenclature

b gear face width, mm	η viscosity of lubricant, Ns/m^3
w load per unit of length, N/m	r_{b2} base radius of gear, m
m_n normal module, mm	b_0 half width of the Hertzian line contact, m
ε_α transverse contact ratio	P_H maximum Hertzian pressure, Pa
ε_β axial contact ratio	α Braus viscosity-pressure coefficient, m^2/N
ε_γ total contact ratio	β Reynolds viscosity-temperature coefficient, k^{-1}
β standard helix angle, ($^\circ$)	x contact coordinate in rolling direction, m
β_b base helix angle, ($^\circ$)	z coordinate across lubricant film, m
h film thickness, m	$\lambda, \lambda_1, \lambda_2$ thermal conductivities of lubricant and solids, W/mk
E elastic modulus, Pa	ρ, ρ_1, ρ_2 densities of lubricant and solids, kg/m^3
t temperature, K	c, c_1, c_2 specific heat of lubricant and solid, J/kgK
t_0 ambient temperature, K	P_{bt} transverse circular pitch, m
r_{b2} base radius of gear, m	P_{ba} axial pitch, m
α_w pressure angle ($^\circ$)	n_1 rotational speed of pinion, $r \text{ min}^{-1}$
δ deformation, m	k stiffness of contact point, N/m
L length of all the contact lines, m	TE transmission error, μm

II. THE LOAD DISTRIBUTION MODEL OF HELICAL GEAR

a) The contact model of the helical gear under heavy load

For operating helical gear pair under heavy load, even though the driving pinion rotates at a constant speed, the gear as well as fall behind the angle

$\Delta\theta$ than the theoretical location because of the deformation of driving and driven gear along the action line. As Fig.1 shows, the meshing condition viewing from helical gear transverse direction, the profile of the solid line is the theoretical location, and the dashed line is the actual location under deformation. N_1N_2 is the theoretical action line. Thus for any point K at the action line, the deformation along the action line is

$\delta_k = r_{b2} \cdot \Delta\theta$. Here assuming the stiffness of the contact point TE is k , then the load per unit of length of point TE is $w_k = k\delta_k$. For helical gears, the contact lines at the same time always more than one (depend on the total contact ratio), so setting L denotes the sum of the length of all the contact lines, the sum load of the

helical gear is the integral of w_k , at any moment, it should be balanced to the extern load, the balanced load equation as follow:

$$\int_0^L w_k dl = \int_0^L k(l)r_{b2}\Delta\theta dl = \frac{9549P}{n_1 r_{b1}} = W_{sum} \quad (1)$$

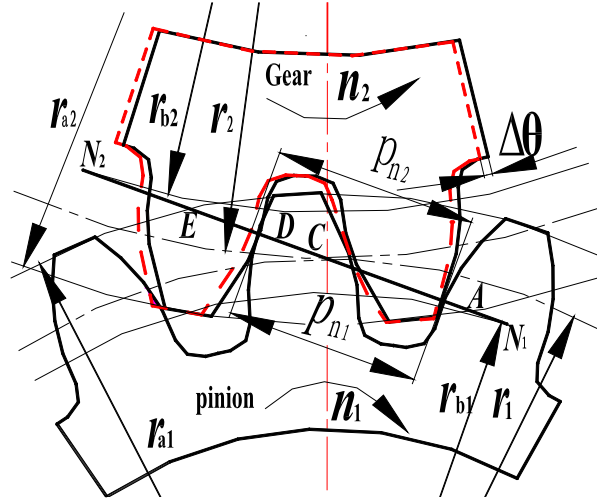


Fig. 1: The contact model of helical gear in transverse under heavy load

b) The sum length of the contact lines

The analysis model of the helical gear is shown as Fig.2, the contact plane $N_1N_2N_3N_4$ is the tangent plane of two gear base circle. K_1K_2 is one of the contact line. The actual action line is A_1E_1 . The transverse contact ratio calculated by Equ.2.

$$\epsilon_a = A_1E_1 / P_{bt} \quad (2)$$

Where $P_{bt} = \pi \cdot m_t$ is the transverse circular pitch, m_t the transverse module.

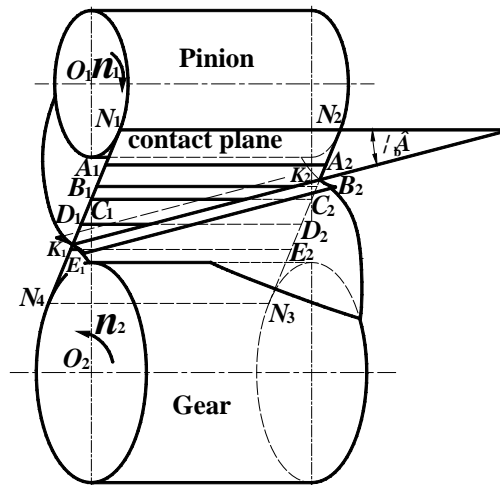


Fig. 2: The analysis model of the helical gear

Viewing from the transverse direction, for $\epsilon_a \in (1,2)$, we can divide the A_1E_1 into three regions, A_1B_1 , B_1D_1 , and E_1D_1 , the A_1B_1 and D_1E_1 are the double contact tooth regions (the number of tooth contact at the same time is 2), B_1D_1 is the single contact tooth region. So we can divide the actual contact plane into three regions. It shows as the Fig.3. The $A_1B_1A_2B_2$ and $D_1D_2E_1E_2$ are the double contact tooth regions, $B_1B_2D_1D_2$

is the single contact tooth region. In double contact tooth regions, the contact lines always occur double in the same location. The coordinate system is established to describe the actual contact plane $A_1A_2E_1E_2$. The axial direction and action line direction are described by B and Γ [10]. Γ is the dimensionless parameter defined as follow:

$$\Gamma = (N_1K - N_1C) / N_1C$$

Where C is the pitch point, K the contact point, thus $\Gamma \in [\Gamma_{A_1}, \Gamma_{E_1}]$, $B \in [0, b]$.

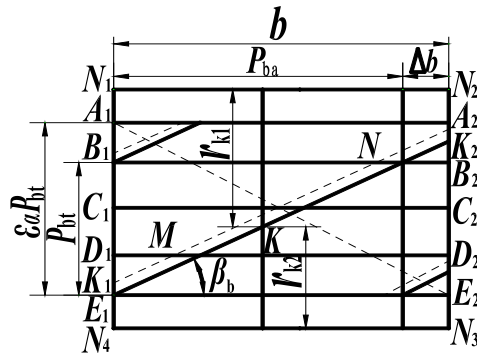


Fig. 3: Analysis model of helical real action plane

Now assuming A_1 is the gear pair approach point (begin meshing), the contact line will move along with the line A_1E_2 to the recess action point E_2 . Axial contact ratio is expressed by the ε_β .

$$\varepsilon_\beta = b / P_{ba} = b \cdot \tan \beta_b / P_{bt} \quad (3)$$

The total contact ratio $\varepsilon_\gamma = \varepsilon_\alpha + \varepsilon_\beta$. When one of the ε_α and ε_β is an integer, the sum length of contact lines is constant. When $\varepsilon_\beta = n$, the sum length can be expressed as:

$$L_n = n \varepsilon_\alpha P_{bt} / \sin \beta_b \quad (4)$$

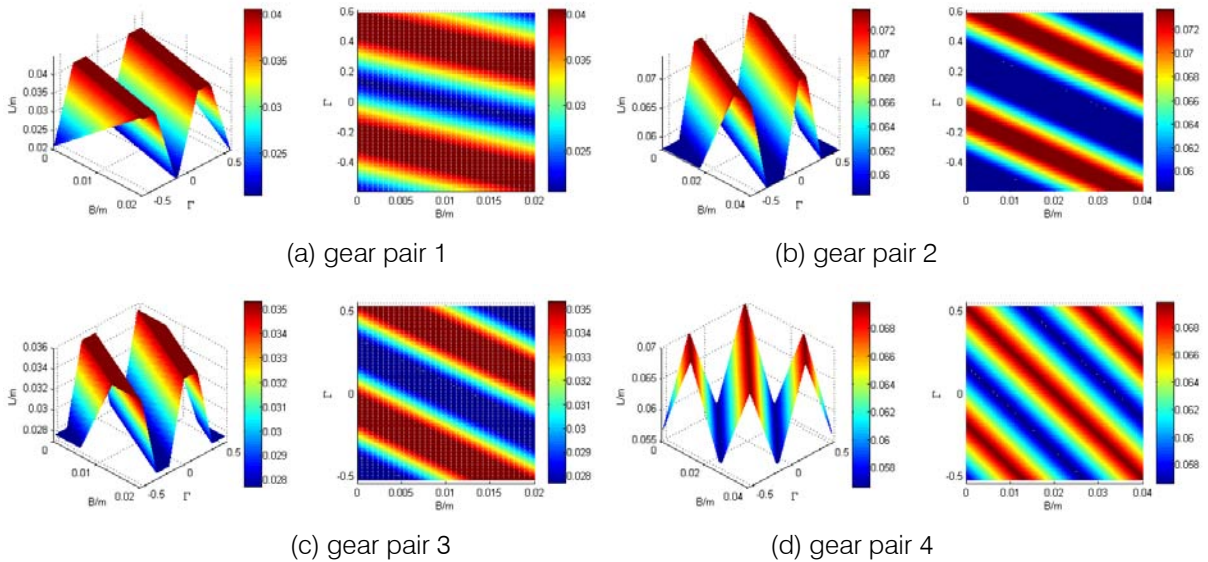


Fig. 5: The result of the sum length of contact lines

Table 1: Gear data and operating conditions

	Gear Pair 1	Gear Pair 2	Gear Pair 3	Gear Pair 4
Number of teeth (pinion/gear)	23/30	23/30	23/30	23/30
Normal pressure angle	20	20	20	20
Normal module, mm	3	3	3	3
Face width, mm	20	40	20	40
Input power(kw)	50	50	50	50
Modulus of elasticity E_1/E_2 , GPa	206/206	206/206	206/206	206/206
Poisson ratio, ν_1/ν_2	0.3/0.3	0.3/0.3	0.3/0.3	0.3/0.3
Helix angle, °	9.8	9.8	20.2	20.2

Pinion speed, r/min^{-1}	2000	2000	2000	2000
transverse contact ratio ϵ_α	1.59	1.59	1.49	1.49
Axial contact ratio ϵ_β	0.36	0.72	0.73	1.47
total contact ratio ϵ_γ	1.95	2.31	2.22	2.96

The length distribution of contact lines with the parameters listed in Table 1 shows as Fig.5. For different gear pairs, the distribution of load per unit of length is different. Compare the gear pair one and two or three and four, the face width doubled, and the length of the contact line almost double as well. The wider the tooth width, the longer the total length. But the value that the maximum minus the minimum has the upper limit

value. We are letting the length ratio $\zeta = L_{\min} / L_{\max}$, the length ratio under different helix angle is show in Fig.6. It is obvious that when $\epsilon_\gamma < 2$, the length ratio is only 0.5, and the fluctuation of length is greatly, the maximum is as double as the minimum length. When $\epsilon_\gamma > 2$, the length ratio is close to 1.

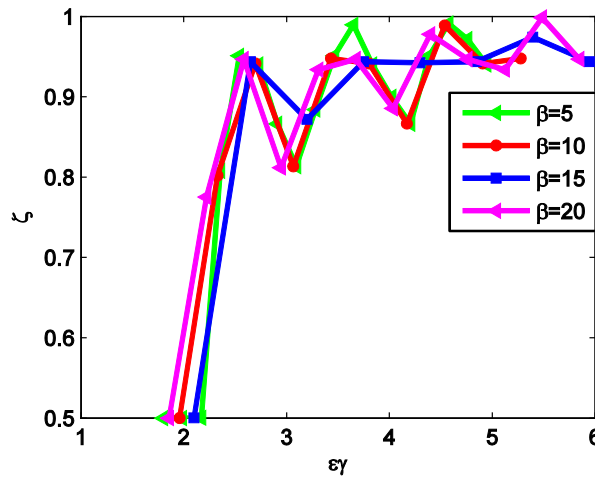


Fig. 6: The length ratio varying with the total contact ratio

c) *The tooth meshing stiffness*

The gear profile is a complex graphics and can be simply as the combination of a rectangle and a trapezium, as the Fig.7 shows. The gear deformation includes the bending deformation, shear deformation, and contact deformation. The total is the sum of the rectangle deformation and trapezium deformation. The

total of the contact deformation point along the action line can be expressed as the sum of the bending deformation δ_B , shear deformation, δ_s and lean deformation δ_G .

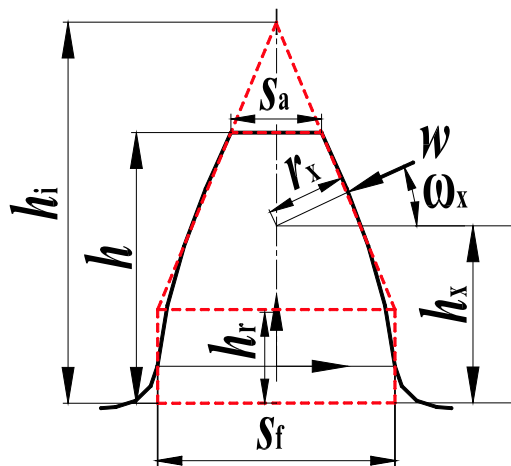


Fig. 7: The stiffness analysis model of gear tooth

$$\delta = \delta_{Br} + \delta_{Bt} + \delta_s + \delta_G \quad (5)$$

Where δ_{Br} and δ_{Bt} means the bending deformation of rectangle and trapezium, δ_s notes the shear deformation.

$$\delta_{Br} = \frac{12w \cos^2 \omega_x}{E_i S_f^3} \left[h_x h_r (h_x - h_r) + \frac{h_r^3}{3} \right]$$

$$\delta_{Bt} = \frac{6w \cos^2 \omega_x}{E_i S_f^3} \left[\frac{h_i - h_x}{h_i - h_r} \left(4 - \frac{h_i - h_x}{h_i - h_r} \right) - 2 \ln \frac{h_i - h_x}{h_i - h_r} - 3 \right] (h_i - h_r)^3$$

$$\delta_s = \frac{2(1 + \nu_1)w \cos^2 \omega_x}{E_i S_f} \left[h_r + (h_i - h_r) \ln \frac{h_i - h_r}{h_i - h_x} \right]$$

$$\delta_G = \frac{24wh_x \cos^2 \omega_x}{\pi E_i S_f^2}$$

Where h is the height of the tooth, h_x the height of contact point, h_r the height of the rectangle, ω_x the

pressure angle of the contact point, $h_i = \frac{h S_f - h_r S_a}{S_f - S_a}, \nu_i$

notes the Poisson's ratio of pinion, E_i the elastic modulus of pinion or gear, w the load per unit of length.

When a pair of tooth meshing, the sum deformation along the action line can be described as the Equ.6.

$$\delta_\Sigma = \delta_1 + \delta_2 + \delta_{PV} \quad (6)$$

Where $\delta_{PV} = \frac{2w[(1 - \nu_1^2) + (1 - \nu_2^2)]}{\pi E}$ is the contact deformation of the meshing point, so the stiffness of this point can be expressed as Equ.7.

$$k = w / \delta_\Sigma \quad (7)$$

Fig.8 shows the distribution of stiffness along the action line; the maximum occurs close to the pitch point. The regulation of stiffness is similar to the inverse unitary potential $v(\xi)$ in Ref. [7-9], which all reflect the capacity that the tooth bears the deformation.

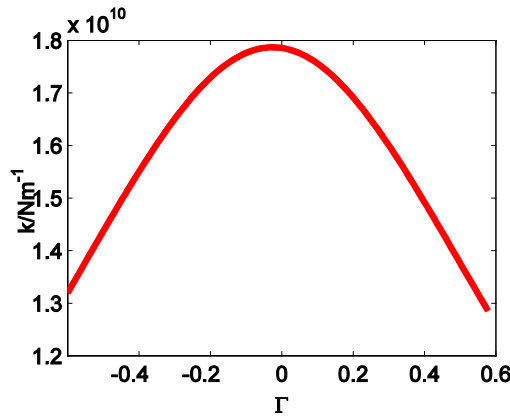


Fig. 8: Gear teeth stiffness along the action line of gear pair 1

d) The load distribution calculation process of helical gear

In Fig.3, the sum length is shown as follow:

$$W_{sum} = \int_0^{L_{sum}} k(l) \cdot TE \cdot dl \quad (8)$$

For the convenience of numerical calculation, the line A_1E_1 is divided into N nodes, and $l_\Delta = A_1E_1 / (N - 1)$, so the total load can be expressed as Equ.9, the number of the contact line is m .

$$W_{sum} = \sum_{j=1}^m \sum_{i=1}^n k_{ij} \max((TE_{ij} - \Delta_x), 0) \cdot l_\Delta / \sin \beta_b \quad (9)$$

The load distribution calculation process of helical gear is shown as Fig.9. According to the equations above, we can calculate the load distribution of every point on the contact plane. Firstly, letting $L=L_0$, $k=k_c$, and TE_0 will be calculated; secondly, from the

Equ.9, the sum load was obtained, then modified the TE according to Equ.10, until the sum load satisfied the Equ.11, then repeat this process until the results of all points were obtained.

$$TE_1 = \frac{W_{sum}}{w} TE_0 \quad (10)$$

$$\frac{|w - W_{sum}|}{W_{sum}} \leq 10^{-5} \quad (11)$$

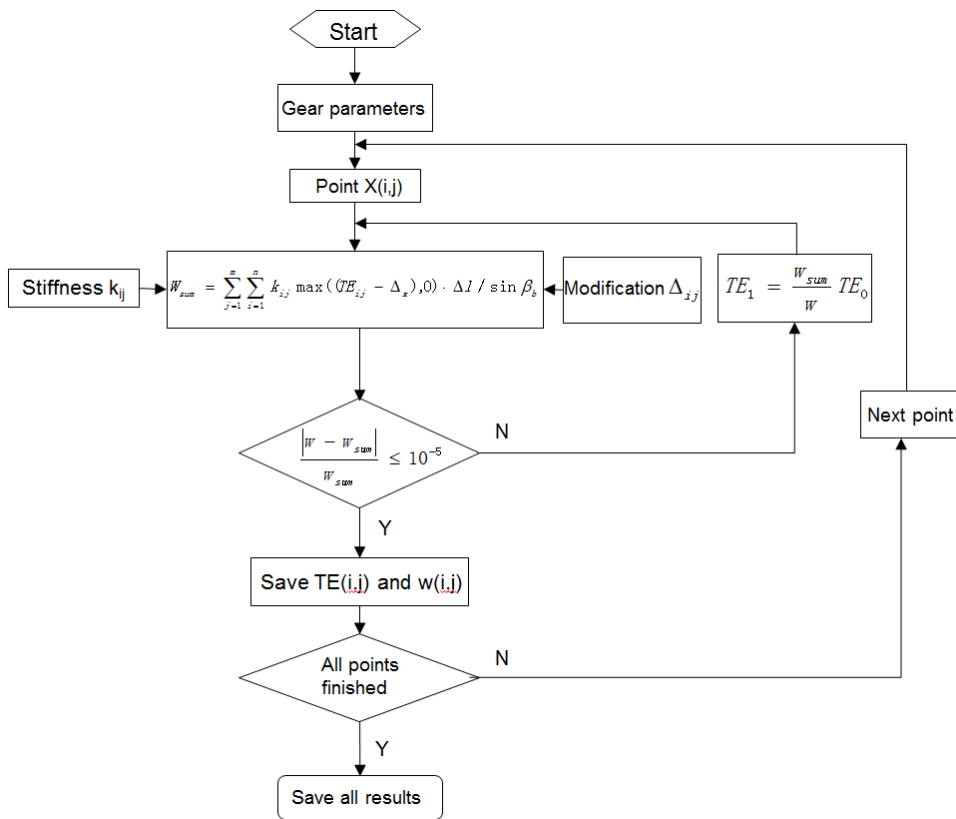


Fig. 9: The load distribution calculation process of helical gear

e) The contact stress of the helical gears

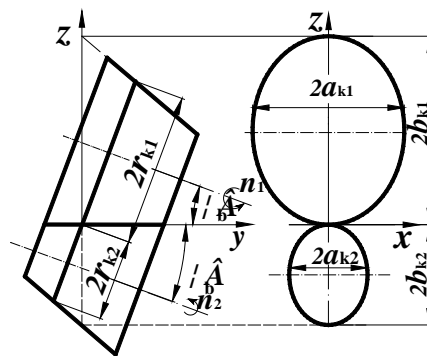


Fig. 10: The contact model of helical temperature

The contact model of the helical gear can be regarded as two tapered rollers [20]. In this model, the actual geometric model is two oval in oxz coordinate systems, and the geometric parameters as follows:

$$a_{Ki}|_{i=1,2} = \frac{r_{Ki} \cos^2 \beta_b}{1 - 2 \sin^2 \beta_b} \quad b_{Ki}|_{i=1,2} = \frac{r_{Ki} \cos \beta_b}{1 - 2 \sin^2 \beta_b} \quad (12)$$

Where the subscript 1 means the pinion, 2 for gear. The curvature of the contact point of two oval are as follows:

$$R_i|_{i=1,2} = \frac{a_{Ki}^2}{b_{Ki}} = \frac{r_{Ki} \cos^3 \beta_b}{1 - 2 \sin^2 \beta_b} \quad (13)$$

According to the Hertz contact theory, the maximum contact press of the helical gear is expressed as Equ.14.

$$\delta_H = \frac{\pi}{4} \sqrt{\frac{Ew}{2\pi R}} \quad (14)$$

Where $R = \frac{R_1 R_2}{R_1 + R_2}$ the curvature sum, E is equivalent to

Young's modulus, $\frac{1}{E} = \frac{1}{2} \left(\frac{1 - \nu_1^2}{E_1} + \frac{1 - \nu_2^2}{E_2} \right)$.

f) The load distribution calculation of helical gear without modification

In the calculation process, the modification, setting Δ_{ij} to 0, then the transmission and the unit-line load of contact plane can be obtained. The three-dimension unit-line load distribution is shown in Fig.11. The load distribution on the contact plane is not only depends on the transmission error, but also depends on

the stiffness distribution. The value of the load is small in the dedendum and addendum region of helical gear, and large close to pitch point. For the different helix angles and different face width, the load distribution is different. As we know, the sliding speed is maximum in the dedendum or addendum. From the 4 cases, the biggest occurs in the begin meshing and engaging-out point of, the helical contact plane.

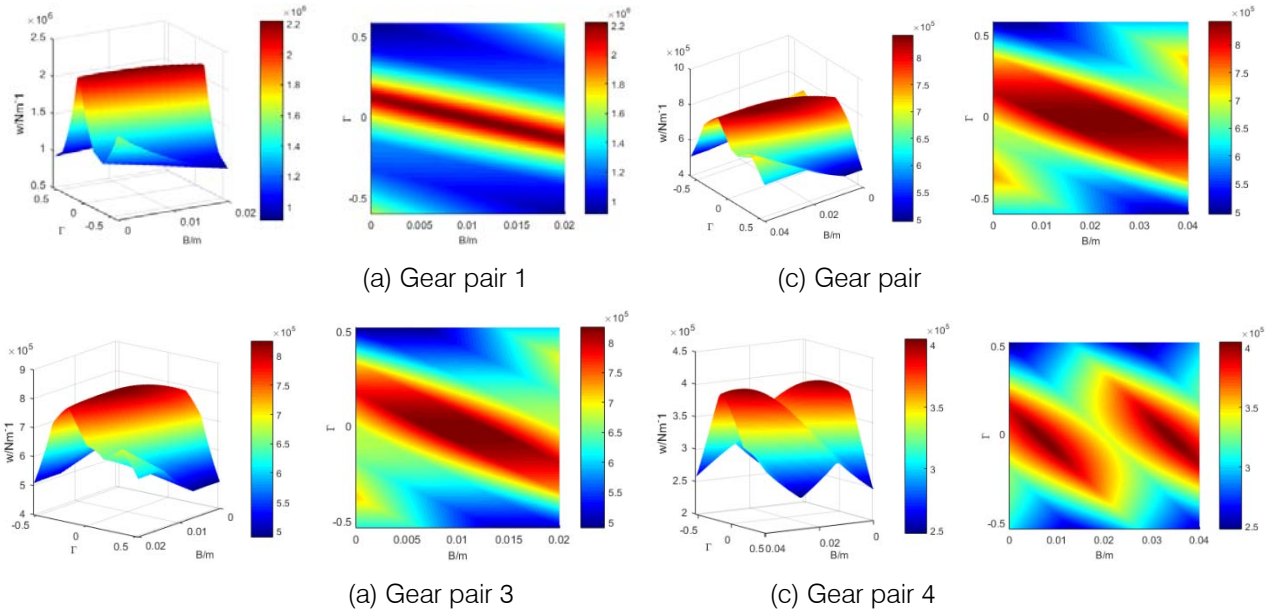


Fig. 11: Unit-line load distribution of helical gears

The load distribution solved in this paper is in good agreement with the results which occur in Ref.8 by the finite elements method (FEM). The results show that the contact stress solved by FEM is larger near the pitch point and small in the dedendum and addendum

region. Thus the load distribution in this paper is consistent with the actual condition to a great extent without the consideration of the end effect, the machine error, and assembly error.

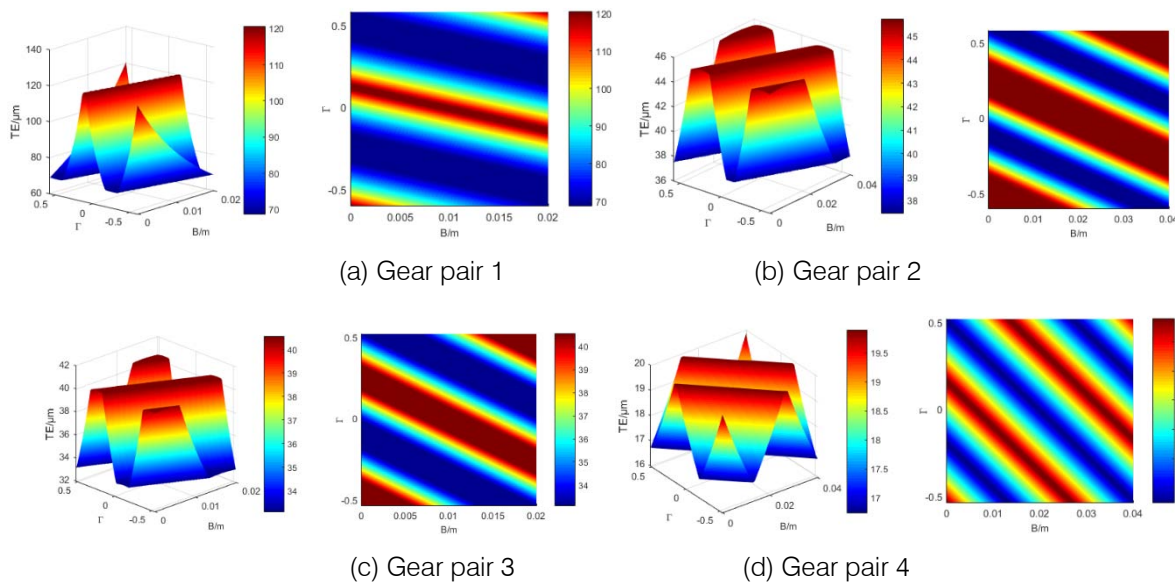


Fig. 12: The transmission error of the helical gears

The transmission errors of helical gear pairs shown in Fig.12, its distribution law corresponding to the distribution of length. The fluctuation of transmission error is the main indicator of the vibration and dynamic load. It is significant to choose the advisable helix angle and face width to make the fluctuation of transmission error minimum.

The contact press distribution of the helical gears is shown in Fig.13. It is similar to the unit-line load.

But the contact stress of foot is greater than that of top of pinion. It is because the sum radius of the curvature of the root is smaller than that of the tooth top. For a helical cylindrical gear without modification, the maximum contact press is located at the engagement of the pinion root. As shown in Fig.14, it is a fatigue pinion of an electric axle after the loading bench test, fatigue pitting at the meshing point of the root of the pinion.

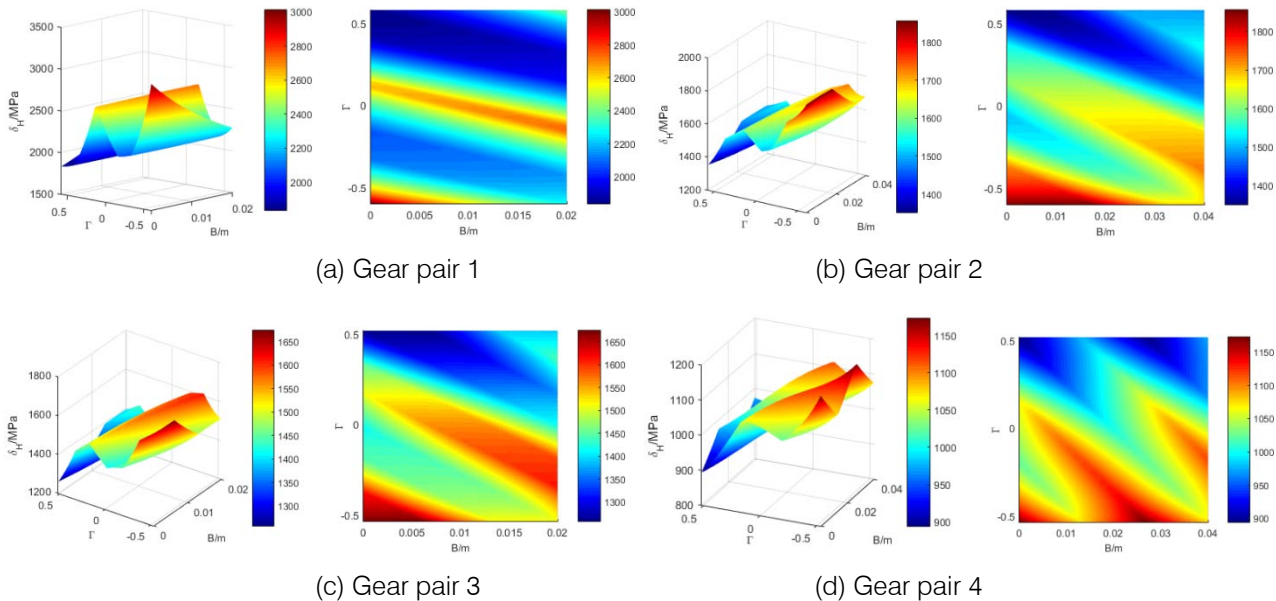


Fig. 13: The contact press of the helical gears

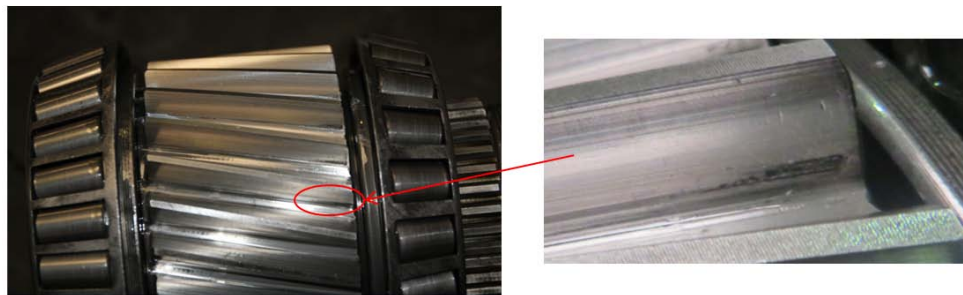


Fig. 14: The fatigue pitting at the meshing point of helical gear

g) *The contact stress with the modification and misalignment*

In practical application, the tooth surface of helical gear needs to be modified. For one reason, the maximum contact press located at the engagement of the pinion root. For the second reason, the shafts, bearings, and the housing will be deformed under the heavy load.

The modification includes the profile modification and helix modification. Profile modification includes profile crowning, pressure angle modification, tip relief, and root relief. The helix modification includes lead crowning, helix angel modification, and end relief. According to the calculation method in Fig.9, the

transmission error(TE), unit-line load distribution, and contact press distribution of helical gear could be obtained. For the four gear pairs in table 1, the modification parameters are shown as table 2.

Table 2: Modification parameters

Modification form	Modification/um
profile crowning(barreling) C_α	10
Lead crowning C_β	10
tip relief	5
End relief	0
Helix angle modification $fH\beta$	0
Pressure angle modification, $fH\alpha$	0

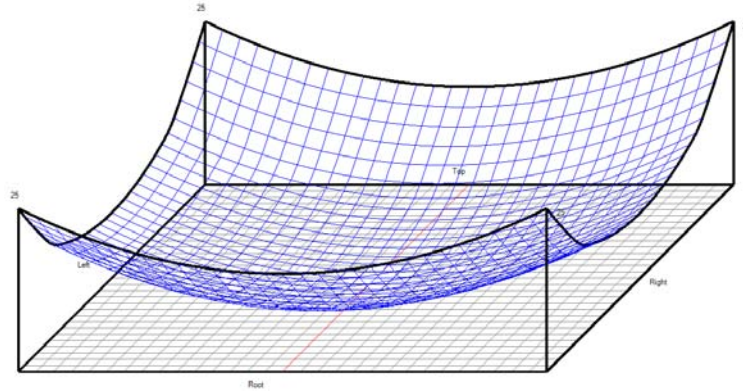


Fig. 15: Modification distribution of contact plane

The modification distribution of the helical gear contact plane is as shown in Fig.15. And the contact press of helical gear is shown in Fig.16. After modification, the contact press distribution of the tooth

surface has been greatly improved. The maximum pressure transferred from the meshing point of the pinion root to the central area of the contact surface.

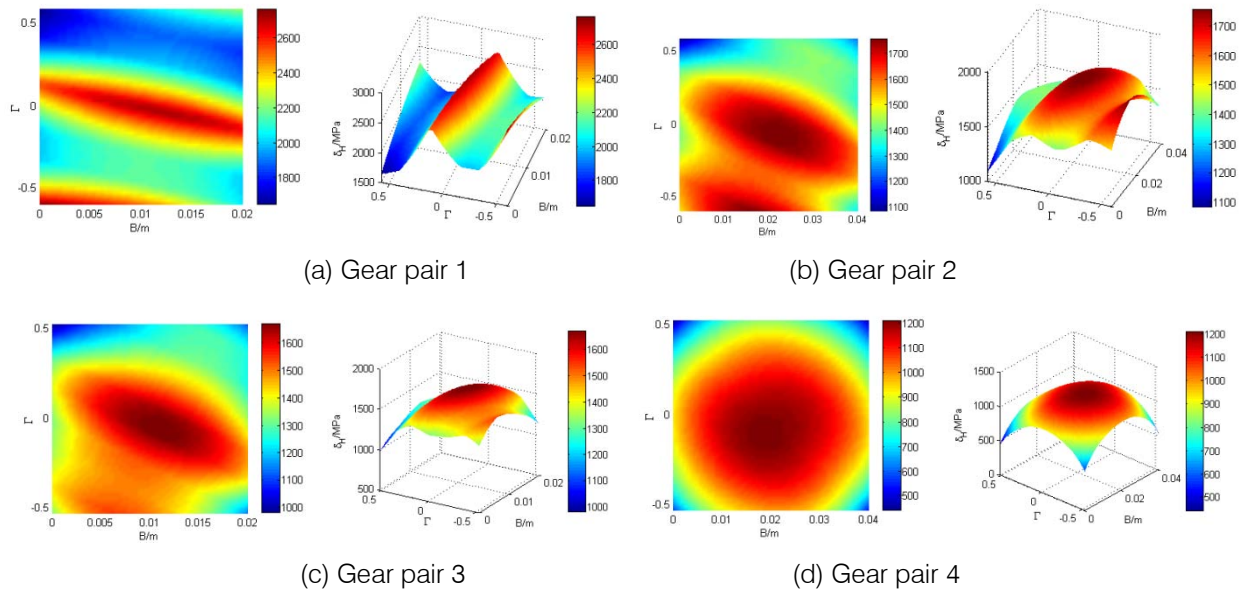


Fig. 16: The contact press of the helical gears with modification

In a transmission system, due to the deformation of the transmission shaft, the machining error of the gearbox, and the changes of the bearing stiffness, the gears pair will operate with misalignment. The contact state with misalignment can be simulated by the helix angle modification. Take gear pair 4 for example, the contact press distribution with different

helix modification is shown in Fig.17. With the increase of tooth inclination deviation, the contact stress inclines to one end, and the maximum stress is also increasing.

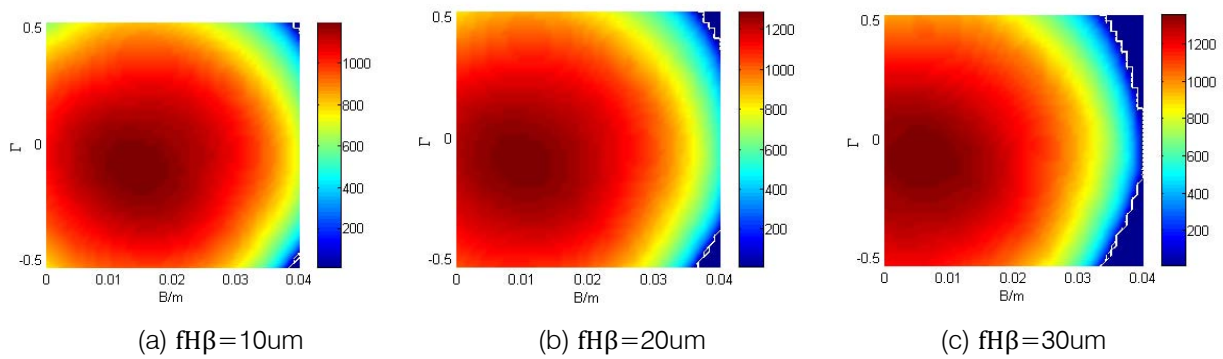


Fig. 17: The contact press distribution with helix modification

h) The feature coordinate system

From the above analysis, all the results in the contact plane were calculated by the numerical method. But in the preliminary design and strength rating process of helical gear, our focus is the maximum stress or the highest contact temperature of the contact plane. For the helical gear, the sliding speed is large in the addendum and dedendum region, and most scuffing

failure occurs in these regions. The sliding speed approximately zero in the region close to the pitch point, so it is safer than the addendum and dedendum region. The 3-dimensional load distribution covers all the information about the contact plane, but it is time-wasting and not intuitionistic. So the feature coordinate system should be established.

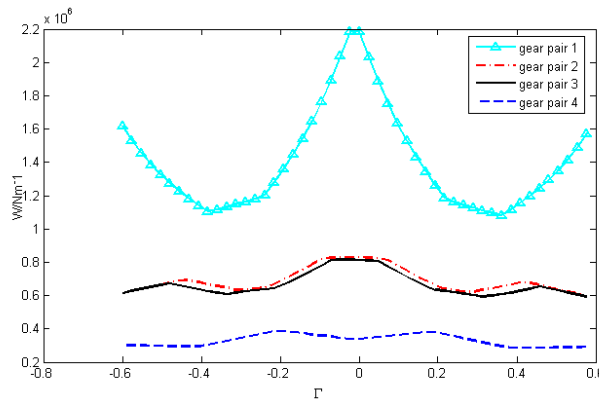


Fig. 18: Unit-linear load and transmission error distribution

In Fig. 3, the line A_1E_2 is recommended as the feature coordinate system, marked by Ψ , defined the same as Γ . The A_1 is the approach point (begin meshing), and E_2 is the recess point. The parameters in feature coordinate cover both the tooth profile and axial information. The unit-line load distribution along with the feature coordinate is shown in Fig.18. Compared the feature coordinate and 3-dimension coordinate, the maximum is the same in the addendum and dedendum region, the value in the feature coordinate system is a little lower than the three-dimension coordinate close to the pitch point, because the dangerous region of helical gear is the addendum and dedendum, so that the feature coordinate can satisfy the need of design and strength rating. Furthermore, the feature coordinate is more succinct than the three-dimension. From the load distribution of gear pair 1 and 3, or gear pair 2 and 4, the helix angle has influenced a lot on the load distribution, in the case, the helix angle from the 9.8 to

20.2, and the maximum load per unit of length from the 3.8×10^5 N/m to 2.7×10^5 , so it is important to choose appropriate helix angle, tooth height, and face width to optimize the load distribution and minimize the dynamic load.

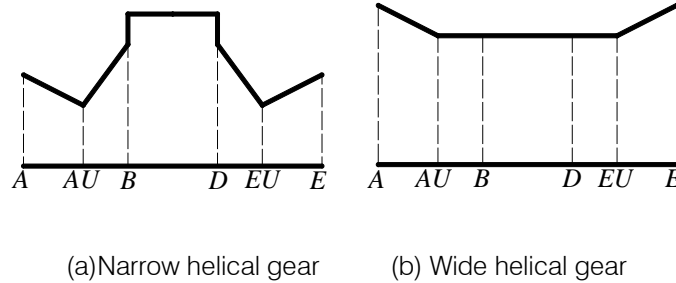


Fig. 19: Load sharing factor for the narrow helical gear and wide helical gear of ISO

In the Ref.10, the load distribution of narrow helical gear is given as the Fig.19, the buttressing effect near the end points A and E of the line of action, compared the results in this paper, the load distribution is similar with the gear pair 1, but is different from the gear pair 2, so the ISO can reflect the characteristic to some extent. Still it can't adapt to all the conditions. In this way, the method proposed by this paper is effective, and the point AU and EU is given by Equ. 15.

$$\Gamma_{AU} - \Gamma_A = \Gamma_E - \Gamma_{EU} = 0.2 \sin \beta_b \quad (15)$$

In the ISO standard theory, the helical gear with the total contact ratio $\varepsilon_\gamma < 2$ was treated similarly to spur gears as well as the buttressing effect. And the wide helical gear ($\varepsilon_\gamma > 2$) was assumed to act near the ends A and E along with the helix teeth over a constant length. From the Fig.6, we know that even though the $\varepsilon_\gamma > 2$, the fluctuation is considerable for some parameters. So the ISO standards are stereotypical and inaccurate.

III. THE THERMAL ELASTOHYDRODYNAMIC LUBRICATION OF HELICAL GEARS

a) The analysis model of the thermal elastohydrodynamic lubrication

When gears pair subjected to heavy loads, the lubricating film may not separate the surfaces adequately, leading to localized damage of the tooth surface. This type of failure is known as scuffing and it is checked by maximum contact temperature and film thickness. Scuffing failure may occur at any stage during the lifetime of a set of gears, and it may lead to failure in a few of hours if the contact temperature is too high. So it is significant to research the scuffing load capacity of the gears.

The high contact temperature is the main reason for scuffing failure, and the interfacial contact temperature conceived as the sum of two components, namely the bulk and flash temperature [10]. The bulk temperature fields are constant with time. Nevertheless, the flash temperature varies with time, and only appears

in the interface of pinion and gear. In the thermal steady state, the bulk temperature of the tooth is higher than the ambient oil temperature.

$$t_B = t_M + t_f \quad (16)$$

Where t_B is the contact temperature, t_M the bulk temperature, and t_f the flash temperature. The bulk temperature can be calculated by the finite element method (FEM). For the pinion of the pair 1, the bulk temperature is 360K (87°C), the ambient oil temperature is 60°C.

The internal energy of oil film will increase due to the compression and viscous damping, and the temperature of oil film and tooth will rise because of the heat convection and conduction. After some time, the whole system will be on a thermal steady state. The bulk temperature of gear was higher than the ambient oil temperature. Therefore, in the inlet zone, the tooth profile is the heat source to heat the lubrication film, and the lubrication film temperature will rise instantly as high as the bulk temperature because that the lubricating film thickness is so thin. Then the temperature of the lubrication film will get higher due to the compression and viscous damping. In this region, the lubricating film is the heat source to heat the gear by convection and conduction. The ambient temperature was chosen as the inlet temperature in the technical literature [16-20]. By this means, the interface temperatures of the inlet contact region solved by the numerical method will lower than the interface bulk temperature; It is not in good agreement with the fact. In this paper, the interface bulk temperature was taken as the inlet temperature, which is more reasonable.

b) The thermal elastohydrodynamic lubrication equations

i. Reynolds equation

For the thermal steady state, the Reynolds equation of helical gear can be expressed in the following form as:

$$\frac{\partial}{\partial x} \left(F_2 \frac{\partial p}{\partial x} \right) = u_2 \frac{\partial(\rho h)}{\partial x} - (u_2 - u_1) \frac{\partial}{\partial x} \left(\frac{\rho F_1}{F_0} \right) \quad (17)$$

Where $F_0 = \int_0^h 1/\eta dz$, $F_1 = \int_0^h z/\eta dz$, $F_2 = \int_0^h \rho \cdot z/\eta(z - F_1/F_0) dz$.

$$\underbrace{\rho \cdot c_p \left(u \frac{\partial t}{\partial x}\right)}_{\text{Convection}} - \underbrace{\lambda \frac{\partial^2 t}{\partial z^2}}_{\text{Heat Conduction}} + \underbrace{\frac{t}{\rho} \frac{\partial \rho}{\partial t} u \left(\frac{\partial p}{\partial x}\right)}_{\text{Compression/Expansion}} = \underbrace{\eta \left(\frac{\partial u}{\partial z}\right)^2}_{\text{Fluid Friction}} \quad (23)$$

The sliding speed of contact point:

$$u_i|_{i=1,2} = \pi \cdot n_i R_i / 30 \quad (18)$$

In this equation, the mass density and the viscosity of lubricant can be described by Dowson and Higginson temperature-pressure-density relationship [21] and Roelands temperature-pressure-viscosity relationship [22] can be expressed as:

$$\rho(p, t) = \rho_0 \left(1 + \frac{0.6 \times 10^{-9} p}{1 + 1.7 \times 10^{-9} p} - 0.00065(t - t_0) \right) \quad (19)$$

$$\eta(p, t) = \eta_0 \exp \left\{ A_1 \left[-1 + (1 + A_2 p)^z \left(\frac{t - 138}{t_0 - 138} \right)^{-s_0} \right] \right\} \quad (20)$$

Where $A_1 = \ln \eta_0 + 9.67$, $A_2 = 5.1 \times 10^{-9}$, $z = \alpha / (A_1 A_2)$, $s_0 = \beta / (A_1 (t_0 - 138))$.

ii. The film thickness is given as

$$h = h_0 + \frac{x^2}{2R} - \frac{4}{\pi E} \int_{x_a}^{x_b} p(x) \ln|x - s| ds \quad (21)$$

Where h_0 is film thickness constant depend on the applied load.

iii. The balanced load equation

The hydrodynamic pressure of the contact region must be in equilibrium with the input load, which calculated by the numerical method in section 2. Thus the pressure equilibrium is expressed by the following equation:

$$w = \int_{x_a}^{x_b} p(x) dx \quad (22)$$

The three-dimensional temperature distribution of oil film was calculated by the energy equation as follows:

The boundary condition for Eq.23 is the thermal interface equation:

$$\begin{cases} t(x, 0) = \frac{\lambda}{\sqrt{\pi \rho_1 c_1 u_1 \lambda_1}} \int_{-\infty}^x \frac{\partial t}{\partial z} \Big|_{z=0} \frac{ds}{\sqrt{x-s}} + t_a \\ t(x, h) = \frac{\lambda}{\sqrt{\pi \rho_2 c_2 u_2 \lambda_2}} \int_{-\infty}^x \frac{\partial t}{\partial z} \Big|_{z=h} \frac{ds}{\sqrt{x-s}} + t_b \end{cases}$$

Where t_a and t_b are the bulk interface temperature of the pinion and gear.

The equation governing the shear stress in the lubricant film is a momentum equation which for the Newtonian fluid is as follow:

$$\frac{\partial p}{\partial x} = \frac{\partial}{\partial z} \left(\eta \frac{\partial u}{\partial z} \right) \quad (24)$$

iv. Numerical method

All equations and boundary conditions mentioned above about thermal were written into dimensionless forms to facilitate the numerical calculation. There are pressure loop and temperature loop in the entire calculation process. In the pressure loop, assuming the temperature of all the nodes is the ambient temperature (360K). In the contact coordinate in the rolling direction (x direction), the whole contact region (from inlet position to outlet position) was divided into 81 non-equidistant nodes; the interval is large in the inlet region and small in the secondary pressure peak region. The distribution of pressure and the film thickness can be calculated by the Newton-Raphson method depending on the Equ.17-24. Divided the film gap (obtained in the pressure loop, z direction) into 21 equidistant nodes. The temperature of all the nodes can be calculated depend on the equ.20-21 and equ.24-25. Then repeat these two processes until the pressure error less than 10^{-5} . The lubricant properties are shown in Table 2.

Table 2: Material properties of the lubricant and gears

Symbol, unit	Value
Ambient viscosity of lubricant, η_0 , Ns/m ²	0.08
Specific heat of lubricant, c , J/kgK	2000
Specific heats of solids, J/kgK	470
Thermal conductivity of lubricant, λ , W/mK	0.14
Thermal conductivities of solids a and b, λ_1 and λ_2 , W/mK	46
Ambient density of lubricant, ρ , kg/m ³	870
Densities of solids a and b, ρ_1 and ρ_2 , kg/m	7850
Barus viscosity-pressure coefficient, α , m ² /N	2.19×10^{-8}
Reynolds viscosity-temperature coefficient, β , K ⁻¹	0.042

IV. THERMAL EHL RESULTS

a) The thermal EHL results of the contact point

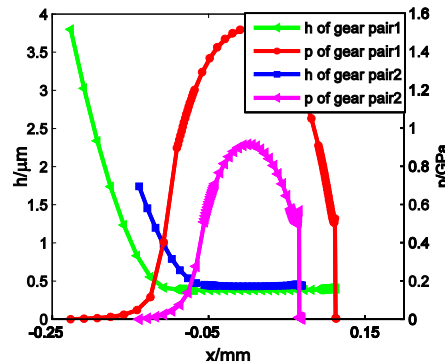


Fig. 20: The pressure and film thickness of oil film

Fig.20 shows the oil pressure and film thickness along the x direction of began meshing point of gear pair one and two. The load per unit of length of gear pair one is 2.73×10^5 N/m, and for gear pair two is 1.02×10^5 N/m shown in Fig.14. For the gear transimission system under heavy load, the film center pressure is higher; in this case, the maximum pressure is as high as 1.51GPa, the minimum film thickness is $0.42 \mu\text{m}$. Because of the heavy load, the curve of oil

pressure and oil thick has't the typical characteristic of thermal EHL. The secondary pressure peak close to the outlet and inconspicuous. The distribution of the pressure is similar to Hertzian pressure distribution. The maximum occurs the location $x=0$ and the heavier of the load, the higher of the maximum. The heavier, the wider the contact zone. Furthermore, it has little influence on the minimum oil thickness.

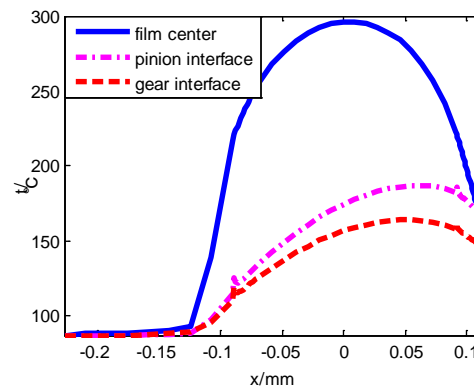
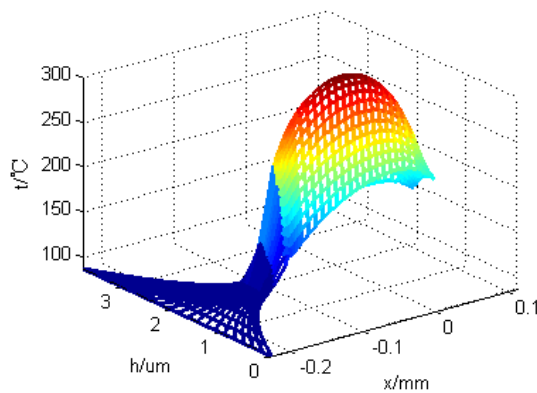


Fig. 21: Three-dimension film temperature and film center and interface temperature of gear pair1

The three-dimension and boundaries temperature distribution of the contact region are shown in Fig.21. The film center temperature is much higher than two boundaries; this is because the heat conducts from the film to all the teeth to maintain the bulk temperature. The distribution of film center temperature is similar to the film center pressure and peaked in the Hertzian maximum, but two boundaries are different from the film center; the temperature increase until close to the outlet and slightly decrease. The reason is in the rear part of the contact zone, the compression effect is no longer generate the heat, so the heat from the film center to the two boundaries via conduction effect and to the inner tooth through convection.

b) Comparison with the Blok's flash temperature

The contact and flash temperature is the main reason for the gear scuffing failure, Blok derived the flash temperature equation in 1937[12] as follow:

$$t_f = 0.7858 \frac{fw|u_1 - u_2|}{(\sqrt{\lambda_1 \rho_1 c_1 u_1} + \sqrt{\lambda_2 \rho_2 c_2 u_2}) \sqrt{b_0}} \quad (25)$$

Where $f=0.06$ is coefficient of friction, w the load per unit of length, $\lambda_i, \rho_i, c_i, u_i$ the heat conduction coefficient, density, specific heat, sliding speed of the pinion and gear, b_0 the half-width of Hertzian line contact.

In the thermal EHL results, the maximum temperature rise of two boundaries is its flash temperature. The flash temperature along the feature coordinate was calculated by the thermal EHL method and Blok equation as show in Fig.22. In the dedendum region of the pinion (close to approach point), the thermal EHL flash temperature is higher than the Blok result, and in the addendum region of the pinion(close to recess point), the Blok temperature is lower than thermal EHL flash temperature. In theory, the temperature-pressure-density and temperature-pressure-viscosity effect and the compression of oil film were considered in the thermal EHL theory. The Blok flash temperature equation is very concise and

corresponding to the experiment to some extent. However, it loses sight of the influence of the bulk temperature, so it is not a good agreement of the experiment under the heavy load. Thus the thermal EHL theory is even close to the actual condition. The safety factor defined as follow [10]:

$$S = \frac{t_s - t_{oil}}{t_{c_{max}} - t_{oil}} \quad (26)$$

Where t_s is the scuffing temperature, t_{oil} the ambient temperature, $t_{c_{max}}$ the maximum contact temperature.

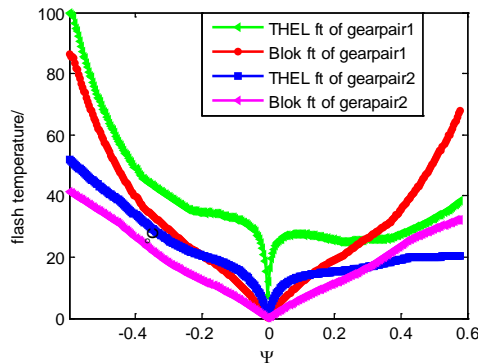


Fig. 22: The TEHL flash temperature and Blok flash temperature of the helical gear in the feature coordinate

c) The minimum thickness method from thermal EHL and Dowson equation

When gear teeth are separated completely by a full fluid film of lubricant, there is no contact between the asperities of tooth surfaces, and usually, there is no scuffing and wear. For the heavy load helical gear, the thickness of oil film is very small, and incidental asperity contact takes place. As the minimum film thickness decreases, the number of contacts increases, abrasive wear, adhesive wear, and scuffing became possible. So the minimum thickness of lubricant film is a property of scuffing load capacity, especially for the gear pair under

heavy load. The minimum thickness equation was given by Dowson and Higginson [22] as the Equ.27. The safe factor can be measured by the thickness ratio. When the thickness ratio $\chi < 1.4$, it is considered as mixed friction. When the thickness ratio is less than 1, the scuffing failure probably takes place to a great extent.

$$h_{min} = \frac{2.65\alpha^{0.54} (\eta_0 u_m)^{0.7} R^{0.43}}{E^{0.03} w^{0.13}} \quad (27)$$

$$\chi = h_{min} / \sqrt{R_{a1}^2 + R_{a2}^2} \quad (28)$$

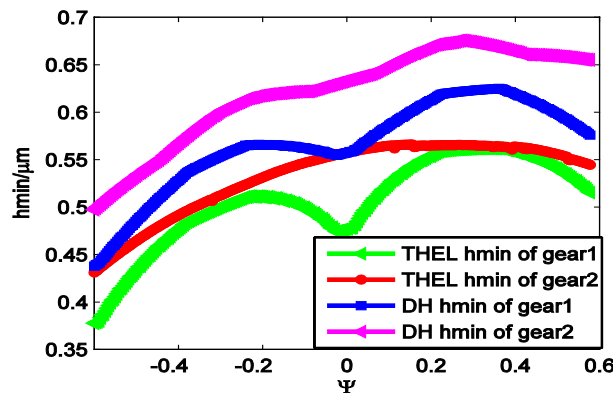


Fig. 23: The minimum thickness of the film in the feature coordinate system

The minimum film thickness solved by thermal EHL and Dowson equation is shown as Fig.23. The minimum thickness curves are similar along the feature coordinate of gear pair one and two. The minimum film thickness is lowest in the dedendum of the pinion, so the dedendum of the pinion is dangerous. The results are consistent with the maximum flash temperature method. The value from thermal EHL is lower than that from the Dowson equation. The Dowson equation didn't consider the influence of temperature on film thickness.

In contrast to the fatigue damage, a single momentary overload may initiate scuffing failure, so the scuffing capacity is crucial for the heavy load and high-speed helical gear system. The minimum film thickness and maximum contact temperature, as well as the flash temperature obtained by the thermal EHL theory, are applied to check the scuffing strength. The scuffing capacity can be checked by the flash temperature or minimum thickness method.

V. CONCLUSIONS

In this paper, a model of non-uniform along the contact line of helical gear teeth, obtained from the meshing stiffness, transmission error, and balanced load equation, has been proposed. The feature coordinate system was established to simply preliminary design and strength rating process. The thermal effect of helical gear lubrication will affect the scuffing load capacity. The thermal EHL method is applied to check the scuffing load capacity.

The following conclusions can be drawn:

1. The length of contact lines depends on the face width and basic helix angle. And the length is not parallel with the axial line. The fluctuation is evident when the total contact ratio less than 2. The distribution of transmission error is similar to the sum length. The distribution of load per unit of length is dependent on the meshing stiffness and transmission, it is similar to the meshing stiffness along the contact line and similar to the transmission error along the *B*-axis. The modification of gears can greatly improve the distribution of contact stress. The maximum contact stress is concentrated in the center of the tooth surface to avoid the contact between the tooth surface. The contact stress inclines to one end, and the maximum stress is also increasing under with misalignment.
2. The feature coordinate system established in this paper can cover both the tooth profile and axial information. It can satisfy the need for preliminary design and strength check of helical gears. The weakest strength region is the dedendum of the pinion. A load of the dedendum region in the feature coordinate system is as same as the three-dimension coordinates system.

3. The thermal EHL theory can provide more information to check the scuffing load capacity. The highest contact temperature and minimum film thickness method were applied to evaluate the scuffing load capacity. The pressure distribution under heavy load is similar to the Hertzian pressure distribution, and the secondary pressure peak close the outlet and inconspicuous. The temperature of the film center is much higher than two boundaries. The film center temperature distribution is similar to the pressure distribution. The two boundaries temperature increase until close to the outlet and slightly decrease. The thermal EHL flash temperature is corresponding to the Blok flash temperature but higher in the dedendum region and lower in the addendum region of the pinion. The minimum thickness film is smaller than the Dowson equation. So the scuffing load capacity that solved by thermal EHL is more practical than the traditional method.

REFERENCES RÉFÉRENCES REFERENCIAS

1. ISO Standard 6336-2:1996, Calculation of Load Capacity of Spur and Helical Gears – Part 2: Calculation of Surface Durability (Pitting), International Organization for Standardization, Geneva, Switzerland, 1996.
2. ISO Standard 6336-3:1996, Calculation of Load Capacity of Spur and Helical Gears – Part 3: Calculation of Tooth Bending Strength, International Organization for Standardization, Geneva, Switzerland, 1996.
3. Zaigang Chen, Yimin Shao. Mesh stiffness calculation of a spur gear pair with tooth profile modification and tooth root crack. *Mechanism and Machine Theory*, 62(2013)63-74.
4. A. Fernandez del Rincon, F. Viadero, M. Iglesias, et al. A model for the study of meshing stiffness in spur gear transmissions. *Mechanism and Machine Theory*, 61(2013)30-58.
5. Y. Zhang, Z. Fang. Analysis of tooth contact and load distribution of helical gears with crossed axes. *Mechanism and Machine Theory*. 34(1999)41-57.
6. I Yesilyurt, FS Gu, Andrew D. Ball. Gear tooth stiffness reduction measurement using modal analysis and its use in wear fault severity assessment of spur gears. *NDT&E International*. 36(2003)357-372.
7. J.I.Pedrero, M.Pleguezuelos, M.Artés, J.A.Antona, Load distribution model along the line of contact for involute external gears, *Mechanism and Machine Theory* 45 (2010)780-794.
8. J.I.Pedrero, M.Pleguezuelos, M.Muñoz. Critical stress and load conditions for bending calculations of spur and helical gear, *International Journal of Fatigue* 48 (2013)28-38.

9. J.I. Pedrero, M.Pleguezuelos, M.Muñoz. Critical stress and load conditions for pitting calculations of spur and helical gear, *Mechanism and Machine Theory* 46(2011)425-437.
10. ISO Standard 13989-1:2000, Calculation of scuffing load capacity of cylindrical, bevel and hypoid gears-Part 1: Flash temperature method. British Standards Institution, London, 2000.The United Kingdom.
11. ISO Standard 13989-2:2000, Calculation of scuffing load capacity of cylindrical, bevel and hypoid gears-Part 1: Integral temperature method. British Standards Institution, London, 2000.The United Kingdom.
12. H.Blok. Theoretical study of temperature rise at surfaces of actual contact under oiliness lubricating conditions, in *Proceedings of the General Discussion on Lubrication and Lubricants*[J]. *Imech E*, 2(1937)222–235.
13. Wang KL, Cheng HS. A numerical solution to the dynamic load, film thickness and surface temperatures in spur gears, part I analysis. *Journal of Mechanical Design*. 103(1981)177–187.
14. Wang KL, Cheng HS. A Numerical solution to the dynamic load, film thickness and surface temperatures in spur gears, part II results. *Journal of Mechanical Design*.103 (1981)188–194.
15. Li-Ming Chu, Hsiang-Chen Hsu, Jaw-Ren Lin, dtal. Inverse approach for calculating temperature in EHL of line contacts. *Tribology International*. 42 (2009)1154-1162.
16. T.Almqvist, R. Larsson. The Navier–Stokes approach for thermal EHL line contact solutions. *Tribology International*. 35(2002)163-170.
17. P. Anuradha, Punit Kumar. Effect of lubricant selection on EHL performance of involute spur gears. *Tribology International*. 50 (2012)82-90.
18. Lars Bobach, Ronny Beilicke, Dirk Bartel, et al. Thermal elastohydrodynamic simulation of involute spur gears incorporating mixed friction. *Tribology International*, 48 (2012)191-206.
19. P.W. Wang, H.Q. Li, J.W. Tong, et al. Transient thermo elastohydrodynamic lubrication analysis, *Tribology International*, 37(2004)773-782.
20. Ping Yang, Peiran Yang. Analysis on the thermal elastohydrodynamic lubrication of tapered rollers in opposite orientation. *Tribology International*, 40(2007)1627-1637.
21. Roelands CJA. Correlation aspects of Viscosity-temperature-pressure Relationship of Lubrication oils. Delft Univeristy of Technology, Netherlands, 1966.
22. Dowson D, Higginson GR. *Elastohydrodynamic Lubrication*. Oxford: Pergamon Press, 1977.

This page is intentionally left blank



GLOBAL JOURNAL OF RESEARCHES IN ENGINEERING: A
MECHANICAL AND MECHANICS ENGINEERING
Volume 20 Issue 1 Version 1.0 Year 2020
Type: Double Blind Peer Reviewed International Research Journal
Publisher: Global Journals
Online ISSN: 2249-4596 & Print ISSN: 0975-5861

Wheel Tooth Profiles of Hydraulic Machines and Mechanical Gears: Traditions and Innovations

By D.F. Baldenko & F.D. Baldenko

Russian State University

Abstract- An analysis of the advantages and disadvantages of the most common types of gears in practice, technical requirements and technological capabilities in their design and manufacture at the present stage of development shows that developments in the field of creating gears with unconventional tooth profiles are relevant. The technical solution proposed in the article refers to cylindrical gears of external and internal gearing, the shape of the teeth of the wheels of which is formed as the envelope of the original contour of the rack, and the number of teeth are assigned depending on the purpose of the mechanism, the required gear ratio and the diametric dimensions. Such mechanisms are used in various branches of mechanical engineering in the form of gear wheels of gearboxes, winches, planetary and wave gears, and also as working bodies of pumps, hydraulic motors, compressors and internal combustion engines with straight and helical teeth.

Keywords: *cycloidal gearing, gear, harmonic profile, involute gearing, main circle, number of teeth, rack, running-in, tooth profile.*

GJRE-A Classification: *FOR Code: 091399p*



Strictly as per the compliance and regulations of:



© 2020. D.F. Baldenko & F.D. Baldenko. This is a research/review paper, distributed under the terms of the Creative Commons Attribution-Noncommercial 3.0 Unported License (<http://creativecommons.org/licenses/by-nc/3.0/>), permitting all non commercial use, distribution, and reproduction in any medium, provided the original work is properly cited.

Wheel Tooth Profiles of Hydraulic Machines and Mechanical Gears: Traditions and Innovations

D.F. Baldenko^α & F.D. Baldenko^σ

Abstract- An analysis of the advantages and disadvantages of the most common types of gears in practice, technical requirements and technological capabilities in their design and manufacture at the present stage of development shows that developments in the field of creating gears with unconventional tooth profiles are relevant. The technical solution proposed in the article refers to cylindrical gears of external and internal gearing, the shape of the teeth of the wheels of which is formed as the envelope of the original contour of the rack, and the number of teeth are assigned depending on the purpose of the mechanism, the required gear ratio and the diametric dimensions. Such mechanisms are used in various branches of mechanical engineering in the form of gear wheels of gearboxes, winches, planetary and wave gears, and also as working bodies of pumps, hydraulic motors, compressors and internal combustion engines with straight and helical teeth.

Keywords: cycloidal gearing, gear, harmonic profile, involute gearing, main circle, number of teeth, rack, running-in, tooth profile.

I. INTRODUCTION

Gears as one of the main structural elements of various mechanisms and machines are known since ancient times, and gearing theory is one of the fundamental applied branches of physical and mathematical science and general engineering. The modern stage of the development of the theory and practice of gearing, based on the use of innovative computer technologies and three-dimensional modeling, allows us to solve new problems, including the development of non-traditional types of gears with optimized geometrical parameters of the teeth. To date, three main types of cylindrical gears of external and internal gearing, differing in the profile of the teeth and the technology of their manufacture, have received wide industrial application [1-3]:

- Involute;
- Cycloidal (including pinworms);
- With circular teeth (Novikov gearing).

Among the variety of gear mechanisms from a technological point of view, it is possible to distinguish involute and cycloidal gears, the face profile of the wheels of which is formed by the method of running-in the tool rack around the main circle.

Profiling from the rack is the most common and universal way to build a profile of the teeth, and in the case of a displacement of the rack relative to the main circumference, this allows you to correct the shape of the teeth, achieving optimal gearing for various operating conditions.

Wheels with an involute tooth profile - the most common in mechanical engineering - have significant technological and operational advantages compared to other types of gears [2]: a simple tool for cutting teeth; a constant position of the general normal to the profiles of the mating teeth, which reduces dynamic loads; insensitivity to a small change in center distance. At present, involute gearing is the basis for the development of the majority of transmission devices for mechanisms and machines of all industries and agriculture, and the theory is most fully developed in relation to this type of gearing [1].

The classical involute tooth profile of mechanical gear wheels and working bodies of volumetric pumps is formed as the envelope of the initial contour of the gear rack, which is an isosceles trapezoid with an angle of 20° and is generally displaced relative to the generating straight and main circle [2]. Currently, the vast majority of cylindrical gears for various purposes have a profile of the side faces of the teeth, built on the basis of standard or partially modified involute engagement.

At the same time, despite the large number of positive operational and technological qualities of involute tooth profiles, one of their significant drawbacks is the tendency to undercuts and self-intersections with small numbers of gear teeth (as is known, for an involute profile without displacement $z_{\min} = 17$, Fig. 1), which reduces the efficiency and scope of involute gears, increases their weight and size and cost indicators, and also limits the ability to design the working bodies of rotary machines. In addition, the convex contact of the surfaces in the case of external gearing of the wheels increases the contact stress and reduces the bearing capacity of the transmission.

Author ^α: Russian Scientific Research Institute of Drilling Techniques.
e-mail: fbaldenko@mail.ru

Author ^σ: Russian State University of Oil and Gas named after Gubkin.

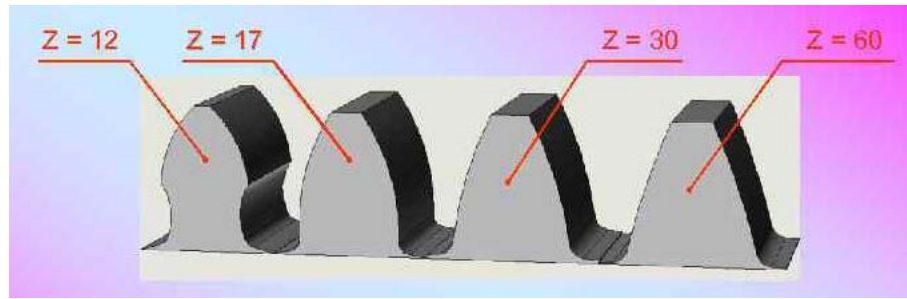


Fig. 1: The influence of the number of teeth on the shape of the profile of an involute tooth

Wheels with a cycloidal tooth profile are characterized by a smooth contour, the possibility of gearing with a minimum number of teeth (including single and double gears) without the risk of trimming the profile and creating gears of internal gearing of the wheels with the number of teeth differing by one (which is used in planetary gearboxes and rotary hydraulic working bodies machines, compressors and ICE). The cycloidal profile has the widest range of tooth shape changes, which allows the development of mechanical gears with almost any necessary combination of tooth numbers and the curvature of the mating wheels. When using cycloidal gearing, it becomes possible to create low-tooth profiles of the same sign of curvature (round, oval, triangular with curved faces), which is required for the development of highly efficient rotary machines. The initial cycloidal profile related to the outer or inner element of the gear pair is formed from a shortened hypo- and epicycloid; their equidistant as well as the envelope of a cycloidal rack [4].

An extracentroid profile formed from a shortened cycloidal curve (when the producing point is not located on a rolling circle) is most widely used in mechanical engineering.

An equidistant profile, which is characterized by a smooth contour and a continuous change in the position of the contact point on the mating surfaces of the stator and rotor (a combination of sliding and rolling), has found widespread application in working bodies of single-screw pumps and hydraulic motors (Fig. 2).

According to the ratio of the number of teeth (lobes), cycloidal mechanisms are distinguished with arbitrary numbers of teeth of the wheels and with the numbers of teeth differing by one

Option $|z_1 - z_2| = 1$ for internal gearing is used in two cases: 1) in planetary gearboxes, which ensures maximum gear ratio and load distribution at the same time over several pairs of mating gear teeth; 2) in the working bodies of rotary volumetric machines in order to form isolated working chambers, hermetically separated from the entrance and exit.

According to the arrangement of profiles with internal gearing, the number of teeth of which differ by

one, schemes can be applied in which a wheel with a smaller number of teeth is an internal or external element.

The choice of one of these schemes for a given initial profile (epi- or hypo) is determined by the design requirements of the designed machine and depends on the method of constructing the conjugate profile (as an internal or external envelope) and the ratio of the radii of the initial circles (centroid) of the initial and conjugate profiles.

An option when a larger number of teeth falls on the stator profile is characteristic of the working bodies screw pumps (kinematic ratio 1:2) and hydraulic motors (3:4 ... 9:10) with equidistant engagement (Fig. 2), while the option where the stator has one less number of teeth than the inside its rotor belongs to the well-known schemes of internal combustion engines and compressors with eccentric non-equidistant gearing and a kinematic ratio of 3:2 and 2:1 (Fig. 3).

The relative movements of the conjugate cycloidal tooth profiles distinguish between mechanisms: with variable touch conditions (when the contact point moves along both the original and the conjugate profile), with partially variable contact conditions along only one of the profiles (for example, along the stator), while the mating profile is engaged at one constant point.

Variable contact conditions of the profiles are characteristic for the engagement of equidistant cycloidal mechanisms (when both rolling speeds along the conjugate profiles are not equal to zero). The constant contact conditions of one of the profiles relate to the case of engagement of profiles formed directly from hypo- or epicycloids without equidistant procedures.

Provided that one of the profiles is constantly touched, it is possible to create a local seal assembly (moving at the profile point of the inner element) or fixed (at the profile point of the outer element), depending on the mechanism scheme, respectively, on the surface of the rotor or stator.

Examples of cycloidal mechanisms with constant conditions of contact of one of the profiles (Fig. 3) are the Wankel engine and rotary compressor

(constant contact of the tips of the protrusions of the teeth of the rotor), as well as a gas engine with constant contact of the tips of the protrusions of the teeth of the three-lobe stator.

The cycloidal tooth profile has been widely used in the oil and gas industry in the development of single-screw hydraulic machines with an elastic stator lining (pumps for oil production and downhole hydraulic motors for drilling wells), the working body of which is a screw gerotor mechanism with *internal* equidistant cycloidal gearing (Fig. 2).

For multi-lobe screw gerotor mechanisms ($z_2 \geq 2$), the conjugated end profiles of the helical surfaces of the stator and rotor are formed by the method of rolling in a cycloidal rack, the initial contour of which was proposed at the Perm branch of the All-Union Scientific Research Institute of Drilling Techniques [5]. In the general case, for a given contour diameter of the gerotor mechanism, the shape of the cycloidal profile is

determined by a combination of five dimensionless geometric parameters (gear ratio, gearing coefficients (epi or hypo), eccentricity, tooth shape, and rack displacement), which complicates the manufacturing technology (due to the need to perform equidistant procedures for the contour of the rack) and the choice of the optimal shape of the profiles described by complex mathematical expressions, depending on the combination of the five above dimensionless parameters.

External cycloidal gearing can be used in mechanical gears and working bodies of pumps and compressors, since it allows to obtain a large gear ratio in one stage due to the absence of restrictions on the number of teeth up to before using a single-tooth gear (the cross-section of which is a circle with a displaced center as in the classical and tested Moineau pump scheme, Fig. 2a), which was used by Russian engineers (Tomsk University) in eccentric-cycloidal gearing [6].

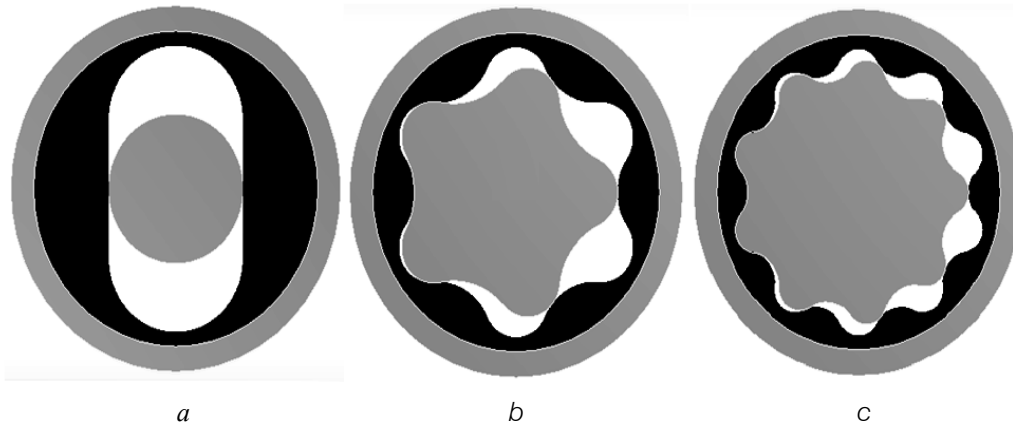


Fig. 2: Cross-sections of single-screw hydraulic machines with equidistant hypocycloidal profile and different kinematic relation [4]:

$a - 1:2$; $b - 5:6$; $c - 9:10$

Cycloidal gearing in various oil field mechanisms (cylindrical gears of draw works and mud pumps, top drive systems of drilling rigs and sucker-rod pumps, beam pumping units; rack and pinion lifts; planetary gears) can provide the following operational advantages in the future: reduced number the teeth of the driving gear ($z = 1 \div 6$) and, as a result, the minimum weight and size indicators and increased gear ratios; preferential rolling of profiles in the vicinity of the pole with slight slip; rational conjugation conditions (convex-concave contact in many phases of engagement); high efficiency; reduced vibration; improved technological capabilities in the manufacture and hardening of wheels. Calculations show the real possibility of creating a cycloidal planetary gearbox with a gear ratio of $i = 6 \div 16$ (Fig. 4) [7], which significantly exceeds the capabilities of a similar scheme with traditional gearing (involute or Novikov gearing) and gives a new impetus to the development of highly efficient gear turbodrills and borehole pumps for oil production. An interesting feature

of the presented scheme of the cycloidal planetary gearbox is also the fact that the number of teeth of all wheels is simultaneously a multiple of 2 and 3.

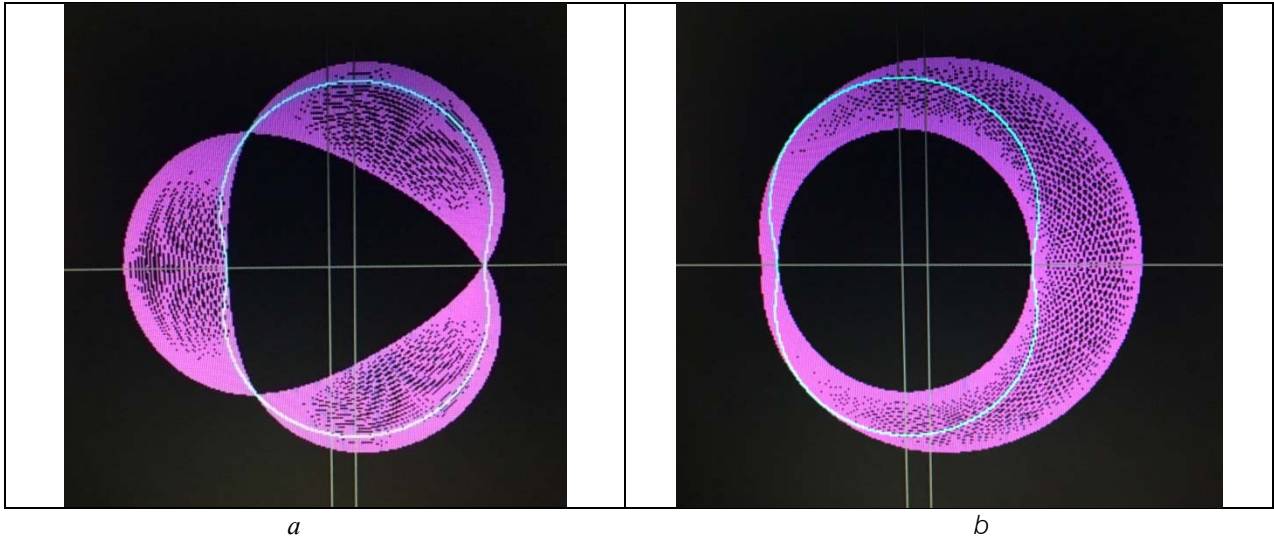


Fig. 3: Non-equidistant (skeletal) profiles of the working bodies of rotary machines, formed during the running-in of two-way shortened epicycloid:

a – on an external centroid; b – on the internal centroid

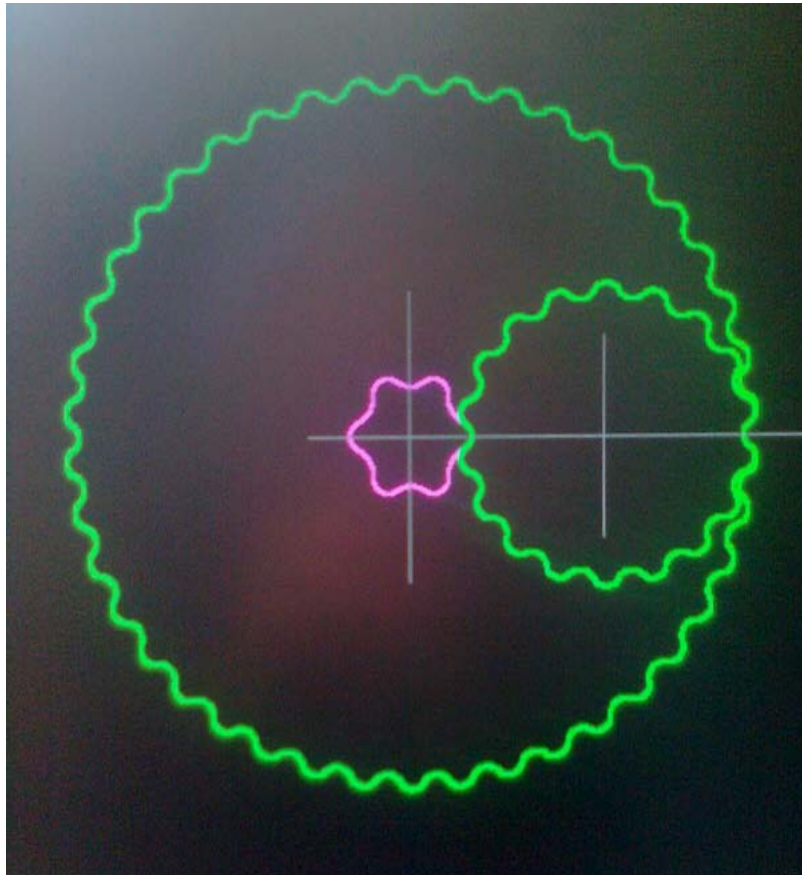


Fig. 4: Cycloidal planetary reducer according to the scheme 6-18-42 ($i = 8$):

— hypocycloidal wheel; — epicycloidal wheel

Improving the shape of traditional wheels and developing new types of gears is attracting more and more attention due to the influence of gear mechanisms on the basic technical characteristics of machines, as

well as the general scientific and technological progress, the development of materials science, machine tool building and digital technologies.

Great prospects for improving involute and cycloidal transmissions open when modifying their nominal end profiles. There are various schemes for modifying external and internal gearing associated with high-altitude and longitudinal teeth correction, transition to an asymmetric profile shape [2, 4, 8], which allows to improve the characteristics of a rotary machine, as well as increase the load capacity, efficiency and durability of mechanical transmission. For cycloidal working bodies of down hole hydraulic motors with the execution of the teeth of one of the wheels (stator) of elastic material, the modification of gearing can be carried out proceeding from the conditions of rational redistribution of elastomer deformation and reduction of mechanical losses in the pole tooth zone due to the effect of a hydrodynamic wedge.

Among the unconventional types of gears that have appeared recently in the technical literature and patent fund, innovative wheel designs can be noted: 1) with a non-involute tooth profile, the curvature of which varies according to a certain law depending on the slip in the mate [9]; 2) with a radius profile of the teeth, consisting of tangent arcs of the circumferences of the heads and legs with their centers on the pitch circle [10]; 3) with an engagement line made in the form of a lemniscate [11]. The inventors of these inventions substantiate the technical and technological advantages

of their geometry in comparison with the involute profile and indicate the areas of possible use of gears.

This article proposes a new alternative type of gearing [12], characterized in that the initial contour of the rack is made in the form of a harmonic curve (sinusoid or cosine wave), displaced in general relative to the producing straight line, and the end profile of the gear teeth is formed as an envelope families of harmonic curves when they are run in the main circle of a certain radius, selected depending on the required number of teeth of the wheel. At the same time, the number of wheel teeth can take on any value, starting from one, which creates the premise of expanding the kinematic capabilities of the gear mechanism and obtaining a high ratio in one stage.

The main difference and advantage of the harmonic curve over the cycloid is its smoothness, which does not require the execution of equidistance procedures and makes it possible to use the harmonic itself directly as the initial loop contour, rolled around the main circle of radius r_z . Thus, when the end profile is formed from a harmonic rack, similar to the case of involute gearing, a transition is made from a three-stage scheme (rack - equidistant of the rack - offset equidistant) to a two-stage scheme (rack - the offset rack), in which the initial contour of the rack I coincides with the original circuit II (Fig. 5).

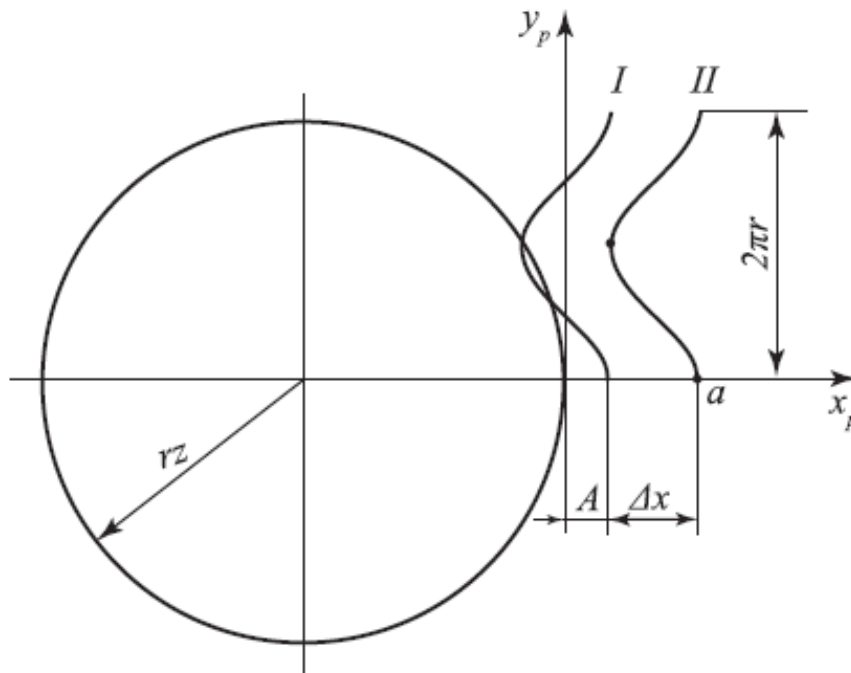


Fig. 5: The initial position of the rack during the formation of a harmonic profile

The coordinates of the initial contour of the harmonic rack relative to the generating line (tool axes x_p, y_p) can be represented in the form:

$$x_p = x_0 + \Delta x$$

$$y_p = y_0, \tag{1}$$

where x_0, y_0 are the initial coordinates of the harmonic I symmetrically located relative to the generating line; Δx

is the displacement of the initial rack contour relative to the generating line.

If we use the cosine wave as a harmonic (Fig. 5), then

$$\begin{aligned} x_o &= -uA\cos\psi \\ y_o &= r\psi, \end{aligned} \tag{2}$$

where ψ is the angular parameter varying from 0 to 2π ; r is the radius of the unit circle; A – harmonic amplitude equal to half the height rack; u is a profile type coefficient: $u = 1$ when forming an epigarmonic profile (from a positive cosine, when the protrusion of the rack is directed from the center of the main circle), $u = -1$ when forming a hypogarmonic profile (from a negative cosine, when the protrusion of the rack is directed to the center main circle, Fig. 5).

In Fig. 6 shows the current positions of the rods during the formation of epi- and hypogarmonic profiles using the positive and negative cosine waves, respectively. The difference between the families of these curves from the point of view of the initial position of the staff consists in the location of the point corresponding to the maximum diameter of the profile:

in the case of the formation of a hypogarmonic profile, this point (a, Fig. 5) is located on the x_p axis at the beginning of the angular pitch of the staff ($\psi = 0$), while during the formation of the epigarmonic profile, a similar point will be located in the middle of the angular step ($\psi = \pi$).

In the current position, when running along the main circle, the generating line and the rail connected with it are rotated through the angle φ_p . Since running without slip, the family of curves of the rack is described by the following parametric equations:

$$\begin{aligned} X &= (x_p + rz)\cos\varphi_p - (y_p - rz\varphi_p)\sin\varphi_p \\ Y &= (x_p + rz)\sin\varphi_p + (y_p - rz\varphi_p)\cos\varphi_p. \end{aligned} \tag{3}$$

The harmonic gear profile is the inner envelope of the family of run-in racks (Fig. 6). To go from (3) to the envelope equation it is necessary to establish the relationship between ψ and φ_p . Her can be obtained through general geometric constructions, given that the normal to the envelope passes through the pole - the point of contact of the generating line and the main circle.

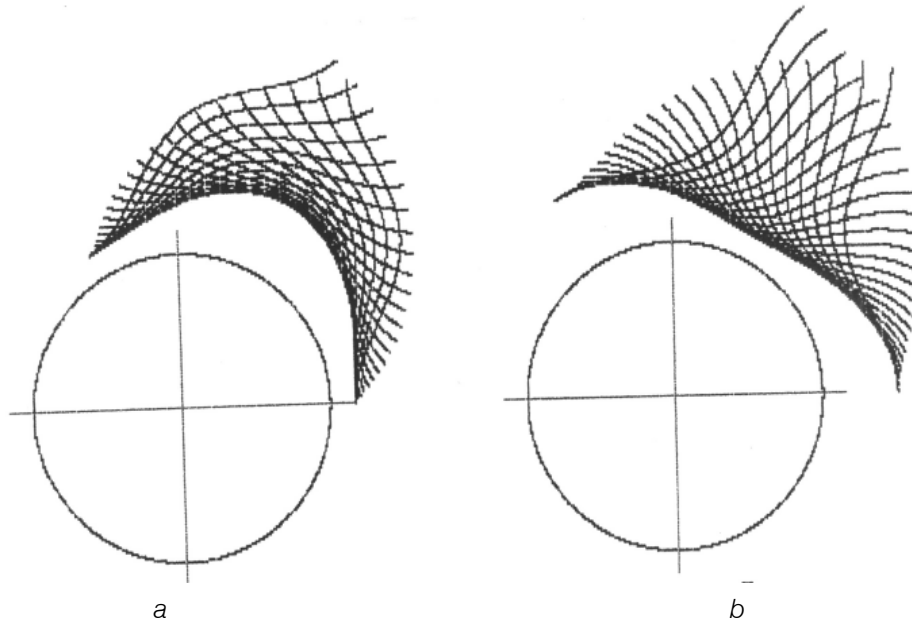


Fig. 6: The scheme of formation of one branch of a harmonic profile ($\varphi_p = 2\pi/z$) according to the method of running-in a rack ($z = 3$):

a - epigarmonic; b - hypogarmonic

A distinctive feature of a closed harmonic profile is the independence of its shape from the pattern of formation: epi- and hypogarmonic profiles are identical (phase-shifted by an angle π/z). Therefore, in contrast to the cycloidal one, such a profile can be called the general term “harmonic”, without specifying from which

curve (sine or cosine) the rail is formed and without adding an epi- or hypo prefix.

The average diameter D_a of the harmonic profile (in the pitch circle of the teeth) does not depend on the harmonic amplitude, and the height of the teeth h – from the rack offset:

$$D_a = 2(rz + \Delta x). \quad (4)$$

$$h = 2A. \quad (5)$$

- displacement coefficient of the original rack contour

$$c_\Delta = \Delta x / r.$$

The choice of the numerical values of these dimensionless geometric parameters depends on the type and required characteristics of the gear pair.

Gears with a harmonious tooth profile (Fig. 7, 8) can be used in various mechanisms of external and internal gearing with parallel axes.

The shape of the harmonic end profiles of a pair of gears engaged in meshing (the initial one is index 1 and the conjugate one is index 2) is completely determined by a combination of three dimensionless geometric parameters:

- gear ratio $i = z_2 : z_1$;
- harmonic shape coefficient $c_A = A / r$;

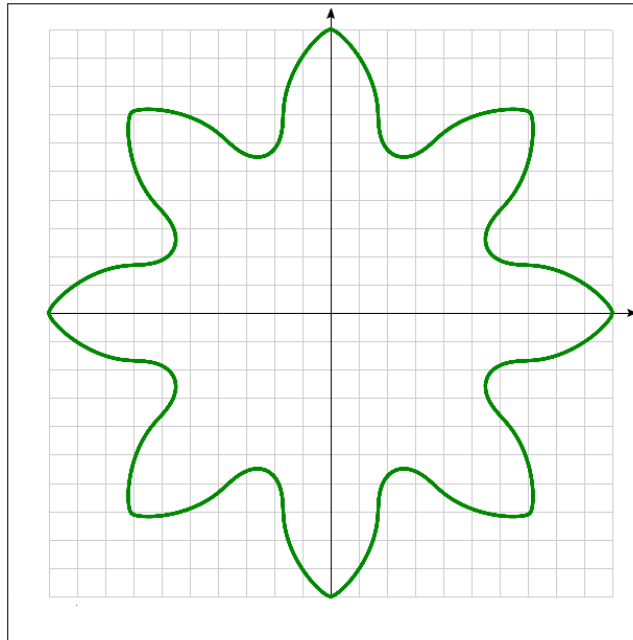


Fig. 7: Gear with nominal harmonic profile ($z = 8$; $c_A = 2$; $c_\Delta = 0$)

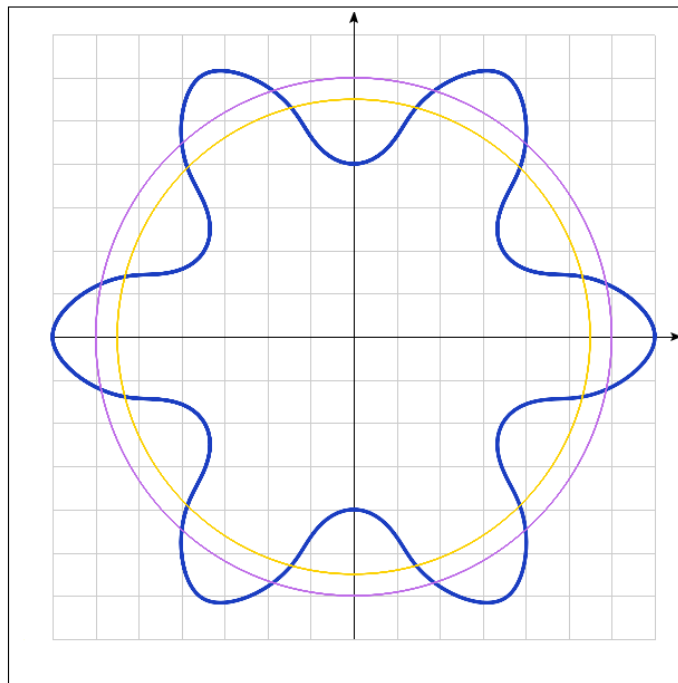


Fig. 8: Gear with a shifted harmonic profile ($z = 6$; $c_A = 1,5$; $c_\Delta = -0,5$) and drawing the main and dividing circles

In the general case, when the initial harmonic profile of the wheel is selected by the z_1 tooth (the construction scheme of which is shown in Figs. 5 and 6), the conjugate profile of the second wheel is formed as the envelope of the initial profile during the running-in of the initial circles of the wheels, the ratio of the radii of which corresponds to gear ratio z_2/z_1 .

In practice, when constructing a mating profile, you can use the simplified method in which the mating profile is performed similarly to the initial one by the method of running from the general contour of the rack

[4]. In relation to the proposed gearing, this means that when the profiles of the mating wheels are formed, the harmonic shape remains unchanged ($A_1=A_2=A$), and only the magnitude of the rack shift ($\Delta x_1; \Delta x_2$) changes [12].

As an example in Fig. 9 shows an embodiment of a gear pair of external harmonic gearing without bias with a ratio of 7:25 in the characteristic gearing phase corresponding to the contact of the tooth protrusion of the driving gear with the tooth cavity of the driven wheel.

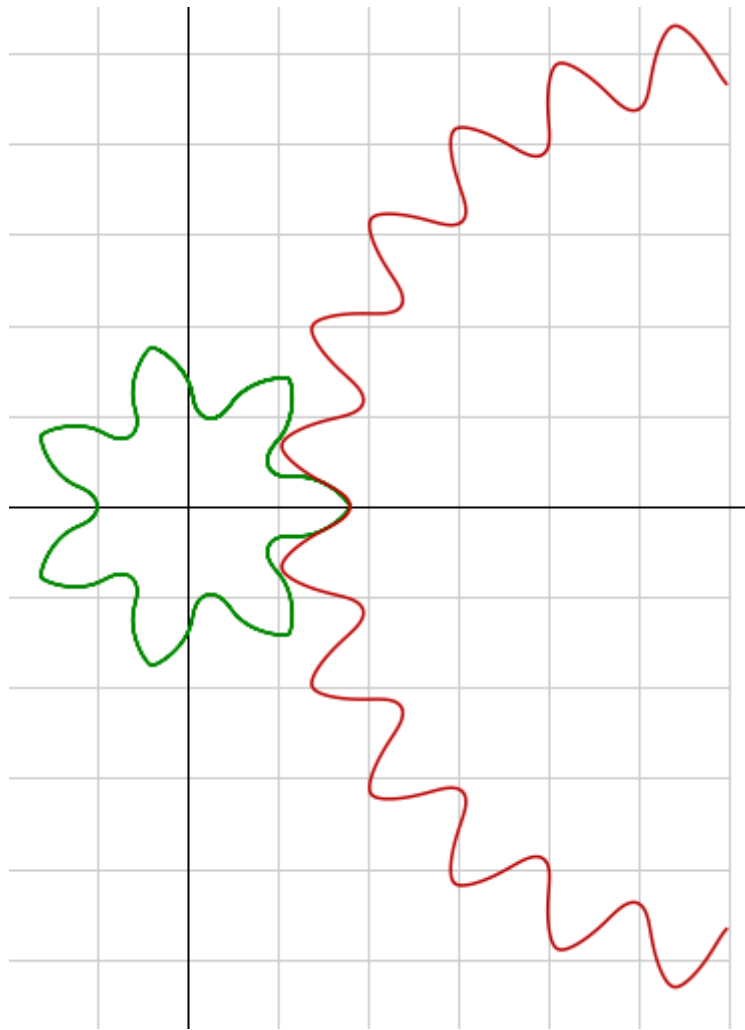


Fig. 9: Gearing of wheels with a harmonic profile ($c_A = 2$; $c_\Delta = 0$)

When designing gears with a harmonic profile, the shape of their teeth can vary widely depending on the combination between the dimensional parameters (r ; A ; Δx) or dimensionless coefficients (c_A ; c_Δ), which will ensure the best gearing performance (with geometric, kinematic and power points of view), including by choosing the optimal curvature and relative sliding of the profiles for various gear ratios of the mechanism.

Thus, by changing the relationship between dimensionless profile coefficients, it is possible to give the tooth a different shape (from smooth to pointed at

the top) depending on the purpose and gearing pattern (mechanical transmission or working parts of the hydraulic machine), a given characteristic and operating conditions of the mechanism.

An engagement with a harmonic tooth profile formed by the method of rolling in a rack accumulates the positive properties of similar involute and cycloidal gears (Fig. 10) and has the following advantages:

- compared to cycloidal gearing, it is possible, as in the case of involute gearing, to use the original rack contour identical to both profiles in the design and

manufacture of mating gears of external gearing. This is due to the fact that the initial harmonic curve I (Fig. 5) in the interval from 0 to 2π is located symmetrically with respect to the longitudinal axis yp and has the same curvature of its vertices; therefore, the teeth of the rack are characterized by the identical shape of their protrusions and depressions. In the case of external cycloidal engagement, the wheel profiles are represented by conjugated hypo- and epicycloidal curves (Fig. 4), the profiling of which is carried out from the corresponding initial contours;

- compared to involute gearing, it is possible, due to smoothness, lack of transition curves and less tendency to undercuts and sharpenings of the sinusoidal curve, to develop wheel profiles with a minimum number of teeth, up to the limit modifications of single and double tooth designs in

the form of a cam and a guitar. This opens up new kinematic, constructive and technological possibilities when creating gear transmission mechanisms and working bodies of hydraulic machines with external and internal gearing, including a decrease in their overall dimensions.

In addition to mechanisms with cylindrical wheels, a harmonic end profile of teeth can also be used in the development of bevel and worm gears.

The technical result of the proposed type of gearing is to increase the efficiency and flexibility of the process of designing and manufacturing gears (including on modern gear-processing equipment), which in the long run creates real prerequisites for further expanding the scope and improving mechanical gears and volumetric rotary machines in various branches of technology.

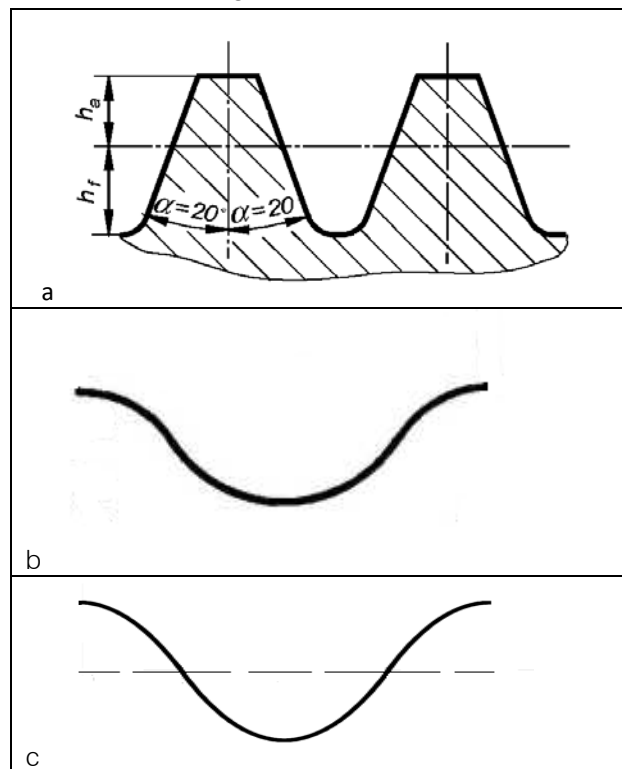


Fig. 10: The initial contours of the gear racks for cutting teeth of various profiles:

a - involute; b - cycloidal; c - harmonic

REFERENCES RÉFÉRENCES REFERENCIAS

1. *Litvin F. L.* Theory of gears. Moscow, Science, 1968.
2. *Vulgakov E.B.* Theory of involute gears. Moscow, Mechanical Engineering, 1995.
3. *Korotkin V.I., Onishkov N.P., Kharitonov Yu.D.* Novikov Gearing: Achievements and Developments (Mechanical Engineering Theory and Applications). Nova Science Pub Inc, 2011.
4. *Baldenko D.F., Baldenko F.D., Gnoevykh A.N.* Single screw hydraulic machines (in two volumes). Moscow, IRC Gazprom, 2005-2007.
5. Patent 671463 of the USSR. Gerotor mechanism / A.V. Tsepkov et al.; 11.11.1974.
6. European Patent 2530359A1. Eccentrically cycloidal engagement of toothed profiles (variant embodiments) / V.V. Stanovskoy and etc.; 17.01.2011.
7. *Baldenko F.D.* Prospects for the use of cycloidal gearing in the oil and gas industry // Territory Neftegaz. 2014, No 6.
8. *Kapelevich A.* Direct Gear Design for Asymmetric Tooth Gears. AKGears, LLC. USA, 2016.

9. US Patent 5271289A. Non-involute gear / *M.L. Baxter Jr.*; 16.12.1992.
10. *Pakhomov S.N.* Radius alternative to involute gearing // Modern equipment and technologies. 2016, No 4.
11. US Patent 20070207051. Toothed member and a corresponding locusus / *A. Katz*; 11.03.2005.
12. Patent 184504 of the Russian Federation. A gear wheel with a harmonic tooth profile / *D.F. Baldenko, F.D. Baldenko*; 15.03.2018.





GLOBAL JOURNAL OF RESEARCHES IN ENGINEERING: A
MECHANICAL AND MECHANICS ENGINEERING
Volume 20 Issue 1 Version 1.0 Year 2020
Type: Double Blind Peer Reviewed International Research Journal
Publisher: Global Journals
Online ISSN: 2249-4596 & Print ISSN: 0975-5861

Mathematical Modeling for Optimization of Periodicity in the Preventive Maintenance Plans

By Rodrigo Fernandes Corrêa & Acires Dias

Universidade Federal de Santa Catarina

Abstract- This study aims to present the development of a model for optimization of periodicity in the preventive maintenance plans of industrial assets, through the study of the lifespan of systems justified by use, time, condition, and costs. The mathematical modeling used was implemented computationally using the MATLAB[®] software. The aim of this model is to provide increased reliability to the facilities, in line with the financial results of the business. The line of research is integrated into the Reliability Centered Maintenance (RCM) management process.

Keywords: *preventive maintenance; periodicity; lifetime; mathematical modeling; residual cost; maintenance cost.*

GJRE-A Classification: FOR Code: 091307



Strictly as per the compliance and regulations of:



Mathematical Modeling for Optimization of Periodicity in the Preventive Maintenance Plans

Modelagem matemática para otimização de periodicidade nos planos de manutenção preventiva

Rodrigo Fernandes Corrêa^α & Acires Dias^ο

Abstract- This study aims to present the development of a model for optimization of periodicity in the preventive maintenance plans of industrial assets, through the study of the lifespan of systems justified by use, time, condition, and costs. The mathematical modeling used was implemented computationally using the MATLAB[®] software. The aim of this model is to provide increased reliability to the facilities, in line with the financial results of the business. The line of research is integrated into the Reliability Centered Maintenance (RCM) management process.

Keywords: preventive maintenance; periodicity; lifetime; mathematical modeling; residual cost; maintenance cost.

Resumo- Propõe-se, com este trabalho, apresentar o desenvolvimento de um modelo de otimização de periodicidade dos planos de manutenção preventiva de ativos industriais por meio do estudo da vida útil dos sistemas, fundamentado pelo uso, tempo, condição, custos. A modelagem matemática utilizada foi implementada computacionalmente por meio do MATLAB. O objetivo do modelo é proporcionar maior confiabilidade às instalações, alinhadas ao resultado financeiro do negócio. A linha de pesquisa está integrada ao processo de gerenciamento de manutenção centrada em confiabilidade (MCC).

Palavras-chave: manutenção preventiva; periodicidade; vida útil; modelagem matemática; custo residual; custo de manutenção.

1. INTRODUCTION

The maintenance cost is decisive factor on the operational viability of an equipment or process. In the industrial context, the maintenance cost has come to represent, on average, 20% of the fixed cost of products. A given published in ABRAMAN (2011) shows that the maintenance cost of the Brazilian industry represents, on average, 3,95% of the Brazilian GDP. Espinosa Fuentes (2006) and Biasotto (2006) presented

maintenance strategies that were employed in industrial complexes, having, as highlighted, management models that seeks preventive actions such as TPM (Total Productive Maintenance), RCM (Reliability Centered Maintenance), preventive based on condition, in time, in impairments, among others. Methodologies to manage well these management models were presented by Waeyenbergh (2005) and Rigone (2009). According to Smith (1993), the great challenge for optimization of the cost in these strategies is on the “what to do” and “when to do”; i.e., what scope and with what periodicity. The correct definition of a periodicity defines the cost in all technical preventive measures.

This approach is very important for companies encouraging several studies. Christer (1998) addressed the issue of optimizing the frequency of preventive maintenance, from the failure rate of equipment; Ferreira (2010) addressed the mathematical modeling using method of approval, Bayesian network, to optimize the use of the most appropriate maintenance techniques to a given preventive/corrective process. Haicanh et al. (2014) addressed the mathematical modeling with genetic algorithm to check the dependence of components that suffers preventive maintenance and that affects positively and negatively the maintenance cost.

Given the importance of the periodicity optimization in the preventives maintenances, the objective is, with this work, develop a mathematical model that assists in the dimension of periodicity in the preventive maintenance plans (PM) and answer questions of research such as:

- ✓ What is the influence of the difference between corrective MTTR and preventive MTTR in the maintenance cost?
- ✓ What is the financial impact of the preventive maintenance in accordance with the cost of the outgoing time?
- ✓ What is the influence of residual cost (due to premature component exchange) in maintenance cost?
- ✓ What is the preventive periodicity that provides lower maintenance cost over the lifetime of the process?

Author α: Programa de Pós-graduação em Engenharia Mecânica, Universidade Federal de Santa Catarina – UFSC, Rua Eng. Agrônomo Andrei Cristian Ferreira, s/n, Trindade, CEP 88040-900, Florianópolis, SC, Brazil. e-mail: rodrigo.correa@portobello.com.br

Author ο: Departamento de Engenharia Mecânica, Universidade Federal de Santa Catarina – UFSC, Rua Eng. Agrônomo Andrei Cristian Ferreira, s/n, Trindade, CEP 88040-900, Florianópolis, SC, Brazil. e-mail: acires.dias@ufsc.br

Premature exchange is a term used in this work to designate replacement of the item before it reaches the end of life.

II. PERIODICITY IN THE PM PLAN

Although the preventive maintenance enable anticipation of correction of damage, before the fault occurs, it also generates unavailability in the process, because for each maintenance event there is the need to stop the process, making setup of the periodicity and the execution time of a preventive maintenance becomes complex, due to this and other factors such as:

- The periodicity of preventive maintenance of each equipment should be combined with all the equipment of the process, to generate a better use of the stop time of the process.
- Difficulty to define which components will be swapped, from the knowledge of the useful life of the same.
- Dimensioning of labor for the execution of activities.
- Concentration of the largest possible number of activities to enjoy the impairment of the process.

The definition of great periodicity, that provides lower cost and higher reliability in systems, is one of the challenges of preventive maintenance.

a) Definition of the periodicity on PM

Act in a conservative manner in relation to the reliability generates a high cost in maintenance due to premature component exchange and the excessive use of maintenance labor. The experience of one of the authors, by 17 years in the industrial maintenance, in mechanical level of corrective and preventive maintenance, as a planner, analyst, engineer, coordinator and maintenance manager, allowed to experiment decisions that, for increased reliability, demanded questions, such as: "intensify the preventive maintenance, it increases the scope or reduces the periodicity"?

By acting in a conservative manner in relation to the cost of maintenance, with objective of obtaining a good use of components to make maximum use of its useful life, you can also compromise the reliability of the system due to the uncertainty that exists on the useful life of each component, (region of periodicity 17 to 20 in Figure 1). Consequently, there will be the possibility to reduce the cost of maintenance and raise the cost of the process, due to the low reliability, generating unavailability in the process.

As shown on Figure 1, the region of great periodicity (between 9 and 12), that provides better financial result of the system, depends on many factors, such as: cost of preventive maintenance, profitability of the process and especially the knowledge of the useful life of the systems. For this it is necessary an in-depth statistical control of failures and time of occurrence. Still

according to Figure 1, the reduction of periodicity provides better reliability, but can derail the profitability of the process due to the increase in maintenance costs.

b) Useful life in preventive maintenance

For Smith (1993, 2004), preventive maintenance is the operation of the services or tasks of inspection that has been planned for the achievement of specific points in time and preserves the function of the operation of the equipment or systems.

For Bertsche (2008), preventive maintenance is a maintenance method, where the tasks are performed preventively; that is, to a predetermined time, or after a specified periodicity or a quantity of operating hours these activities are performed.

For both authors, the preventive maintenance can be based on time, condition or failure.

It is based on time, when it's set a determined time of use or a number of cycles for the execution of certain repairs, adjustments or replacement of components.

It is based on condition when applied techniques of visual inspection, routine or more depth as techniques of vibration analysis, thermo graphic analysis, analysis of oil and ultrasound, also defined as predictive.

It is based on failure, when the repair occurs after detecting the fault. Whereas the failure won't damage other components and won't generate consequences to safety and the environment, planning tools, parts and labor and looks forward to the occurrence of the failure to perform the repair.

These preventive actions are ways to predict the moment of equipment failure, that is, predict the end of it's useful life. Failure analysis techniques can be seen in Kumamoto & Henley (1996), Dias et al. (2011) and Dias (2012).

As shown on Figure 2, the higher the intensity of inspection the lower the uncertainty of the estimation of component life, to the point at which they can act in the exact moment of the failure "based on the failure", when, then, there is a use of 100% of component life.

Leaving the component fail, in view of the cost of maintenance, has a better exploitation of the component, with the use of 100% of it's useful life. In this sense, there would be no premature component cost, due to this recovery; however, in most situations, the predominant maintenance policy would be corrective.

According to Souza (2009), normally the assessment of useful life of components is based on past experience and on statistical data provided by the manufacturers. On the incompatibility of adjustments with the production program, many equipment can't be reviewed at certain times, sacrificing components that could be in good conditions if done the exchange in the

right time. These are the reasons that generate the main criticisms of the preventive maintenance policy. It is observed, on Figure 3, the statistical distribution of 10 systems for the sliding equipment; you may ask: how

can you define the periodicity of an intervention of equipments from the distribution of the useful life of its system?

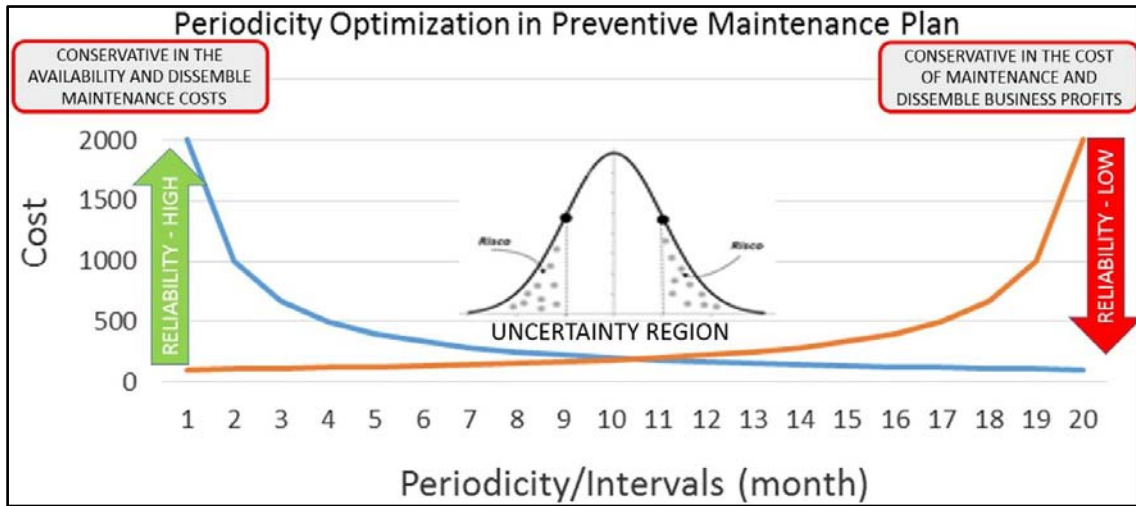


Figure 1: Cost effects on the periodicity of preventive maintenance (Corrêa & Dias, 2014).

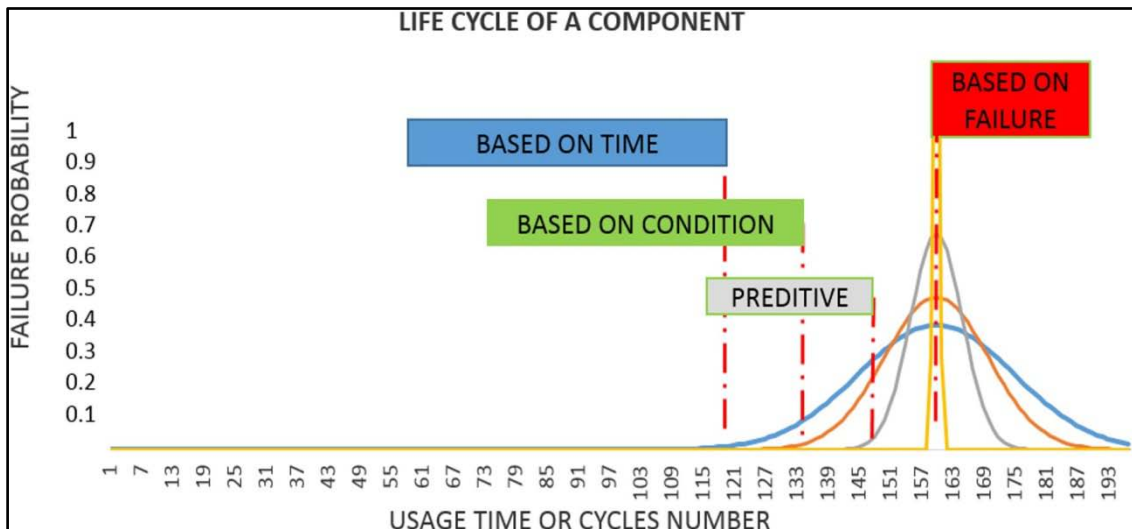


Figure 2: Definition of periodicity in function of useful life (Corrêa & Dias, 2014).

Can the periodicity of preventive maintenance of this equipment be defined, based only on knowledge of the useful life of each system?

In case the answer was “yes”, there would be the definition of impairments of the equipment in function of time, generating a stop for each “mode” of the distribution that represents the useful life of each system, as shown on Figure 4.

Figure 4 shows 27 stops on the equipment, on a period of 25 months. As in this example is not being considered the MTTR (medium time to repair) and nor the hours cost of outgoing process to which the equipment is inserted, the cost generated by stopping the process is not significant; that means, the maintenance cost is generated only by the cost of parts and labor.

It’s important to observe in this figure, that some systems are replaced more than once, during the useful life of the evaluation, that means, the system that has an average life of 4 months for a useful life of 25 months of evaluation is necessary to be replaced 6 times, generating 6 impairments to process.

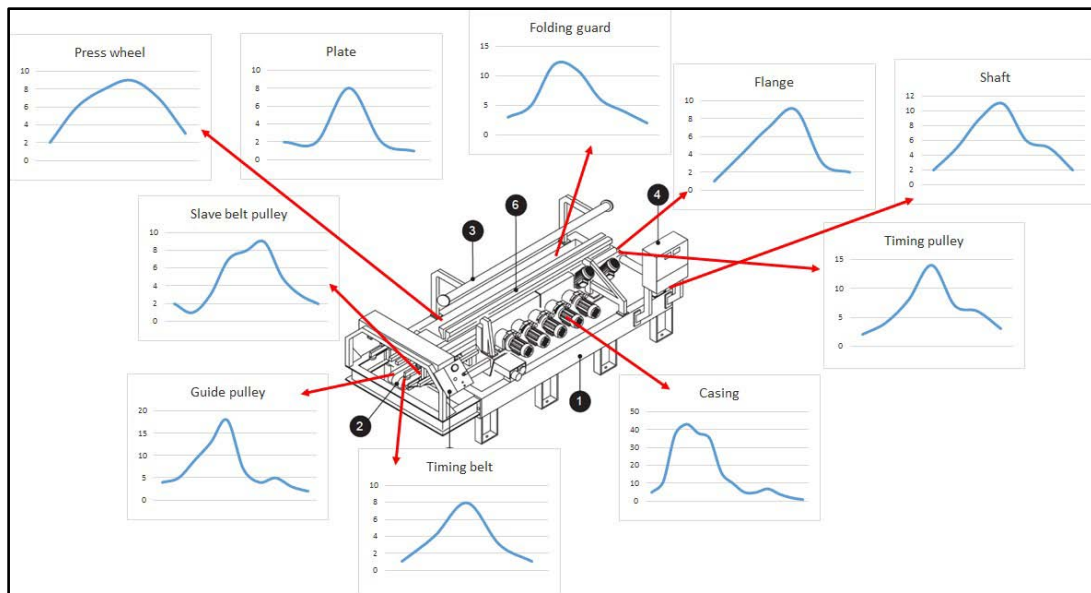


Figure 3: Distribution of the function of “useful life” for the equipment systems (Corrêa & Dias, 2014).

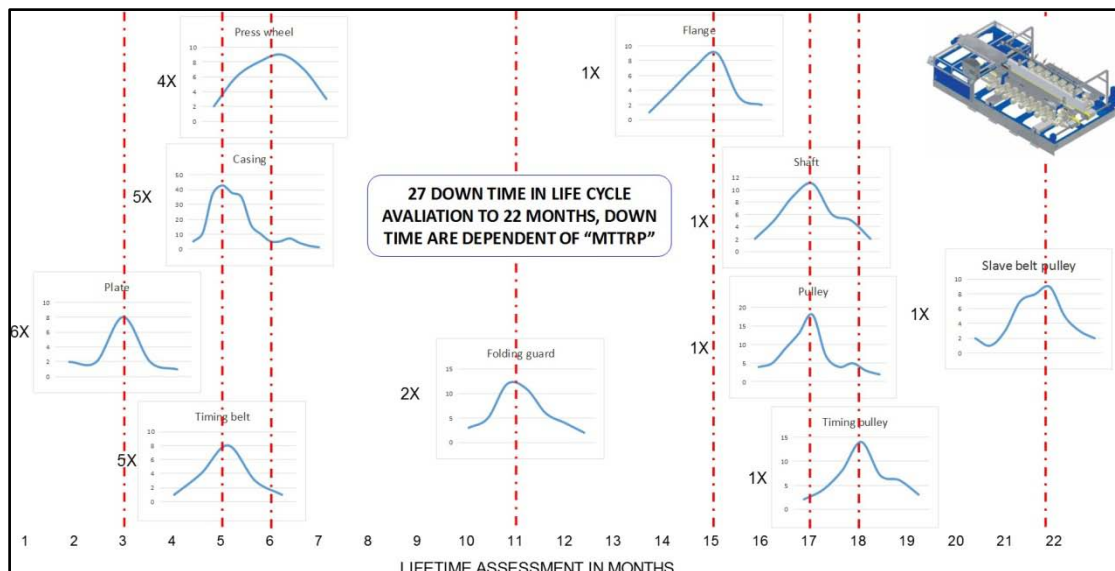


Figure 4: Distribution of function of “useful life” of systems, distributed in time (Corrêa & Dias, 2014).

This way, the definition of periodicity more favorable financially is to act on a corrective form, making repairs on each component at the end of its useful life, despite having a high unavailability due to the large number of impairments.

c) Evaluation of periodicity

To better understand the comments made earlier, note the evaluation of a hydraulic press, represented in six systems with their respective MTTR, useful life and cost of repair, as Table 1.

Each system has an estimated life from statistical data with an uncertainty for each value displayed: each useful life was estimated from a probabilistic distribution and may be normal, lognormal or Weibull. It was, also, considered the residual cost of component, i.e., the value of the component that was

replaced without having been used its useful life in full. The likely total useful life less the effective life of work. This approach is the process of maintenance cost as the following Equation 1 and 2:

$$CM = CCn + CRn + CP \tag{1}$$

And: CM – Cost of maintenance (R\$); CCn - Cost of component “n” (R\$); CRn – Residual cost of component “n” (R\$); CP – Cost of impairment (R\$).

$$CP = (MTTRn \times CHC) \tag{2}$$

And: MTTRn – Medium time to repair system “n” (h); CHC – Cost of outgoing time of system (R\$/h). The residual cost seen in Figure 5 is represented by means of the function of a descending straight line. Whenever a component is replaced before the end of its estimated

useful life, the cost of the repair is being added to the residual cost of the component replaced.

In the example in Figure 5, the component "COMP1" has an estimated useful life of 20,000 hours. Opting to replace it preventively before of 20,000 hours, (as the example in Figure 5 that shows an exchange at 10,000 hours), it has a residual cost. When you choose to replace a component or make a repair of a system before the end of its useful life, the cost of maintenance will be: the cost of a new component (necessary parts for the repair) plus the residual cost of the system or component, that still didn't reach the end of its useful life.

Imagine, now, that the hydraulic press shown as an example on Table 1 is insert in a process in which the cost of outgoing time of process is R\$ 0.00 for hour of impairment. In this case, you can stop the process at any time without financial effect on the process. From the point of view of cost of maintaining more economical, the option would be replace each component, only on the end of its useful life, having, then, a better use of systems and lack of residual cost for maintenance.

For this situation, there would be 14 impairments on the process, totalizing 120 hours stopped, as shown in Figure 6 by the end of each component useful life, has a stop in the process for actuation of maintenance.

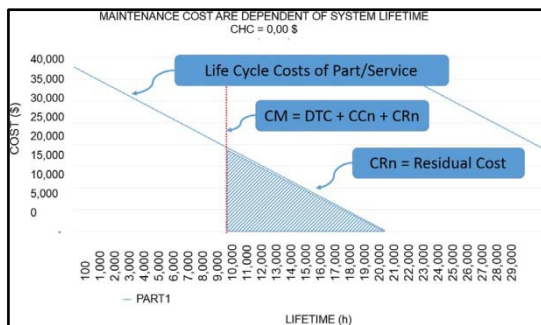


Figure 5: Representation of residual cost for a system (Corrêa & Dias, 2014).

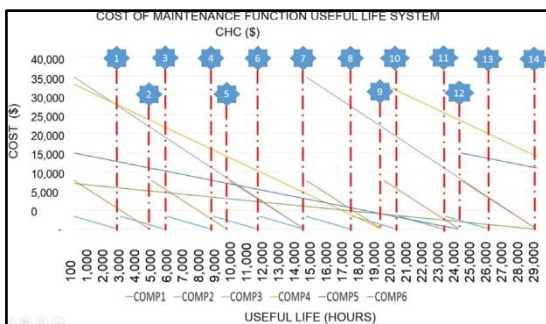


Figure 6: Representation of residual cost of the six systems of a press (Corrêa & Dias, 2014).

For the example shown in Figure 6, operates according to the policy of corrective maintenance (MC),

taking in consideration that the fault generated on the equipment due to the use of the comprehensive life of each equipment does not cause any side effect, such as: damage to other systems, security or the environment. From the economic point of view, for the scenario presented previously, act as a corrective action would be the most viable for the profitability of the process.

There are other factors that should be considered in this analysis such as; availability of labor to act correctively, specialty of labor, tooling, spare parts and MTTR, which will be exemplified with more details to follow.

You can make a new analysis for the same equipment, this time it is installed in a process whose hour cost of resigning is \$ 7,000.00 for hour of impairment. In this case, obviously, the strategies should be other. To better understand it will be compared both systems, represented in Figure 7, by COMP3 and COMP5.

When replaced the component COMP3 with 15,000 hours that represents its useful life, the maintenance cost will be, cost of component COMP3 + cost of impairment (CP).

If in this intervention is also chose to replace the component "COMP5", in order to take advantage of impairment of the process, the cost of this maintenance would be: cost of components COMP3 and COMP5 + impairment cost (CP) + residual cost of the component COMP5 (Crcomp5). According to the data shown on Table 1, the cost of this maintenance would be:

$$CP = MTTR_{max} \times CHC = 15 \times 7,000 = R\$ 105,000.00.$$

$$CM = C_{comp3} + C_{comp5} + CP + C_{rcomp5}$$

$$CM = 13,000 + 20,000 + 105,000 + 8,000$$

$$CM = R\$ 146,000.00$$

Another option would be replace each component by the end of its useful life. For this situation there would be two impairments on the process, as represented by Figure 8.

In the example above, there would be an impairment in instant 15,000 hours, and another impairment in instant 25,000 hours.

For 15,000 hours has the CM as:

$$CP = MTTR_{comp3} \times CHC = 10 \times 7000 = R\$ 70,000.00.$$

$$CM = C_{comp3} + CP$$

$$CM = 13,000 + 70,000 = R\$ 83,000.00$$

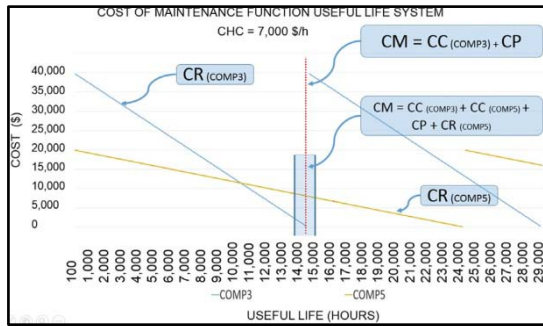


Figure 7: Cost of maintenance with CHC greater than zero and residual cost (Corrêa & Dias, 2014).

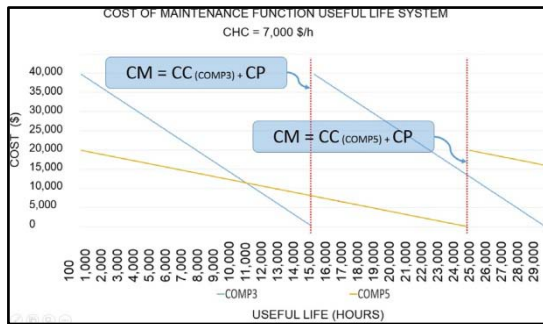


Figure 8: Cost of maintenance with CHC greater than zero without residual cost (Corrêa & Dias, 2014).

For 25.000 hour has the CM as:

$$CP = MTTR_{comp5} \times CHC = 15 \times 7,000 = R\$ 105,000.00.$$

$$CM = CC_{comp5} + CP$$

$$CM = 20,000 + 105,000 = R\$ 125,000.00$$

In the period of 25,000 hours has a cost of maintenance of two impairments, totalizing in R\$ 208,000.00.

When is compared both scenarios presented in Figure 7 and 8, you can observe: on Figure 7, in the period of 25,000 hours, has only one impairment in the process totalizing a maintenance cost, for the period, of R\$ 146,000.00. Now in Figure 8, in the same period of 25,000 hours, has two impairments, totalizing a cost of maintenance of R\$ 208,000.00. It can be observed, by means of example cited, that the scenario represented in Figure 7 has a lower cost of maintenance, consequently more profitable for the business; therefore, the replacement of components or premature revisions of systems, depending on the profitability of the process, are necessary.

III. MODELING

The mathematical modeling has as objective the structuring of systems variables to be studied in order to obtain calculations optimization of the periodicity of preventive maintenances.

For this modeling, the model takes into consideration some characteristics of the systems:

1. All intervention of preventive maintenance takes into consideration the replacement of all the evaluated components.
2. The time of execution of the preventive maintenance is based on the component that has the largest time of preventive repair MTTRp, within the evaluated system.
3. The events of corrective maintenance occurs so that it does not cause any harm to safety, environment or damage the underlying component; i.e., the damage caused in the corrective event is mainly the component, causing only financial impact.
4. All the systems are represented by a RBD (Block Diagram of Reliability) in series being that any failure in a single component requires that stops all the process.

The model is based in the estimated useful life, medium time to repair and the outgoing time of the process of each component to be evaluated. To have a result that is consistent with this model, should only be evaluated systems for which it possess information about the useful life of components well defined.

In the productive processes (systems) can exist a multitude of components, but this model is proposed to make a great assessment of periodicity from most significant components that has a greater representativeness in the cost of repair and the time of impairment of the process.

a) Declarations of variables

To start the modeling, first shall be informed all the variables involved in the model, as follows:

$MTTR_{cn}$ = Medium time to repair the corrective of component "n".

$MTTR_{max}$ = Maximum medium time to repair the preventive of system.

V_{un} = Average useful life of component "n".

VUT_n = Use of the component life "n".

V_{umax} = Maximum useful life of the system.

V_{umin} = Minimum useful life of the system.

V_{us} = Useful life of evaluation of the system.

CC_n = Cost of component "n".

CR_n = Residual cost of the useful life of component "n".

CRT = Total residual cost of the useful life of the system.

CHC = Cost of outgoing time of the system.

CRP_p = Cost of preventive repair.

CRP_c = Cost of corrective repair.

CMV_u = Cost of maintenance for the evaluated useful life.

N_c = Number of systems.

W_p = Periodicity of preventive.

W_{pot} = Periodicity of preventive optimized.

$CR(w)$ = The total residual cost of the useful time of the system in accordance with the periodicity.

b) Equations

As previously mentioned, the residual cost of the component represented by the variable CR_n , is a periodic descending function as a function of time. Each period represents the component replacement.

To model this event, the function that best represents is a series of Fourier, saw-tooth type, according to Equation 3.

$$y(t) = \frac{2L}{\pi} \sum (-1)^{(n-1)} \times \sin \frac{n \times \pi \times t}{L} \quad (3)$$

To model the CR_n (Residual cost of useful life of component "n"), in the series, was necessary to perform some adjustments in the original equation, as will be shown in the Equation 4.

$$CR_n(t) = \frac{CC_n}{1.5} + \frac{CC_n}{2} \sum_{n=1}^{1000} \frac{(-1)^n}{n} \times \sin \left[\frac{n \times \frac{\pi}{0.5 \times V_{un}} \times \left(t + \frac{V_{un}}{2} + VUT_n \right)} \right] \quad (4)$$

It is observed, initially, that the original Equation 1 is a growing series and the necessity here is decreasing. It was also necessary to insert an additional term, to move the amplitude of the equation that varies positively and negatively around the point "zero". In this modeling is necessary only positive values that represents the $CR_n(t)$. The number of terms for modeling each series is present in the value of 1 to 1000, varying in one unit. It was added the terms $V_{un}/2$ and VUT_n that represents the phase angle in the function, by moving all the function to the beginning of the useful life of each evaluated component and adjusting the life of system utilization in function of the moment to be assessed.

An example of this function can be observed in Figure 9.

After the definition of the equation that represents the cost of each component in function of its useful life, to obtain the cost of useful life of all the systems to be evaluated, applies the Equation 5.

$$CR_T = \sum CR_n(t) \quad (5)$$

From obtaining the cost of the useful life of the system in function of time, is needed to know the cost of preventive repair in function of time, that is, what is the cost of repair for a determined moment. This may be calculated by means of the Equation 6.

$$CRP_p(t) = \sum CC_n + MTTR_{max} \times CHC + CR_T \quad (6)$$

It is recalled that the cost of instantaneous repair considers the exchange of all the components.

For the present study, no matter the instantaneous cost to perform a certain repair, but what is the cost of the repairs in function of the periodicity.

The system will simulate many frequencies in function of a determined useful life, denominated V_{us} (useful life of evaluation of the system). The V_{us} is the life that absorbs the maximum useful life of the component of a determined system. Therefore the V_{us} will be two times higher than the maximum life of a determined component of the evaluated system, or defined by the user, and may be entered its value during the entry of data in the program.

The life of the initial assessment, i.e., the lower periodicity evaluated, is defined by a quarter of the value of the smallest life of a determined component of the system evaluated. According to Equation 7.

$$W_p = F \times V_{u_{min}} \Rightarrow \left[\frac{V_{u_{min}}}{4}, 2 \times V_{u_{max}} \right] \quad (7)$$

For each periodicity evaluated within the range defined in the Equation 7, you get the cost of preventive repair in function of the periodicity, according to Equation 8. The periodicities simulated for the Equation 8 arise from the Equation 7, that increments a "F" factor equal to 0.5.

$$CRP_p(W_p) = \sum CRP_p \quad (8)$$

It is observed that as the periodicities are incremented, the cost of maintenance gets another variable, generated by the corrective events. Thus, for each periodicity that exceeds the time of the useful life of a determined component, has a corrective event which can be calculated by the Equation 9.

$$CRP_c(w_p) = \sum [(CC_n + MTTR_{cn} \times CHC) \times \left(\frac{2 \times V_{u_{max}}}{V_{u_n}} \right)] \quad (9)$$

The total cost of maintenance for the life of evaluation of the system in function of the periodicity can be calculated by the Equation 10.

$$CM_{vu} = CRP_p(W_p) + CRP_c(W_p) \quad (10)$$

With the function obtained in the Equation 8, is possible to define the periodicity great for the evaluated system, which is the lowest value of the function generated through the Equation 8.

IV. NUMERICAL APPLICATIONS

The modeling was developed through the software MATLAB, according to Willian (2013).

The main objective of the program is to provide the experts and managers of the maintenance area the ease of evaluation of various scenarios of the industrial

process that comprise the cost of preventive maintenance. In addition, gives the visibility to the economic viability of the projects of industrial processes.

ceramic industrial process, as Figure 10. The variables of entry can also be exemplified in this figure.

a) Data entry

To evaluate the mathematical modeling and the program implemented, will be used a simple model of a

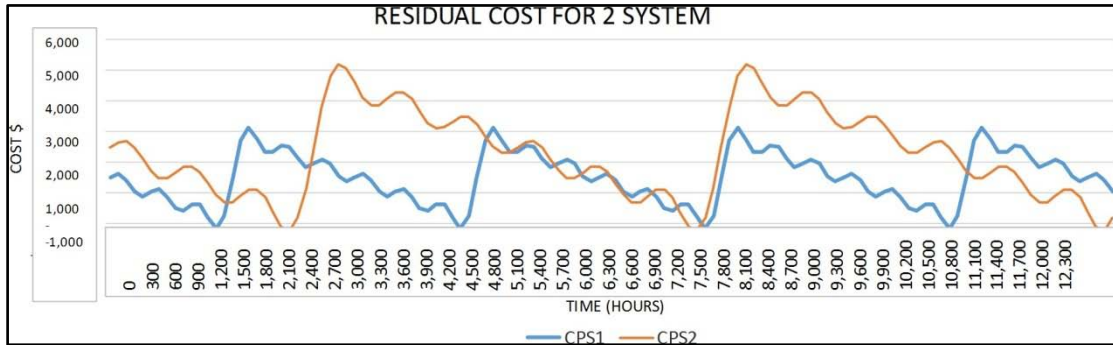


Figure 9: Residual cost of two systems for the number of terms in the Fourier systems, n=5.

In Figure 11, it is possible to observe the data entry page of the designed program named POPMP (Program to Optimize Preventive Maintenance of Periodicity).

b) Results

In Figure 12 can be observed the function of the residual cost of each component of the system in function of its useful life that was modeled in the series saw-tooth Fourier, according to the Equation 2.

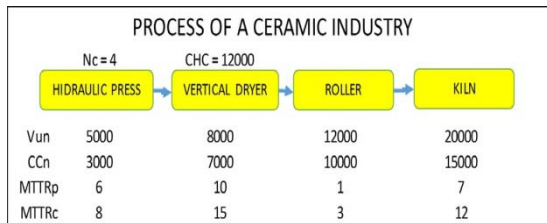


Figure 10: Model of a system for simulation of modeling in MATLAB.

```

***** DATA ENTRY *****
ENTER THE VALUE COST OF OUTGOING TIME OF SYSTEM ($/h)-----:12000
ENTER THE TIME OF BUFFER PROCESS (h)-----:0
ENTER THE NUMBER OF SYSTEM -----:4
ENTER THE USEFUL LIFE OF EVALUATION (h)-----:40000

* ENTER THE USEFUL LIFE OF COMPONENT 1 (HOUR) -----:5000
* ENTER THE USE OF THE COMPONENT LIFE 1 (HOUR)-----:10
* ENTER THE COST OF COMPONENT 1 ($) -----:3000
* ENTER THE MTTRp (Preventive) OF COMPONENT 1 (HOUR) --:6
* ENTER THE MTTRc (Corrective) OF COMPONENT 1 (HOUR) --:8

* ENTER THE USEFUL LIFE OF COMPONENT 2 (HOUR) -----:8000
* ENTER THE USE OF THE COMPONENT LIFE 2 (HOUR)-----:10
* ENTER THE COST OF COMPONENT 2 ($) -----:7000
* ENTER THE MTTRp (Preventive) OF COMPONENT 2 (HOUR) --:10
* ENTER THE MTTRc (Corrective) OF COMPONENT 2 (HOUR) --:15

* ENTER THE USEFUL LIFE OF COMPONENT 3 (HOUR) -----:12000
* ENTER THE USE OF THE COMPONENT LIFE 3 (HOUR)-----:10
* ENTER THE COST OF COMPONENT 3 ($) -----:10000
* ENTER THE MTTRp (Preventive) OF COMPONENT 3 (HOUR) --:11
* ENTER THE MTTRc (Corrective) OF COMPONENT 3 (HOUR) --:13

* ENTER THE USEFUL LIFE OF COMPONENT 4 (HOUR) -----:
    
```

Figure 11: POPMP, modeling in MATLAB.

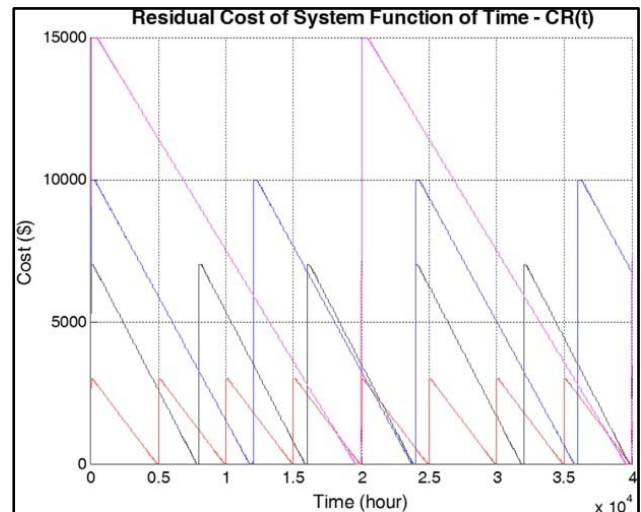


Figure 12: POPMP, residual cost in function of useful life.

In Figure 13 was obtained the total residual cost of the system, calculated by the Equation 3 and the cost of preventive repair calculated by the Equation 4, in function of time. It is observed that at this point of the program, there is only the cost of instantaneous maintenance in function of time and not according to the periodicity that is the main purpose of the POPMP. From this point the program begins to simulate the periodicities, initially considering a quarter of minimum useful life of the system, in this example, 5.000 hours. The system initially will design a periodicity of 1.250 hours, as Figure 14.

From this point, the program begins to increment the periodicity in 0.5 times the value of minimum useful life as Equation 5 (see Figure 15).

For each periodicity simulated, the system calculate the total residual cost, taking in consideration that all the components will be replaced in the preventive event for a determined periodicity.

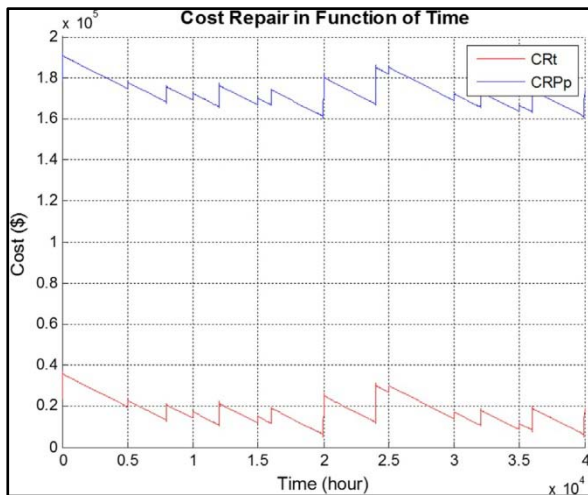


Figure 13: POPMP, cost of preventive repair x time.

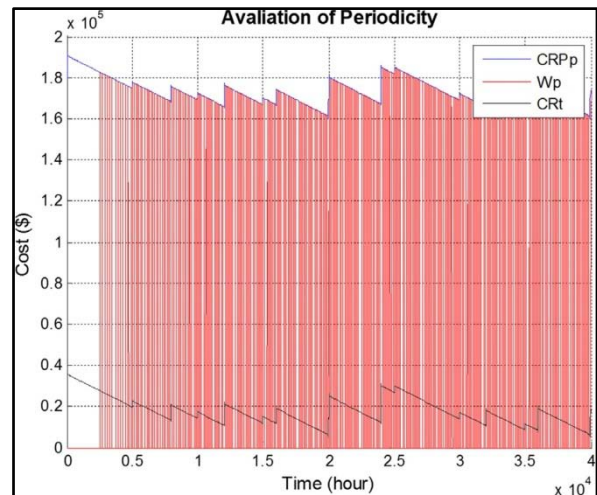


Figure 14: POPMP, evaluation of the periodicity.

In Figure 16, observes the behavior of the total residual cost in function of the periodicity. It is possible to observe that the smaller the preventive periodicity, greater are the residual costs. That means that the smaller the periodicity, the total life of the components will be used less, there is, therefore, a greater occurrence of premature exchanges.

For each periodicity simulated, being that the number of simulated periodicity depends on the difference between the minimum and the maximum useful life of the system, the system calculates the cost of preventive repair in function of periodicity, according to the Equation 6 (see Figure 17).

After calculating the cost of preventive repair in function of the periodicity, the system calculates the cost of corrective repair in function of the periodicity according to the Equation 7. It is worth remembering

that, for each component that have a shorter life that the evaluated periodicity, the program considers a corrective event, calculating its cost from the cost of the component, MTRC (medium time to repair corrective) of the respective component, and outgoing time of the process (see Figure 17), variable CRPc of the legend.

Finalizing with the Equation 8, comes the total cost of maintenance for the useful life of evaluation in function of the periodicity (see Figure 18).

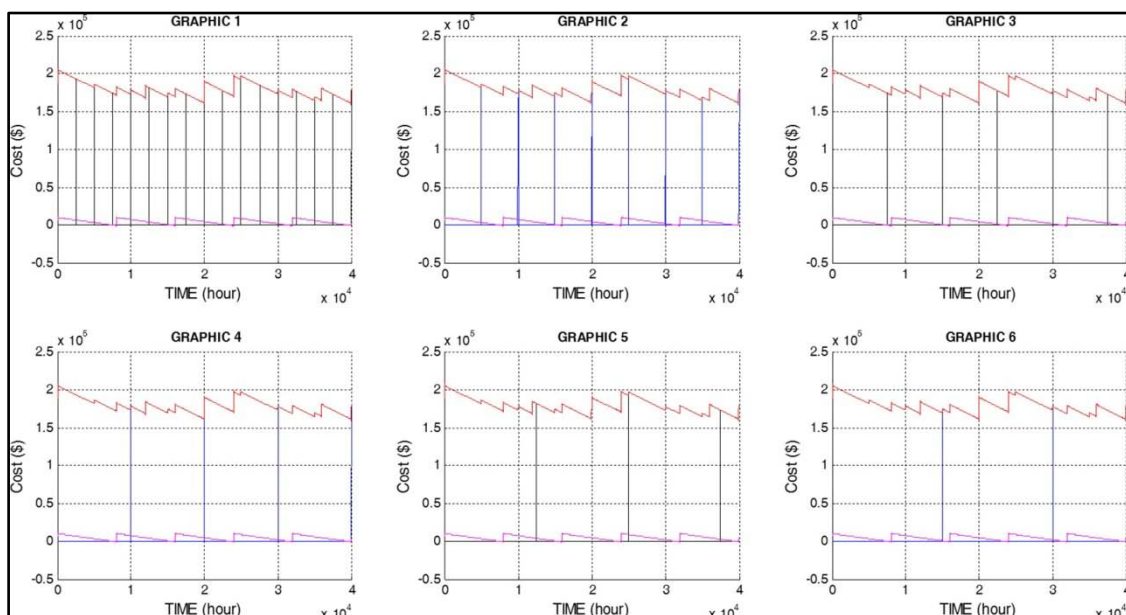


Figure 15: POPMP, interaction of the periodicities.

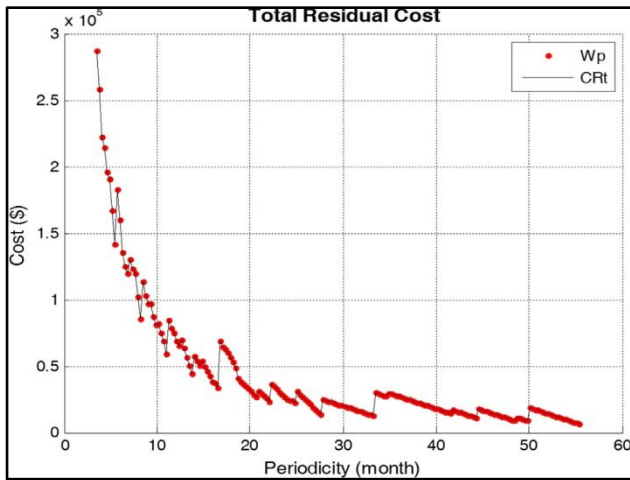


Figure 16: POPMP, total residual cost in function of the periodicity.

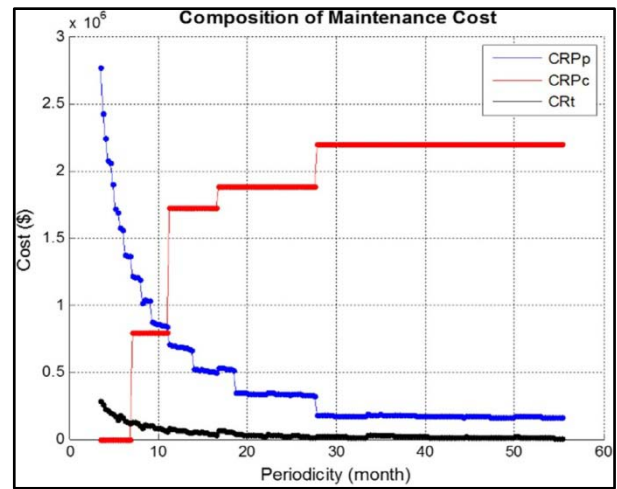


Figure 17: POPMP, cost of preventive repair in function of the periodicity.

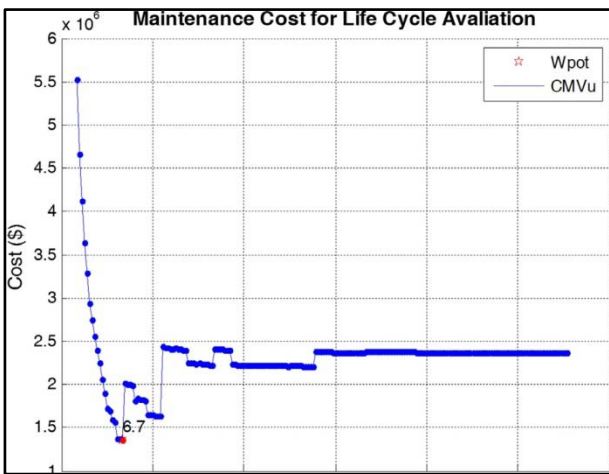


Figure 18: POPMP, maintenance cost of useful life evaluated in function of the periodicity.

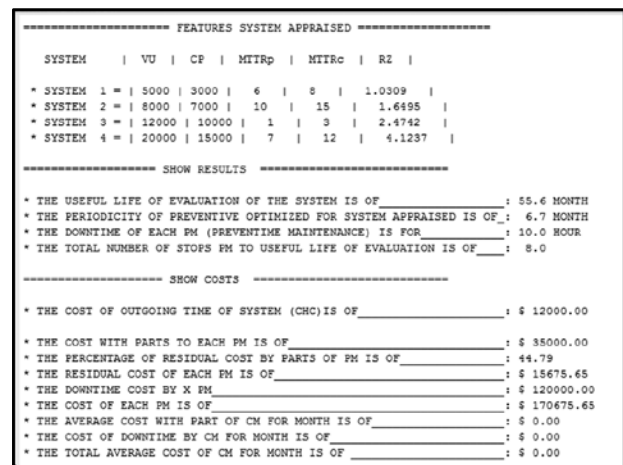


Figure 19: POPMP, the output of the results.

It can be observed that for the system evaluated in the proposed modeling, the periodicity optimized is located in periodicity 6, 7 months (approximately 4.824 hours). Thus, if its elaborated a plan of maintenance planning a stop of 10 hours (see maximum MTRp in Figure 10) to each 6,7 months, with the replacement of all four components of the system, it will be obtained the lowest cost of maintenance for the life of 55,6 months of the system.

According to the results presented in Figure 19, the total accumulated cost of maintenance for the periodicity of 6,7 months, is approximately R\$ 1.359.000,00 for a life of 55,6 months. Each impairment will have a total maintenance cost of approximately R\$ 170.675,65. It can be observed that the most representative is the cost of downtime of R\$ 120.000,00 process and, for the simulation made, it has no occurrence of corrective for the evaluated systems, due to the great periodicity having an inferior time to the lowest useful life of component that, in the model, is 5.000 hours, approximately 6, 9 months.

c) CHC influences

Another important observation that can be obtained in the simulation is the influence of the CHC (outgoing time of the system).

To obtain this evaluation, the system will considerate the same model of Figure 10 by inserting a sensitivity analysis of the simulation. Starts the simulation with CHC equal to “zero” and increase its value of R\$ 2.000,00 to each simulation, according to Figure 20. It is observed that the values of CHC are represented by thousands, CHC x R\$ 1.000.

As is incremented the value of CHC, it is observed a converged reduction of periodicity; that occurs due to the residual cost “CR” (due to the premature replacements) lose their significance in relation to the CHC. In this sense, the processes in which the cost of outgoing time has a ratio higher than the cost of the components, the premature replacement of components is advisable to increase the availability of the equipment, avoiding corrective events. It is emphasized that for the process in which CHC has a

ratio higher than cost of the components, the corrective events have most significant costs, due to $MTTR_c$ be in most situations superior to $MTTR_p$. For this reason, the greater the CHC the lesser will be the periodicity, to avoid corrective events.

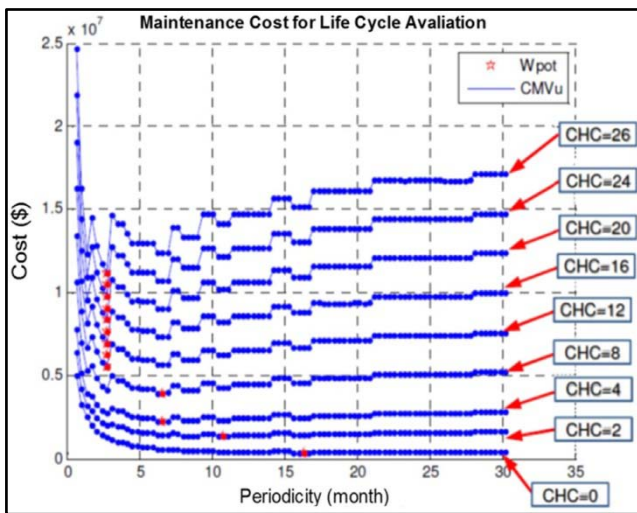


Figure 20: POPMP, CHC influence in the periodicity.

Another observation refers to the occurrence of CHC very low: observe the curve where $CHC = 0$, the periodicity tends to increase, surpassing even the useful life of the component that has the most useful life. That means that for the cases in which the CHC is negligible, the tendency is to apply the strategy of corrective maintenance (MC), whose residual cost will be equal to "zero", because there is no premature replacement.

V. CONCLUSIONS

This article shows a mathematical modeling to optimize periodicity of MP by means of the modeling of industrial systems. Its application enables observe the variation of financial impact in function of the periodicity and conclude that the premature exchange of component is necessary for a certain type of process. In Figure 16 is possible to observe the behavior of the residual cost in function of the periodicity, necessary information for the maintenance manager to make a decision.

In Figures 17 and 18 is possible to observe the behavior of the cost of corrective and preventive maintenance, and which periodicity provides lower maintenance cost over the life of the process.

It is also possible to observe the practical point of view of the modeling. It is known that most of the teams of maintenance of various segments develops knowledge of the behavior and the useful life of their systems; however, when there is need to rearrange all these systems to calculate the great periodicity, that would provide greater financial result to the process, these professionals have difficulty, because the modeling is laborious. In possession of a modeling, the

maintenance manager have conditions to optimize the plan of preventive maintenance and the times of impairment.

It can be conclude that the mathematical modeling implemented as a computational program "POPMP" is of extreme importance to calculate the great periodicity of preventive maintenance of the industrial process and to provide a good visibility of the maintenance costs of the processes. This modeling ensures a periodicity of preventive maintenance that delivers the reliability suitable for each process, in function of the profitability of each business, without overloading the maintenance costs or the costs generated by low availability.

REFERENCES RÉFÉRENCES REFERENCIAS

1. Associação Brasileira de Manutenção – ABRAMAN. (2011). A situação da manutenção no Brasil. In *Anais do 26º Congresso Brasileiro de Manutenção*. Curitiba: Abraman.
2. Bertsche, B. (2008). *Reliability automotive and mechanical engineering*. Berlin: Springer.
3. Biasotto, E. (2006). *Aplicação do BSC na Gestão da TPM: estudo de caso em indústria de processo* (Dissertação de mestrado). Programa de Pós-graduação em Engenharia Mecânica, Universidade Federal de Santa Catarina, Florianópolis.
4. Christer, A. H. (1998). The delay-time modeling of preventive maintenance of plant given limited PM data and selective repair at PM. *Journal of Management Mathematics*, 9(4), 355-379.
5. Corrêa, R. F., & Dias, A. (2014). *Desenvolvimento de uma metodologia para manutenção preventiva* (Dissertação de mestrado). Programa de Pós-graduação em Engenharia Mecânica, Universidade Federal de Santa Catarina, Florianópolis.
6. Dias, A. (2012). Failure analysis. In G. E. Totten & V. J. Negri. *Handbook of hydraulic fluid technology* (2. ed., Cap. 12, pp. 461-530). Hoboken: CRC Press.
7. Dias, A., Calil, L. F. P., Rigoni, E., Sakurada, E. Y., Ogliari, A., & Kagueiama, H. A. (2011). *Metodologia para análise de risco: mitigação de perda de SF6 em disjuntores*. Florianópolis: Studio S. 304 p.
8. Espinosa Fuentes, F. F. (2006). *Metodologia para inovação da gestão de manutenção industrial* (Tese de doutorado). Programa de Pós-graduação em Engenharia Mecânica, Universidade Federal de Santa Catarina, Florianópolis.
9. Ferreira, R. J. P. (2010). A preventive maintenance decision model based on multi criteria method PROMETHEE II integrated with Bayesian approach. *Journal of Management Mathematics.*, 21(4), 333-348.
10. Haicanh, V. U., Do Van, P., Barros, A., & Berenguer, C. (2014). Maintenance planning and dynamic grouping for multi-component systems with positive

and negative economic dependencies. *Journal of Management Mathematics*, 26(2), 145-170.

11. Kumamoto, H., & Henley, E. J. (1996). *Probabilistic risk assessment and management for engineers and scientists*. New York: IEEE Press.
12. Rigone, E. (2009). *Metodologia para manutenção centrada na confiabilidade: sistema baseado na lógica fuzzy* (Tese de doutorado). Programa de Pós-graduação em Engenharia Mecânica, Universidade Federal de Santa Catarina, Florianópolis.
13. Smith, A. M. (1993). *Reliability centered maintenance*. Boston: McGraw Hill.
14. Smith, A. M. (2004). *RCM: gateway to world class maintenance*. Oxford: Elsevier.
15. Souza, V. C. (2009). *Organização e gerência da manutenção* (3. ed.). São Paulo: All Print Editor.
16. Waeyenbergh, G. (2005). *CIBOCOF: a framework for industrial maintenance concept development*. Leuven: Katholieke Universiteit Leuven.
17. Willian, J. (2013). *PALM III: introdução ao MATLAB para engenheiros* (3. ed.). São Paulo: McGraw Hill.



GLOBAL JOURNAL OF RESEARCHES IN ENGINEERING: A
MECHANICAL AND MECHANICS ENGINEERING
Volume 20 Issue 1 Version 1.0 Year 2020
Type: Double Blind Peer Reviewed International Research Journal
Publisher: Global Journals
Online ISSN: 2249-4596 & Print ISSN: 0975-5861

Self-Designed 3-D Printed Mask to Tackle COVID-19

By Hans Agarwal, Anshika Jain, Kapil Goyal & Sumiran Gupta

Abstract- In the current scenario of the pandemic of Covid-19, the mask is becoming an essential part of the human body. For this, we have designed a 3D mask on professional designing software called Solid Works, which will be 3D printed using polylactic acid (PLA) material, which is very light in weight, durable and cheap material. We have designed it in 3 different sizes—small, medium, and large according to the face type; everyone can select the best suitable size for themselves. A gap is significantly provided at the very front of the mask in which one inhale valve and two exhale valves will be attached to the mask so that no one will feel suffocated while wearing this mask and the respiration process can take place smoothly. Then CFD (Computational Fluid Dynamic) analysis of the flow of air passing through the designed mask is done using the simulation software ANSYS to check the ease in breathing while wearing this mask. After 3D printing, this mask on the Stratasys Fortus 400mc 3-D Printing System at Dayalbagh Educational Institute, Agra, India. The inner lining will be done by the silicon fiber padding, which will provide the soft and firm grip of the mask on the face as well as increase the protection against the virus. Then straps will be attached in the provided hooks in the design of the mask. The design of the mask can also be edited according to the face type of the person before 3D printing it to provide a high level of comfort to the wearer.

Keywords: mask, 3-D printing, COVID-19, solid works, ANSYS.

GJRE-A Classification: FOR Code: 091399p



Strictly as per the compliance and regulations of:



© 2020. Hans Agarwal, Anshika Jain, Kapil Goyal & Sumiran Gupta. This is a research/review paper, distributed under the terms of the Creative Commons Attribution-Noncommercial 3.0 Unported License <http://creativecommons.org/licenses/by-nc/3.0/>), permitting all non commercial use, distribution, and reproduction in any medium, provided the original work is properly cited.

Self-Designed 3-D Printed Mask to Tackle COVID-19

Hans Agarwal^α, Anshika Jain^σ, Kapil Goyal^ρ & Sumiran Gupta^ω

Abstract- In the current scenario of the pandemic of Covid-19, the mask is becoming an essential part of the human body. For this, we have designed a 3D mask on professional designing software called Solid Works, which will be 3D printed using polylactic acid (PLA) material, which is very light in weight, durable and cheap material. We have designed it in 3 different sizes—small, medium, and large according to the face type; everyone can select the best suitable size for themselves. A gap is significantly provided at the very front of the mask in which one inhale valve and two exhale valves will be attached to the mask so that no one will feel suffocated while wearing this mask and the respiration process can take place smoothly. Then CFD (Computational Fluid Dynamic) analysis of the flow of air passing through the designed mask is done using the simulation software ANSYS to check the ease in breathing while wearing this mask. After 3D printing, this mask on the Stratasys Fortus 400mc 3-D Printing System at Dayalbagh Educational Institute, Agra, India. The inner lining will be done by the silicon fiber padding, which will provide the soft and firm grip of the mask on the face as well as increase the protection against the virus. Then straps will be attached in the provided hooks in the design of the mask. The design of the mask can also be edited according to the face type of the person before 3D printing it to provide a high level of comfort to the wearer.

Keywords: mask, 3-D printing, COVID-19, solid works, ANSYS.

I. INTRODUCTION

Corona virus is taking hold across the globe; we see countries implementing social distancing measures, travel restrictions, and policies like work from home. Even the more developed countries are also seeing their healthcare systems overloaded by COVID-19.

According to the World Health Organization (WHO), people can transmit the virus to others while showing no signs or symptoms of COVID-19. A mathematical model from a 2020 study supports this, suggesting that 40–80% of transmission stems from those showing no symptoms [1].

Types of face mask people are currently using:

- Surgical mask
- Cloth face coverings
- Respirators, such as FFP2, N95, or the equivalent

We are making a 3-D printed mask for better protection with advanced technological valves to make sure the proper breathing process.

3-D printing is an additive manufacturing process by which three-dimensional solid objects are made by industries using a digital file containing the 3-D design details [2]. The creation of 3-D printed objects takes place in an additive manner, i.e., by laying down of material in successive layers. Each layer is a cross-section of the 3-D printed object. 3-D printing is used by people to build complex shapes using less material as compared to traditional manufacturing.

Nowadays, 3-D printing is becoming popular in aviation industries. 3-D printing is used for printing different parts of aircraft engines. Earlier individual components were constructed and had to be welded together by welding, but now, by use of many parts, 3-D printing is consolidated to a single component which is lighter in weight, uses lesser material, and, most importantly, it is about four-five times stronger. 3-D printing reduces the cost of labor as well as material and improves quality and thus, overall benefits the aviation industries [3]. GE Aviation is a company that has already started using 3-D printers for better efficiency, economical products that are lighter and stronger, and build using automated machinery with higher accuracy [4].

3-D printing starts with designing a 3-D model, i.e., Computer-aided design (CAD) model, a 3-D model, can be created or can be downloaded using the online 3-D repositories. Therefore 3-D scanners, apps, coding, or 3-D modeling software may be used to create designs.

PLA (poly lactic acid) is a green material and an alternative to petrochemical commodity plastics. Its mechanical characteristics are its superior tensile and flexural strength. PLA (poly lactic acid) is very light, with a density of 1.210 - 1.420 g-cm⁻³. PLA can be used in areas of high temperature without wear and tear as it has a high melting point of 423 to 433 K[5]. It is insoluble in water, making it useful during rains and humid weather conditions.

Author α σ ρ: Mechanical Engineering Department, Dayalbagh Educational Institute, Faculty of Engineering, Agra, India.
e-mails: agarwalhans.999@gmail.com, anshika174@gmail.com, kapil3012000@gmail.com

Author ω: Electrical Engineering Department, Dayalbagh Educational Institute, Faculty of Engineering, Agra, India.
e-mail: sumirangpt1@gmail.com

II. LITERATURE REVIEW

In previous research papers, there were various findings of masks, their usages, their comfort, their reusability, and the material appropriate for filtering out the germs. The researches show that 80% of the germ transmission can be lessened the masks are worn properly by the people. The comment is stated in some of the findings of Professor M.Fasher, D.Dwyer, and N.Ovdin along with few other prominent medical scientists [6]. In findings with different experiments by Van der Sande in 2008 / Netherlands, it was found that masks made from any material can reduce the viral transmission of diseases [7]. In 2013 a research by Davies in the United Kingdom proved that the surgical mask was three times more effective from the homemade masks in blocking any type of virus transmission. It also stated that homemade masks should be the last option to use. In 2011 in a meta-analysis by Jefferson, it was affirmed that N95 was more effective for any kind of respiratory viruses [8].

A research paper in 2013 by K.P. Chellamani, D. Veerasubramanian, and R.S. Vignesh Balaji showed the efficiency of the masks on the basis of the filtration, pressure difference, splash difference, etc. [9]. The Annals of Occupational Hygiene, Volume 48, Issue 8, November 2004, developed the prototype for half-mask face pieces from 3-d printing technology and the respiratory filters [10]. The previous researches show the use of different masks and their effectiveness in preventing the germs. In 2020 a demonstration by Amayu Wakoya Gena, DAAD scholarship holder at the chair of Bauphysik at the Bauhaus-Universität Weimar he showed how differently the air spreads by using of the mask and by not using it, this shows wearing a mask is a necessity for stopping the spread of respiratory viruses [11].

III. WORKING OF A MASK

There's no end to airborne diseases where working of a mask must be efficient. It is a type of a protective layer worn particularly over the nose and the mouth (the main entry points of the germs). Hence the making of the mask and its working is designed in a way such that it stops the 99% germs from entering in our body. It has three main components:

1. A filter that filters the germs/filter material that covers the whole nose and mouth.

2. The exhale valve for the warm air of the mouth to go out.
3. A string/band that keeps the mask intact of the mouth and nose.

The efficacy of the mask depends on the three components used appropriately to give the best results. Surgical masks made of the cloth prevent the larger respiratory droplets from entering [12] and hence, are made from single-layer cloth. While designing of mask, the thickness and permeability of the mask depend on the material's ability to absorb the particles; hence according to these parameters, the designing of the mask is done [12].

N95s are usually curved or duck-billed and, form a tight seal over the mouth and nose when fitted in correct manner. They can be uncomfortable to wear for longer durations of time. When surgical masks are worn outside the operation room, it works as a mask to stop the virus, and this mask is usually soft, pleated layers secured to the face with strings or ear loops, and pulled under the chin. So, they are more comfortable than N95s. Both N95s and surgical masks have an inner mesh that contains tiny plastic fibers that work as a filter. Also, both masks are disposable by design, usually discarded whenever they become too dirty, wet, or damaged [13].

The key role of the mask is to reduce the distance of the aerosol droplets while breathing, speaking, coughing and cold. That is why it is of utmost importance that we cover our face with our hand's side elbow while sneezing etc. and that is why masks are prime to wear to reduce the dispersal of the germs [14].

IV. METHODOLOGY

This design will be 3D printed after converting this solid-works file into. stl file format. PLA (Polylactic Acid) material will be used to 3D print the mask. PLA is a thermoplastic derived from renewable resources, so it is quite cheap as compared to the other 3D printing materials that are used for masks. PLA provides better strength with less weight, which makes it important for forming durable products. PLA is semi-transparent, so it yields a glossier surface which seems attractive. Some basic properties of PLA are referred from Table 01 [15], which also gives the strength to the mask made of PLA material.

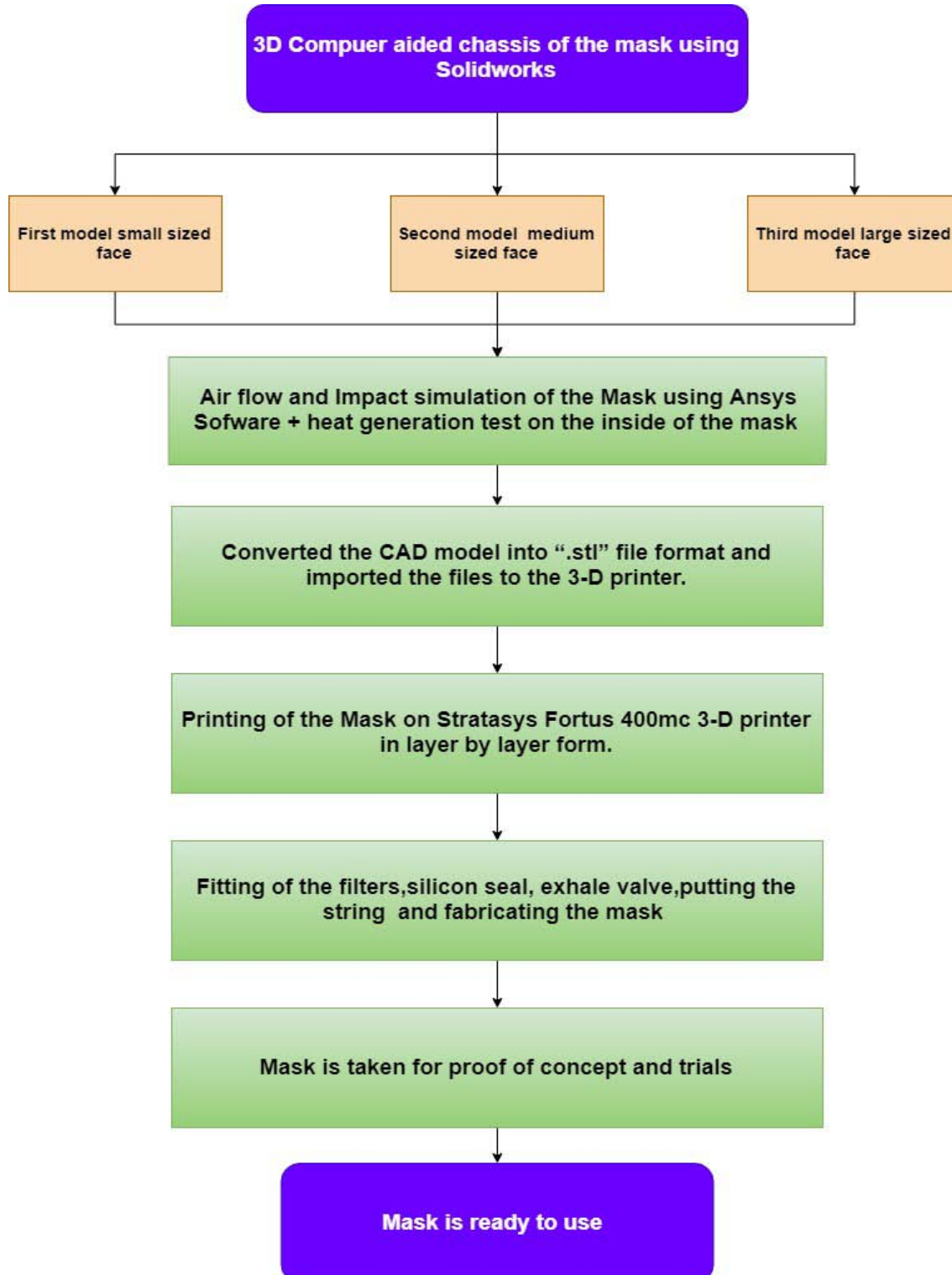
Table 1: [15]

Properties	Value
Tensile Strength	37 MPa
Density	1.3 g/cm ³
Percentage Elongation	6%
Flexural Modulus	4 GPa
Biodegradable	Yes, under the correct conditions
Melting Point Temperature [6]	423 – 433 K

The main criteria for designing this mask in 3-D designing software were to make it flexible for an upgrade according to the face type of the person. If any desired change in the design of a particular portion will be needed, then the whole mask design will not be

disturbed. Changes can be made at that particular part, and this upgrade will automatically transfer from the source file to the main assembly, which will also save the time.

The overall process for manufacturing this mask can be summarized in Flowchart 01:



Flowchart 1

V. DESIGN OF A MASK

We designed the mask in professional 3-D designing software namely, Solid Works, which will be 3-D printed on Stratasys Fortus 400mc 3-D Printing System in the 3-D printing lab, Dayalbagh Educational Institute, Agra, India. The screenshots of 3-D design are

given in Figure 01, Figure02, Figure 03, and Figure 04 with front view, side view, and top view. In the design of this mask, one rectangular slot is provided for an exhale valve or filter, and two elliptical hole slots are provided in the chassis of the mask to fix the inhale valves which prevents suffocation while wearing a mask.

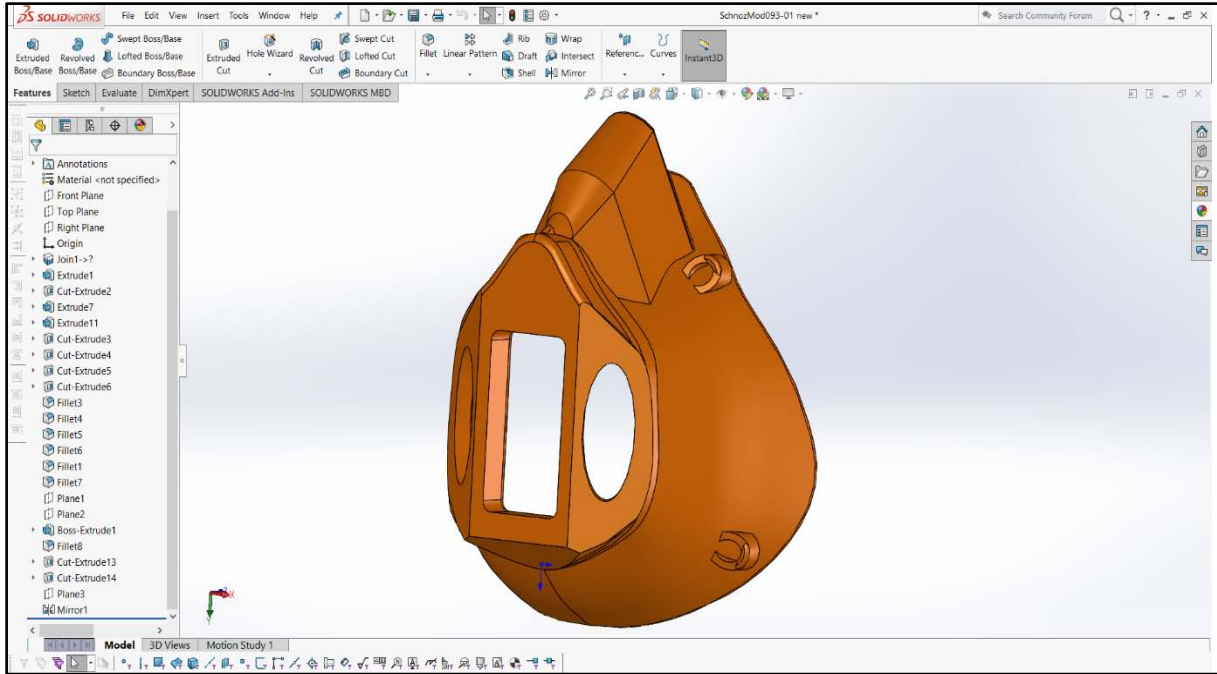


Figure 01: Screenshot of Solid Works 3-D Design of a Mask

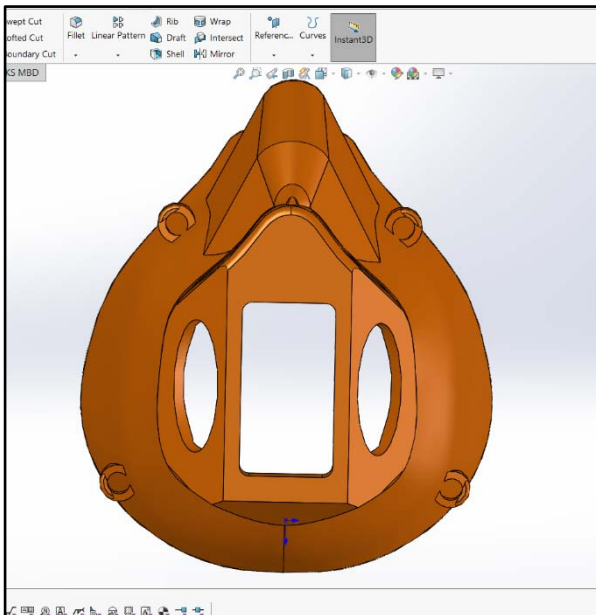


Figure 02: Front View

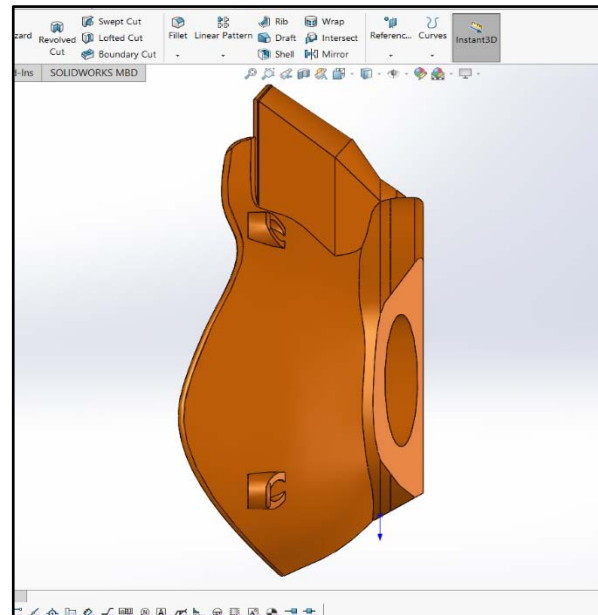


Figure 03: Side View

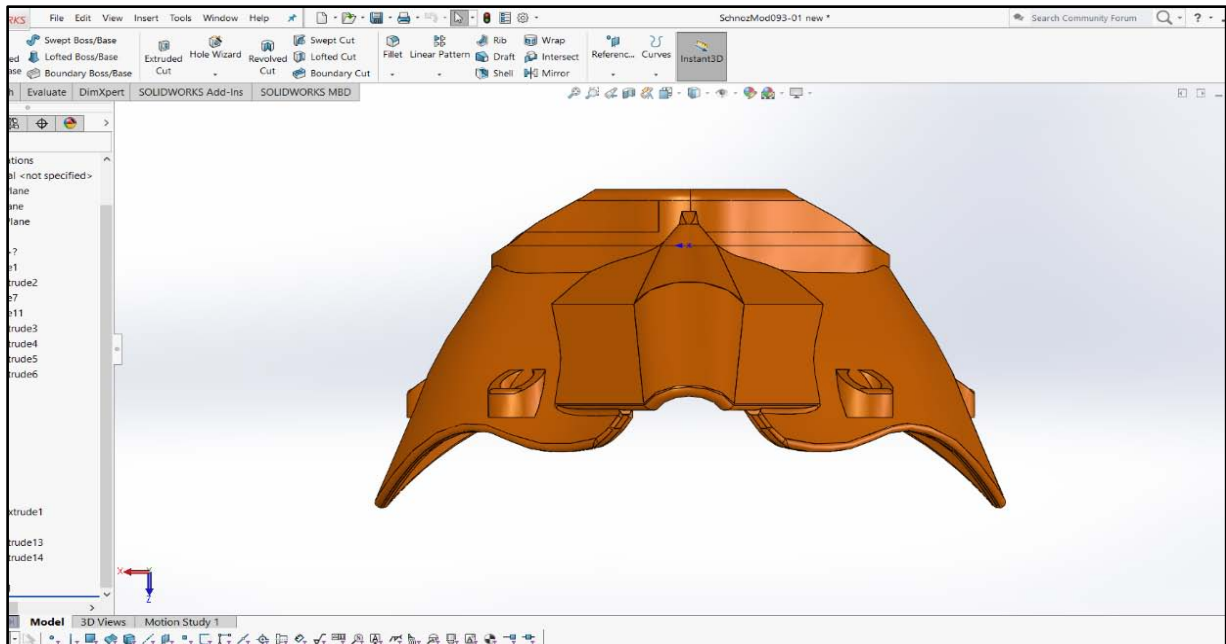
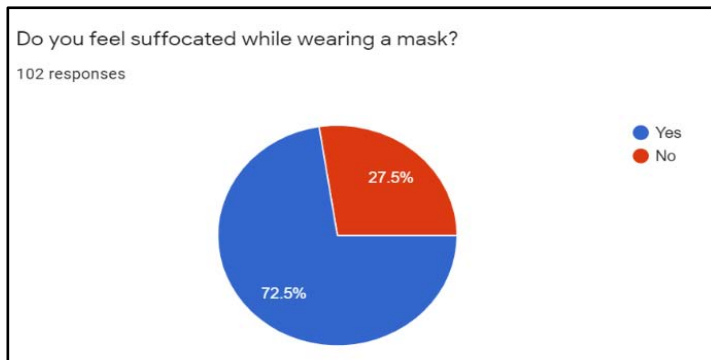


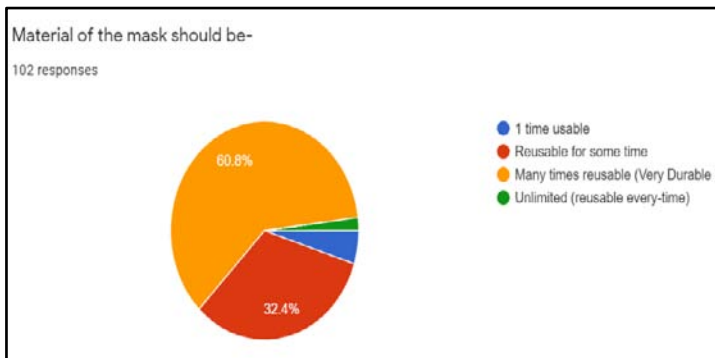
Figure 04: Top View

VI. STATISTICS AND GRAPHS



Nearly 73% of people felt suffocation while wearing mask because there is no or a small filter is provided for air transfer. Our mask will contain 3 valves; 2 for inhale, and 1 for exhale, so that no chances of suffocation will be there, and therefore people can wear it all the time.

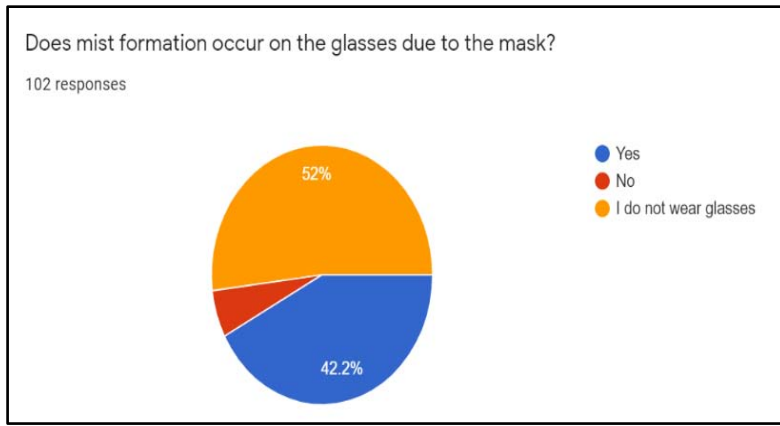
Graph 1



About 61% of the people want the material to be very durable, so we will use PLA (Polylactic Acid) material for the 3D printing of the mask. PLA is very durable, and possess a good resistance to wear and tear.

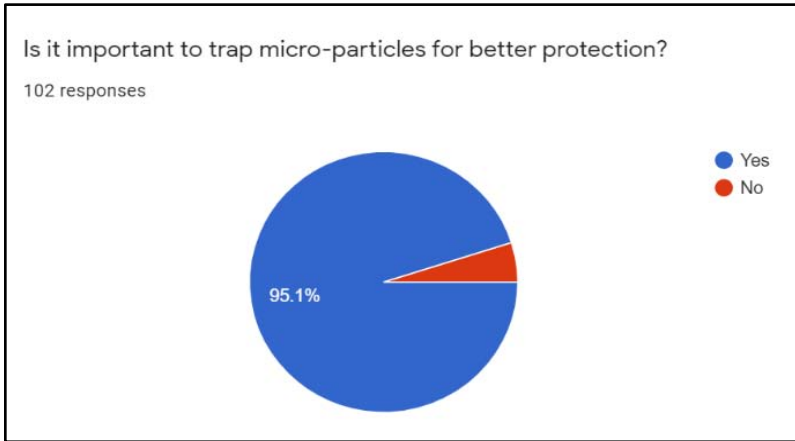
Graph 2





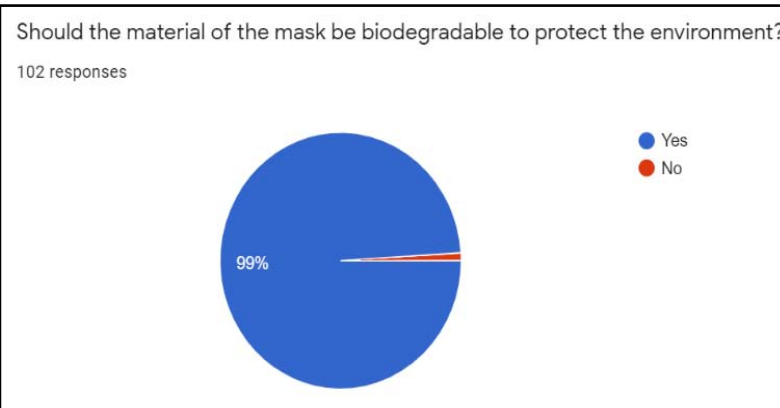
People who wear glasses feel the problem of mist formation on the mask because the distance between the mask and nose is quite less. Our mask will have sufficient distance so that no such problem will occur.

Graph 3



The material that we will use for the valves will be able to entrap the micro particles of Covid- 19, so the mask will allow full protection from the covid-19 infection.

Graph 4



Almost all of the people choose that the material for the mask should be biodegradable. The material PLA that we are using is also biodegradable, so it does not harm environment in any way.

Graph 5

VII. SIMULATION ANALYSIS

The CFD (Computational fluid dynamics) pressure analysis is done by us on the surface of the mask using the simulation software, namely ANSYS, which shows the durability of the material while wearing it. The screenshots shows the overall process with the results in Figure 05, Figure 06, and Figure 07.

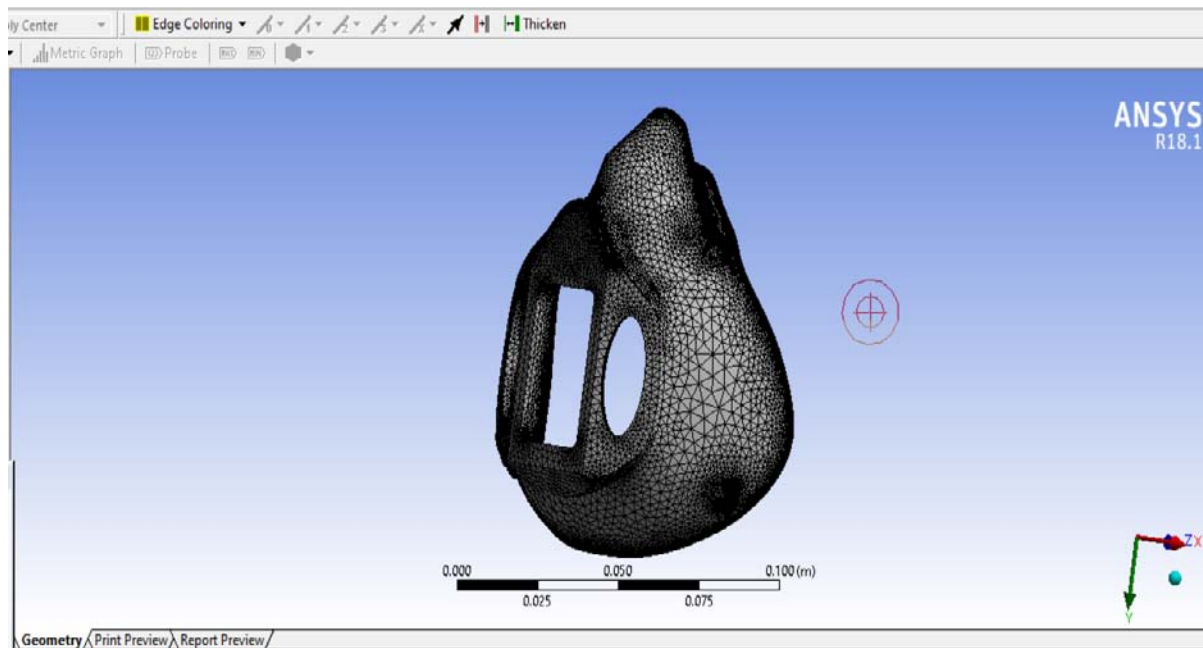


Figure 5: Meshing

The meshing of the mask is shown in Figure 05 and it is done by dividing the mask in very minute elements, and at the edges of the mask, the size of the meshing is very small to get the accurate and desired results. Figure 06 represents the graph of iterations while running the calculation. And finally, result of CFD

pressure analysis is shown with the color codes in Figure 07. As we can see, the red part is occurring at a smallest portion of the mask, and most of the part is either green or blue, so we can state that it can sustain high pressure, and this designed mask holds high durability.

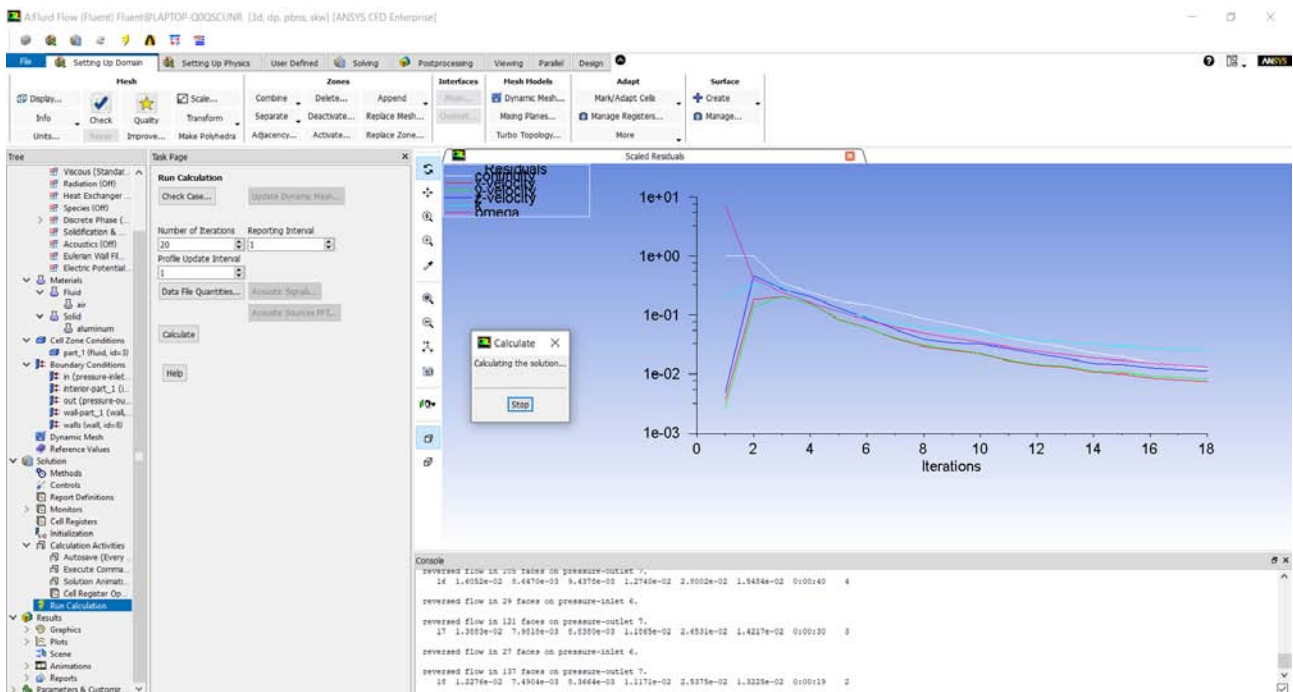


Figure 6: Iteration Graph

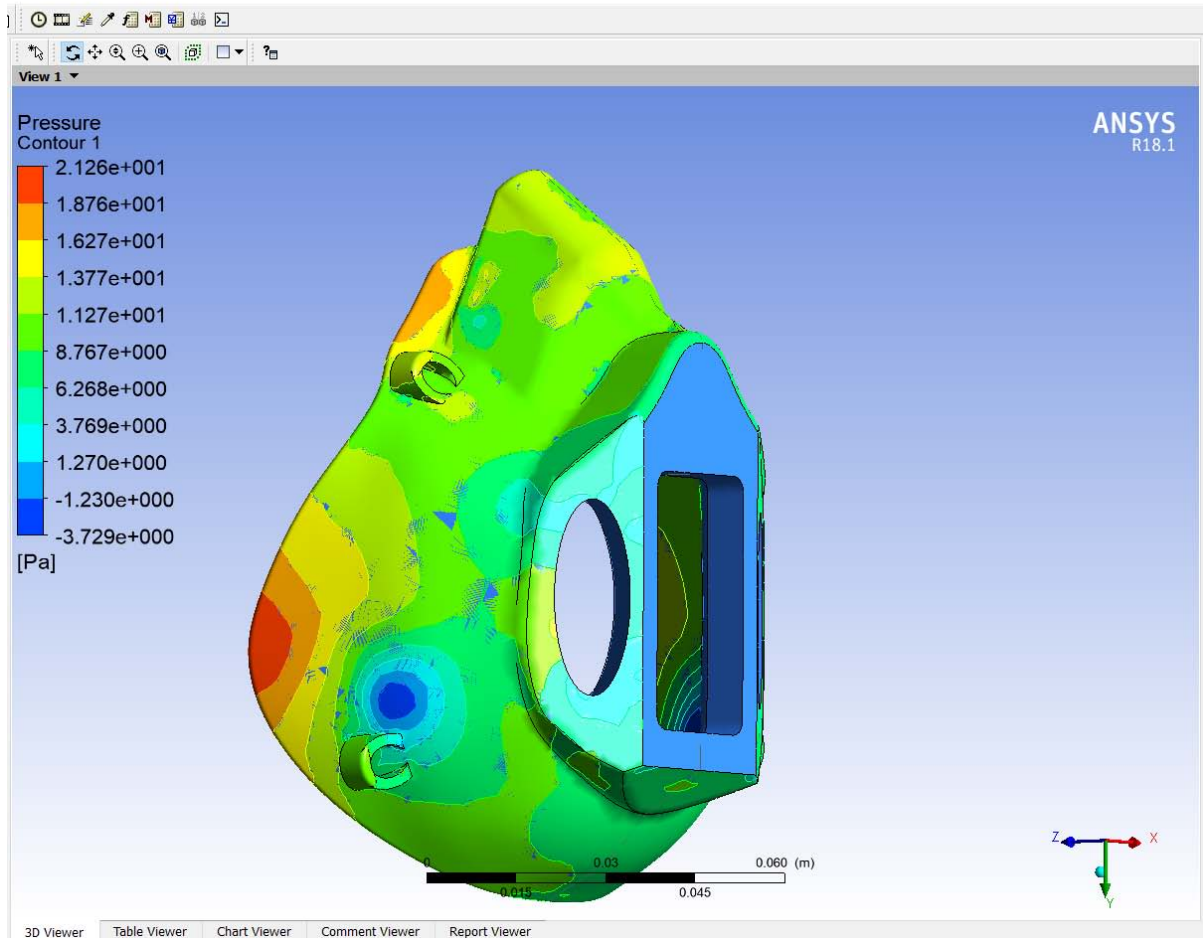


Figure 7: Pressure Simulation

VIII. CONCLUSION

With the Covid-19 pandemic at our doorsteps, face masks have become an integral part of our daily life. The masks which are currently available in the market lacks some basic human comfort and safety aspects such as lack of proper air circulation, mist formation in case of eye-glasses, unsatisfactory entrapment of micro-particles, limited reusability, etc. The prime perspective of our paper is to design a face mask that eliminates all these factors, and provides proper air circulation, no mist formation on eye-glasses, and the mask is made up of durable material having considerable reusability cycle.

The main result of the paper was that the 3-d printed mask is more durable than the regular 3d mask or surgical mask. The mask has better comfort and does not produce mist over the glass due to the exhale valve attached to it. The pie charts from the sample size of more than 100 people of every age show that people need a biodegradable mask that can be used for a sufficient amount of time, so 3-d printed mask is made from a biodegradable material which is durable as well. The mask is also light in weight and has valves which

can be used by people having claustrophobia, the material of the mask has high specific capacity, therefore, it does get heat up quickly; hence the mask overcomes crucial differences of the N95 mask as well as surgical masks.

Our achievement is the design of a 3D printed face mask, which provides all the aforesaid qualities. The mask is made of durable PLA (poly lactic acid) material, which is also biodegradable. This mask will provide all the human comfort and safety measures to the wearer. This mask can also be customized according to the facial anatomy of the wearer as it can be customized digitally on SolidWorks and can be 3D printed easily.

Another advantage of 3d printed mask is that it can have auxiliary attachments (shield) fit into the 3d chassis of the mask, which makes it flexible according to the use and necessity.

With the help of our supervisors in the Dayalbagh Educational Institute, India, we have got all the technical knowledge and resources to complete this project successfully. This paper describes the complete design of an indigenous mask.

REFERENCES RÉFÉRENCES REFERENCIAS

1. "Why face masks are important," Medical News Today, [Online]. Available: <https://www.medicalnewstoday.com/articles/types-of-face-mask#why-they-are-important>. [Accessed 01 06 2020].
2. "3D printing scales up," 3D printing, 05 09 2013. [Online]. Available: <https://www.economist.com/technology-quarterly/2013/09/05/3d-printing-scales-up>. [Accessed 18 09 2019].
3. "Tractus3D," Tractus3D, [Online]. Available: <https://tractus3d.com/what-is-3d-printing/advantages-of-3d-printing/>. [Accessed 18 09 2019].
4. "what is 3d printing," october 2018. [Online]. Available: <https://3dprinting.com/what-is-3d-printing/>. [Accessed 19 09 2019].
5. A. Södergård and M. Stolt, "Properties of lactic acid based polymers and their correlation with composition," Progress in Polymer Science, vol. 6, no. 27, pp. 1123-1163, 2002.
6. D. a. N. M.Fasher, "What Research Says About The Effectiveness of Face Masks?" HEALTH JOURNAL, 2018.
7. V. d. Sande, "Papers about effectiveness of basic masks #masks4all," 2008. [Online]. Available: https://docs.google.com/document/d/1HLrm0pqBN_5bdyysOeoOBX4pt4oFDBhsC_jpbIXpNtQ/edit#. [Accessed 03 06 2020].
8. Jefferson, "Papers about effectiveness of basic masks #masks4all," 2011. [Online]. Available: https://docs.google.com/document/d/1HLrm0pqBN_5bdyysOeoOBX4pt4oFDBhsC_jpbIXpNtQ/edit#. [Accessed 03 06 2020].
9. D. V. a. R. V. B. K.P. Chellamani*, "Surgical Face Masks: Manufacturing Methods and Classification," Journal of Academia and Industrial Research (JAIR), vol. 2, no. 6, pp. 320-324, 2013.
10. J. R. J. L. DON-HEE HAN, "Development of Prototypes of Half-Mask Facepieces for Koreans Using the 3D Digitizing Design Method: A Pilot Study," The Annals of Occupational Hygiene, vol. 48, no. 8, pp. 707-714, 2014.
11. A. Wakoya, "Keep your distance: A new video from the Bauhaus-Universität Weimar illustrates how germs can spread through the air.," Bauhaus. Journal online, 20 03 2020. [Online]. Available: <https://www.uni-weimar.de/de/universitaet/aktuell/bauhausjournal-online/titel/abstand-halten-neues-video-der-bauhaus-universitaet-weimar-verdeutlicht-wie-sich-atemluft-ausbreite/>. [Accessed 03 06 2020].
12. C. F. Y. M. S. F. L. C. C. T. Vittoria Offeddu, "Effectiveness of Masks and Respirators Against Respiratory Infections in Healthcare Workers: A Systematic Review and Meta-Analysis," Clinical Infectious Diseases, vol. 65, no. 11, pp. 1934-1942, 2017.
13. F. JABR, "It's Time to Face Facts, America: Masks Work," 30 03 2020. [Online]. Available: <https://www.wired.com/story/its-time-to-face-facts-america-masks-work/>. [Accessed 04 06 2020].
14. M. M.-C. K. M. J. Y. K. P. H.-H. C. B. J. S. L. P. J. J. M. M.-J. K. M. D. K. O. M. M.-K. L. M. S.-H. C. M. M. S. P. S.-B. H. M. J.-W. C. M. S.-H. K. M. Seongman Bae, "Effectiveness of Surgical and Cotton Masks in Blocking SARS-CoV-2: A Controlled Comparison in 4 Patients," Annals of internal medicine, 06 04 2020.
15. K. Giang, "3dhubs," 3D Hubs: Local 3D printing services, [Online]. Available: <https://www.3dhubs.com/knowledge-base/pla-vs-abs-whats-difference>. [Accessed 06 08 2019].
16. "DroneBot Workshop," DroneBot Workshop, [Online]. Available: <https://dronebotworkshop.com/how-does-a-quadcopter-work/>. [Accessed 12 09 2019].
17. V. Kadamatt, "HOW QUADCOPTERS WORK & FLY: AN INTRO TO MULTIROTORS," 20 11 2017. [Online]. Available: <http://www.droneybee.com/how-quadcopters-work/>. [Accessed 13 09 2019].
18. M. B. J. D. Mr. Kalpesh N. Shah, "Quadrotor – An Unmanned Aerial Vehicle", IJEDR, vol. 2, no. 1, pp. 1299-1303, 2014.
19. T. N. C. P. Pooja Srivastava, "Quadcopter for Rescue Missions and Surveillance," IOSR Journal of Computer Engineering, vol. 1, pp. 48-52, 2017.
20. H. H. S. L. W. C. J. T. Gabriel M. Hoffmann, "Quadrotor Helicopter Flight Dynamics and Control," in American Institute of Aeronautics and Astronautics.
21. J. Dickey, "Air Wolf 2," quadcopterproject, [Online]. Available: <https://quadcopterproject.wordpress.com/static-thrust-calculation/>. [Accessed 18 09 2019].



This page is intentionally left blank



GLOBAL JOURNAL OF RESEARCHES IN ENGINEERING: A
MECHANICAL AND MECHANICS ENGINEERING
Volume 20 Issue 1 Version 1.0 Year 2020
Type: Double Blind Peer Reviewed International Research Journal
Publisher: Global Journals
Online ISSN: 2249-4596 & Print ISSN: 0975-5861

A Study of Automated Optical Inspection of Rapid Influenza Diagnostic Tests

By Wen-Tung Hsua & Cheng-Ho Chenb

National Chin-Yi University of Technology

Abstract- Rapid influenza diagnostic test (RIDT) is one of the most common tools for screening patients suspected of influenza infection. The principle is to detect the surface antigen of influenza virus with known antibodies, and then to interpret it with the naked eye in the form of immune chromatographic assays. It has the advantage of obtaining speedy results (10-30 minutes) and ease of operation (which can be interpreted with the naked eye). There is a variety of rapid influenza diagnostic tests (RIDTs) available in the market, with different sensitivities and specificities depending on the design of the antibody location and reagent composition. Despite its advantages of speed and convenience, a high percentage of test results (20 to 50% or higher) do not correctly reflect the patient's status. In addition to possible misses in the specimen collection process that will affect the tests; the naked eye may not be able to distinguish the unapparent results and cause false negatives. At the same time, because a healthcare worker may not accurately grasp the time of interpretation, false positives can also occur due to excessive test times. To minimize incorrect diagnoses, we propose an interpretation system using machine vision. The system replaces the function of a healthcare worker by a camera and computer. The camera captures the image of the test piece then sent it to the computer for processing and identification; the result can provide the medical staff reference.

Keywords: rapid diagnosis; optical inspection; influenza; machine vision.

GJRE-A Classification: FOR Code: 091399



A STUDY OF AUTOMATED OPTICAL INSPECTION OF RAPID INFLUENZA DIAGNOSTIC TESTS

Strictly as per the compliance and regulations of:



RESEARCH | DIVERSITY | ETHICS

© 2020. Wen-Tung Hsua & Cheng-Ho Chenb. This is a research/review paper, distributed under the terms of the Creative Commons Attribution-Noncommercial 3.0 Unported License (<http://creativecommons.org/licenses/by-nc/3.0/>), permitting all non commercial use, distribution, and reproduction in any medium, provided the original work is properly cited.

A Study of Automated Optical Inspection of Rapid Influenza Diagnostic Tests

Wen-Tung Hsua^α & Cheng-Ho Chen^σ

Abstract- Rapid influenza diagnostic test (RIDT) is one of the most common tools for screening patients suspected of influenza infection. The principle is to detect the surface antigen of influenza virus with known antibodies, and then to interpret it with the naked eye in the form of immune chromatographic as says. It has the advantage of obtaining speedy results (10-30 minutes) and ease of operation (which can be interpreted with the naked eye). There is a variety of rapid influenza diagnostic tests (RIDTs) available in the market, with different sensitivities and specificities depending on the design of the antibody location and reagent composition. Despite its advantages of speed and convenience, a high percentage of test results (20 to 50% or higher) do not correctly reflect the patient's status. In addition to possible misses in the specimen collection process that will affect the tests; the naked eye may not be able to distinguish the unapparent results and cause false negatives. At the same time, because a healthcare worker may not accurately grasp the time of interpretation, false positives can also occur due to excessive test times. To minimize incorrect diagnoses, we propose an interpretation system using machine vision. The system replaces the function of a healthcare worker by a camera and computer. The camera captures the image of the test piece then sent it to the computer for processing and identification; the result can provide the medical staff reference.

Keywords: rapid diagnosis; optical inspection; influeza; machine vision.

I. INTRODUCTION

Virus-caused influenza is one of the most severe viral respiratory infectious disease. Avian influenza of 2003 and the swine flu of 2009 have been among the cases in recent years. Once a highly contagious and lethal strain of influenza virus emerges, it often leads to a pandemic. Therefore, aside from the SARS of 2013 and COVID-19 of 2019-2020, which are also virus-caused, influenza has been the focus of international epidemic prevention and monitoring policy. Because influenza shares many symptoms with the common cold, it is often difficult for a clinician to correctly diagnose the disease in a timely fashion. The standard method for detecting influenza viruses is viral culture and molecular biology testing methods such as RT-PCR, both of which can identify subtypes. Still, both

need special equipment and longer testing times. Viral culture takes at least 48 hours, RT-PCR takes 4-6 hours, so clinicians in small clinics, emergency rooms or outpatient settings cannot obtain results in a short period after the examination, resulting in incoherent diagnosis. Consequently, healthcare workers use a series of rapid influenza diagnostic tests (RIDTs) at the point of care. The principle is to detect the surface antigen of influenza virus with known antibodies, and then to interpret with the naked eye in the form of immune chromatographic as says. They are simple to execute and deliver results in less than 30 minutes. They have become an effective way to detect viruses outside the laboratory. Overall, RIDTs had a high specificity of 90-95% but only a modest sensitivity of 50-80%. Studies show the performance of RIDTs depends on the prevalence of influenza virus in the population [1,2]. A study points out RIDTs with a sensitivity of 62.3% compared to the RT-PCR method [3]. In the study, RIDTs performed better in influenza A virus detection. 64.6% sensitivity in influenza A compare to 52.2% in influenza B. During the 2009 H1N1 pandemic, RIDTs showed 10%-70% sensitivity compared to RT-PCR-based tests [4-7]. Drexler et al. used the BinaxNOW rapid antigen-based testing, reported a sensitivity of 11.1% [8]. In the early days of the pandemic, a large study from New York used the RIDTs BinaxNOW influenza A-B test (BinaxNOW), 3M Rapid Detection Flu A-B test (3MA+B) compared to R-Mix culture [9,10] with a sensitivity of 9.6% and 40% respectively. Poor sample quality and inexperience of medical staff may contribute to the low sensitivity. These researches indicate many factor scan affect the sensitivity of RIDTs. It is low in numerous cases, so this study proposes a system to improve detection sensitivity, minimize the human influence, increase efficiency and reduce the demand for screening work force.

II. PROBLEM STATEMENT

Figure 1 illustrates the procedures for taking an RIDT: (a) Collect the patient's nasopharyngeal specimen through a swap, b. Flush it in a solvent provided by the manufacturer, c. Suck up the fluid using a pipette, then drop it to a specified place on the test pad.

Author ^α: Taichung Armed Forces General Hospital, Taichung, Taiwan.
e-mail: wen-tung@830.org.tw

Author ^σ: National Chin-Yi University of Technology, Taichung, Taiwan.
e-mail: chench@ncut.edu.tw

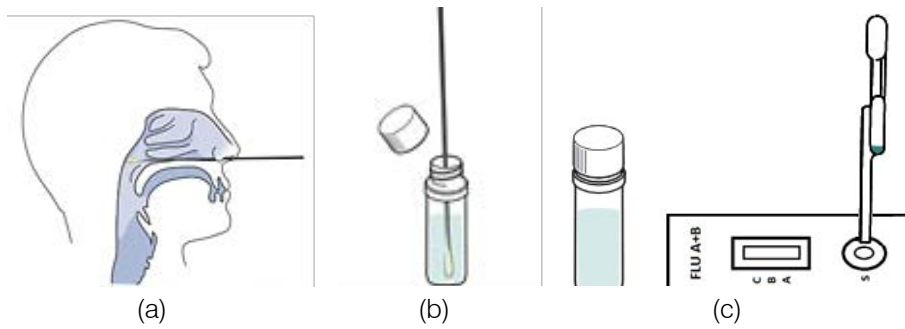


Figure 1: Procedures for Taking a Rapid Influenza Diagnosis Test

After 15 minutes at room temperature, determine whether there is influenza and influenza type (A or B) based on the stripes displayed on the pad, as shown in Figure 2, provided that the control line appears

at the same time. If the control line at C does not appear, it is an invalid detection, repeat the test until a control line shows up.

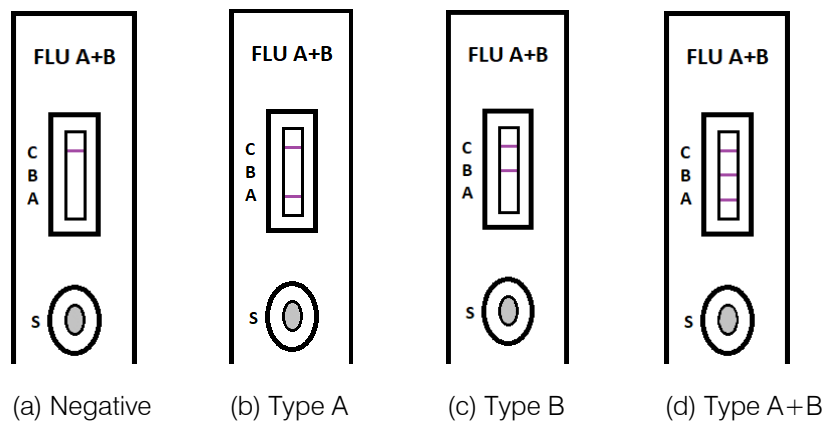


Figure 2: Test Results

The test procedure requires the healthcare worker to make a diagnosis if a stripe, no matter how faint it is, appears at the designated position as long as the control line is also visible. In clinical practice, however, there may be cases too vague for the human to make a definite judgment. Figure 3 displays some

examples with faint stripes. Even if one makes a diagnosis, it is nearly impossible to be consistent. This can explain the high false positives during the peak of the influenza season and high false negatives during the low season.

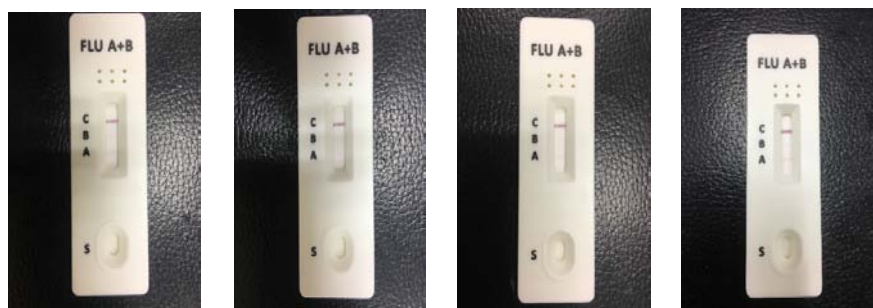


Figure 3: Some test examples with faint stripes

This study applies machine vision technology to develop an automatic interpretation system for RIDTs to assist healthcare workers in the conduct of influenza virus testing, improve the correctness and efficiency, save workforce, and reduce the risk of misjudgment. Other medical tests currently dependent on the naked eye can also implement similar techniques.

III. HARDWARE SETUP

A typical optical inspection system includes a camera, a computer, a light source, and other necessary mechanical and electrical components. Figure 4 depicts a CAD model of the one for RIDT. Figure 5(a) shows the actual mechanism. A groove is

cut in the bedplate to contain the test specimen, as shown in Figure 5(b). Figure 5(c) shows the optical apparatuses in a position to capture the specimen image. The device connects with a computer.

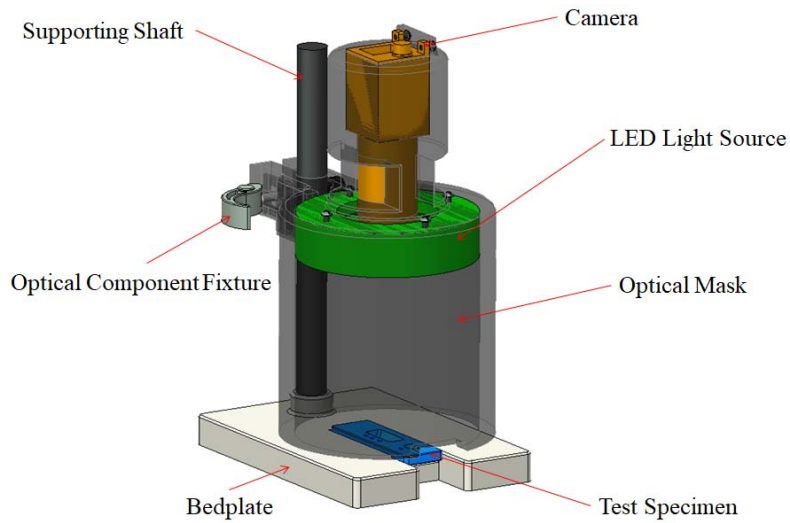


Figure 4: A CAD model of the RIDT inspection system

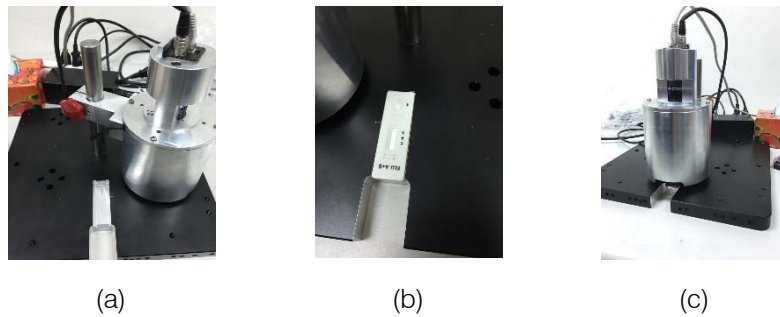


Figure 5: The developed RIDT inspection system

IV. IMAGE PROCESSING

The captured image, shown in Figure 6, is transmitted to the computer, which analyzes the stripes

of the test specimen. The following subsections discuss the image processing techniques employed by the computer program.



Figure 6: The captured image of a test specimen

a) *Image Pre-Processing*

First, the test pad and the area showing the test lines are identified by image pre-processing. The specimen is overall much brighter than its background. The program separates them by a binary threshold, Figure 7(a). To find the region where the test lines may appear, the image is then processed by the Laplace-of-

Gaussian (LoG) operator, Figure 7(b). The edges of possible features are found by the zero-crossing operation, Figure 7(c). The components are joined by the connection operation, Figure 7(d). The software finds the test region by selecting the one with the rectangularity between 0.9 and 1, and an area larger than 5000 pixels, Figure 7(e).

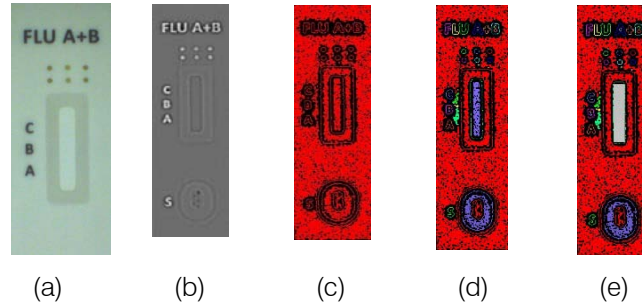


Figure 7: Image pre-processing of the test specimen

b) *Identification of Diagnosis Line*

The camera takes the image of the test specimen every minute. The suggested time for RIDTs inspection is 15 minutes. Figure 8(a) is the image taken after 15 minutes. The test region is identical to the previous step, as shown in Figure 8(b). The gray value is

then spread from 0 to 255 to enhance the image. Figure 8(c) portrays the enhanced image. The program identifies lines on the image by using partial derivatives of a Gaussian smoothing kernel; and shows the extracted lines in red, as in Figure 8(d).

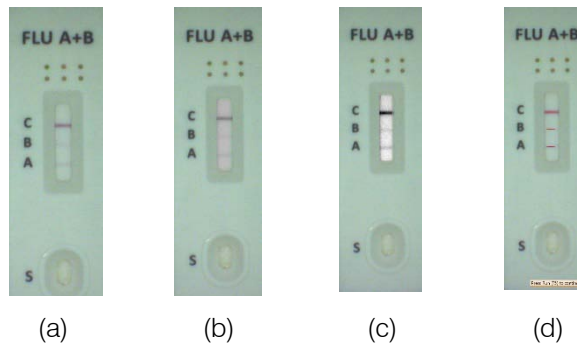


Figure 8: Specimen Image Processing after 15 minutes

c) *Gray-value Calculation*

The program also calculates the gray changes of the test region. It averages the values of each row in the test region, and subtracts the initial numbers from those of later times. Significant changes in gray value indicate test lines, as illustrated in Figure 9. The

horizontal axis represents the row position of the test region, as 0 being the top-most row. The vertical axis denotes the difference of gray values between the initial specimen and the specimen after 15 minutes. Three peaks appear in positions that correspond to the three stripes.

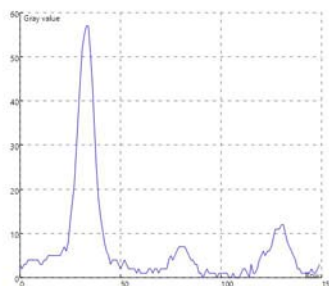


Figure 9: Gray value variations of the test specimen after 15 minutes

From Figures 8 and 9, healthcare workers can easily see the test results. The program can also provide the identification result of the specimen at any specified

time. Figure 10 shows the results at (a) 5 minute, (b) 10 minute, (c) 15 minute and (d) 20 minute.

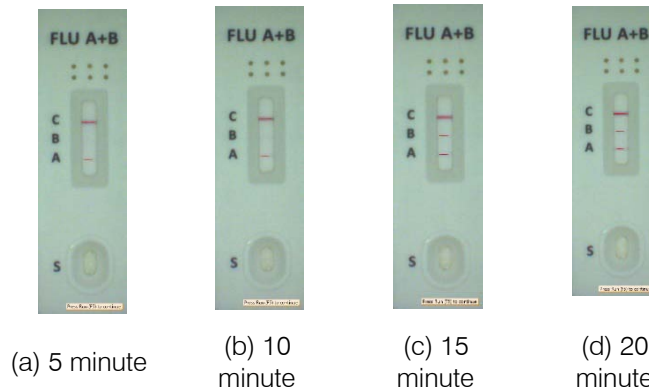


Figure 10: Specimen identification results at different times

The identification results can then be stored and analyzed. Figure 11 shows the changes in gray values from 1 to 20 minutes at A, B, and C positions,

respectively. It can provide a basis for accessing the test results.

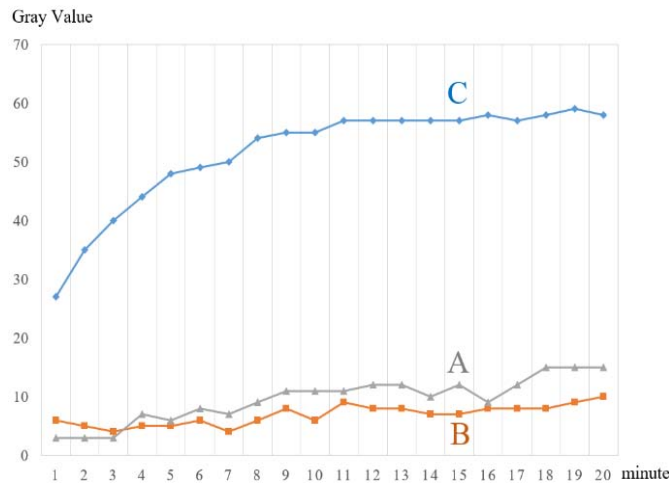


Figure 11: Gray value changes along time at A, B and C line positions

V. CONCLUSION

This research studies the implantation of optical inspection in RIDTs and development of a working system. The experimental results show that it can provide useful assistance to the healthcare workers. With more clinical cases, its consistency and sensitivity can be examined. One may also extend the method to similar rapid tests in medical practices, e.g., COVID-19 diagnosis tests. A proper application of optical inspection techniques will reduce the medical staff's workload and possible human errors, in the meantime, increase test sensitivity and consistency.

ACKNOWLEDGMENT

This research is partially supported by Taiwan Taichung Armed Forces General Hospital Medical Service Fund No. 103A23.

REFERENCES RÉFÉRENCES REFERENCIAS

1. Cruz, A.T.; Demmler-Harrison, G.J.; Caviness, A.C.; Buffone, G.J.; Revell, P.A. Performance of a rapid influenza test in children during the H1N1 2009 influenza outbreak. *Pediatrics* 2010, 125, e645–e650.
2. Harper, S.A.; Bradley, J.S.; Englund, J.A.; File, T.M.; Gravenstein, S.; Hayden, F.G.; McGeer, A.J.; Neuzil, K.M.; Pavia, A.T.; Tapper, M.L.; et al. Seasonal influenza in adults and children—diagnosis, treatment, chemoprophylaxis, and institutional outbreak management: Clinical practice guidelines of the Infectious Diseases Society of America. *Clin. Infect. Dis.* 2009, 48, 1003–1032.
3. Chartrand, C.; Leeflang, M.M.; Minion, J.; Brewer, T.; Pai, M. Accuracy of rapid influenza diagnostic

- tests: A meta-analysis. *Ann. Intern. Med.* 2012, 156, 500–511.
4. Drexler, J.F.; Helmer, A.; Kirberg, H.; Reber, U.; Panning, M.; Muller, M.; Hofling, K.; Matz, B.; Drosten, C.; Eis-Hubinger, A.M. Poor clinical sensitivity of rapid antigen test for influenza A pandemic (H1N1) 2009 virus. *Emerg Infect. Dis.* 2009, 15, 1662–1664.
 5. Gordon, A.; Videa, E.; Saborio, S.; Lopez, R.; Kuan, G.; Balmaseda, A.; Harris, E. Diagnostic accuracy of a rapid influenza test for pandemic influenza A H1N1. *PLoS ONE* 2010, 5, e10364.
 6. Gordon, A.; Videa, E.; Saborio, S.; Lopez, R.; Kuan, G.; Reingold, A.; Balmaseda, A.; Harris, E. Performance of an influenza rapid test in children in a primary healthcare setting in Nicaragua. *PLoS ONE* 2009, 4, e7907.
 7. Louie, J.K.; Guevara, H.; Boston, E.; Dahlke, M.; Nevarez, M.; Kong, T.; Schechter, R.; Glaser, C.A.; Schnurr, D.P. Rapid influenza antigen test for diagnosis of pandemic (H1N1) 2009. *Emerg Infect. Dis.* 2010, 16, 824–826.
 8. Diederer, B.M.; Veenendaal, D.; Jansen, R.; Herpers, B.L.; Ligtvoet, E.E.; Ijzerman, E.P. Rapid antigen test for pandemic (H1N1) 2009 virus. *Emerg Infect. Dis.* 2010, 16, 897–898.
 9. Ginocchio, C.C.; Zhang, F.; Manji, R.; Arora, S.; Bornfreund, M.; Falk, L.; Lotlikar, M.; Kowerska, M.; Becker, G.; Korologos, D.; et al. Evaluation of multiple test methods for the detection of the novel 2009 influenza A (H1N1) during the New York City outbreak. *J. Clin. Virol.* 2009, 45, 191–195.
 10. Crawford, J.M.; Stallone, R.; Zhang, F.; Gerolimatos, M.; Korologos, D.D.; Sweetapple, C.; de Geronimo, M.; Dlugacz, Y.; Armellino, D.M.; Ginocchio, C.C. Laboratory surge response to pandemic (H1N1) 2009 outbreak, New York City metropolitan area, USA. *Emerg Infect. Dis.* 2010, 16, 8–13.
 11. CDC. Evaluation of rapid influenza diagnostic tests for detection of novel influenza A (H1N1) Virus—United States, 2009. *MMWR Morb. Mortal. Wkly. Rep.* 2009, 58, 826–829.
 12. Faix, D.J.; Sherman, S.S.; Waterman, S.H. Rapid-test sensitivity for novel swine-origin influenza A (H1N1) virus in humans. *N. Engl. J. Med.* 2009, 361, 728–729.
 13. Crawford, J.M.; Stallone, R.; Zhang, F.; Gerolimatos, M.; Korologos, D.D.; Sweetapple, C.; de Geronimo, M.; Dlugacz, Y.; Armellino, D.M.; Ginocchio, C.C. Laboratory surge response to pandemic (H1N1) 2009 outbreak, New York City metropolitan area, USA. *Emerg Infect. Dis.* 2010, 16, 8–13.
 14. Andresen, D.N.; Kesson, A.M. High sensitivity of a rapid immune chromatographic test for detection of influenza A virus 2009 H1N1 in nasopharyngeal aspirates from young children. *J. Clin. Microbiol.* 2010, 48, 2658–2659.

GLOBAL JOURNALS GUIDELINES HANDBOOK 2020

WWW.GLOBALJOURNALS.ORG

MEMBERSHIPS

FELLOWS/ASSOCIATES OF ENGINEERING RESEARCH COUNCIL

FERC/AERC MEMBERSHIPS

INTRODUCTION



FERC/AERC is the most prestigious membership of Global Journals accredited by Open Association of Research Society, U.S.A (OARS). The credentials of Fellow and Associate designations signify that the researcher has gained the knowledge of the fundamental and high-level concepts, and is a subject matter expert, proficient in an expertise course covering the professional code of conduct, and follows recognized standards of practice. The credentials are designated only to the researchers, scientists, and professionals that have been selected by a rigorous process by our Editorial Board and Management Board.

Associates of FERC/AERC are scientists and researchers from around the world are working on projects/researches that have huge potentials. Members support Global Journals' mission to advance technology for humanity and the profession.

FERC

FELLOW OF ENGINEERING RESEARCH COUNCIL

FELLOW OF ENGINEERING RESEARCH COUNCIL is the most prestigious membership of Global Journals. It is an award and membership granted to individuals that the Open Association of Research Society judges to have made a 'substantial contribution to the improvement of computer science, technology, and electronics engineering.

The primary objective is to recognize the leaders in research and scientific fields of the current era with a global perspective and to create a channel between them and other researchers for better exposure and knowledge sharing. Members are most eminent scientists, engineers, and technologists from all across the world. Fellows are elected for life through a peer review process on the basis of excellence in the respective domain. There is no limit on the number of new nominations made in any year. Each year, the Open Association of Research Society elect up to 12 new Fellow Members.



BENEFIT

TO THE INSTITUTION

GET LETTER OF APPRECIATION

Global Journals sends a letter of appreciation of author to the Dean or CEO of the University or Company of which author is a part, signed by editor in chief or chief author.



EXCLUSIVE NETWORK

GET ACCESS TO A CLOSED NETWORK

A FERC member gets access to a closed network of Tier 1 researchers and scientists with direct communication channel through our website. Fellows can reach out to other members or researchers directly. They should also be open to reaching out by other.

Career

Credibility

Exclusive

Reputation



CERTIFICATE

CERTIFICATE, LOR AND LASER-MOMENTO

Fellows receive a printed copy of a certificate signed by our Chief Author that may be used for academic purposes and a personal recommendation letter to the dean of member's university.

Career

Credibility

Exclusive

Reputation



DESIGNATION

GET HONORED TITLE OF MEMBERSHIP

Fellows can use the honored title of membership. The "FERC" is an honored title which is accorded to a person's name viz. Dr. John E. Hall, Ph.D., FERC or William Walldroff, M.S., FERC.

Career

Credibility

Exclusive

Reputation

RECOGNITION ON THE PLATFORM

BETTER VISIBILITY AND CITATION

All the Fellow members of FERC get a badge of "Leading Member of Global Journals" on the Research Community that distinguishes them from others. Additionally, the profile is also partially maintained by our team for better visibility and citation. All fellows get a dedicated page on the website with their biography.

Career

Credibility

Reputation

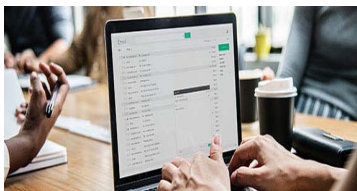
FUTURE WORK

GET DISCOUNTS ON THE FUTURE PUBLICATIONS

Fellows receive discounts on the future publications with Global Journals up to 60%. Through our recommendation programs, members also receive discounts on publications made with OARS affiliated organizations.

Career

Financial



GJ ACCOUNT

UNLIMITED FORWARD OF EMAILS

Fellows get secure and fast GJ work emails with unlimited storage of emails that they may use them as their primary email. For example, john [AT] globaljournals [DOT] org.

Career

Credibility

Reputation



PREMIUM TOOLS

ACCESS TO ALL THE PREMIUM TOOLS

To take future researches to the zenith, fellows receive access to all the premium tools that Global Journals have to offer along with the partnership with some of the best marketing leading tools out there.

Financial

CONFERENCES & EVENTS

ORGANIZE SEMINAR/CONFERENCE

Fellows are authorized to organize symposium/seminar/conference on behalf of Global Journal Incorporation (USA). They can also participate in the same organized by another institution as representative of Global Journal. In both the cases, it is mandatory for him to discuss with us and obtain our consent. Additionally, they get free research conferences (and others) alerts.

Career

Credibility

Financial

EARLY INVITATIONS

EARLY INVITATIONS TO ALL THE SYMPOSIUMS, SEMINARS, CONFERENCES

All fellows receive the early invitations to all the symposiums, seminars, conferences and webinars hosted by Global Journals in their subject.

Exclusive





PUBLISHING ARTICLES & BOOKS

EARN 60% OF SALES PROCEEDS

Fellows can publish articles (limited) without any fees. Also, they can earn up to 70% of sales proceeds from the sale of reference/review books/literature/publishing of research paper. The FERC member can decide its price and we can help in making the right decision.

Exclusive Financial

REVIEWERS

GET A REMUNERATION OF 15% OF AUTHOR FEES

Fellow members are eligible to join as a paid peer reviewer at Global Journals Incorporation (USA) and can get a remuneration of 15% of author fees, taken from the author of a respective paper.

Financial

ACCESS TO EDITORIAL BOARD

BECOME A MEMBER OF THE EDITORIAL BOARD

Fellows may join as a member of the Editorial Board of Global Journals Incorporation (USA) after successful completion of three years as Fellow and as Peer Reviewer. Additionally, Fellows get a chance to nominate other members for Editorial Board.

Career Credibility Exclusive Reputation

AND MUCH MORE

GET ACCESS TO SCIENTIFIC MUSEUMS AND OBSERVATORIES ACROSS THE GLOBE

All members get access to 5 selected scientific museums and observatories across the globe. All researches published with Global Journals will be kept under deep archival facilities across regions for future protections and disaster recovery. They get 10 GB free secure cloud access for storing research files.



ASSOCIATE OF ENGINEERING RESEARCH COUNCIL

ASSOCIATE OF ENGINEERING RESEARCH COUNCIL is the membership of Global Journals awarded to individuals that the Open Association of Research Society judges to have made a 'substantial contribution to the improvement of computer science, technology, and electronics engineering.

The primary objective is to recognize the leaders in research and scientific fields of the current era with a global perspective and to create a channel between them and other researchers for better exposure and knowledge sharing. Members are most eminent scientists, engineers, and technologists from all across the world. Associate membership can later be promoted to Fellow Membership. Associates are elected for life through a peer review process on the basis of excellence in the respective domain. There is no limit on the number of new nominations made in any year. Each year, the Open Association of Research Society elect up to 12 new Associate Members.



BENEFIT

TO THE INSTITUTION

GET LETTER OF APPRECIATION

Global Journals sends a letter of appreciation of author to the Dean or CEO of the University or Company of which author is a part, signed by editor in chief or chief author.



EXCLUSIVE NETWORK

GET ACCESS TO A CLOSED NETWORK

A AERC member gets access to a closed network of Tier 1 researchers and scientists with direct communication channel through our website. Associates can reach out to other members or researchers directly. They should also be open to reaching out by other.

Career

Credibility

Exclusive

Reputation



CERTIFICATE

CERTIFICATE, LOR AND LASER-MOMENTO

Associates receive a printed copy of a certificate signed by our Chief Author that may be used for academic purposes and a personal recommendation letter to the dean of member's university.

Career

Credibility

Exclusive

Reputation



DESIGNATION

GET HONORED TITLE OF MEMBERSHIP

Associates can use the honored title of membership. The "AERC" is an honored title which is accorded to a person's name viz. Dr. John E. Hall, Ph.D., AERC or William Walldroff, M.S., AERC.

Career

Credibility

Exclusive

Reputation

RECOGNITION ON THE PLATFORM

BETTER VISIBILITY AND CITATION

All the Associate members of AERC get a badge of "Leading Member of Global Journals" on the Research Community that distinguishes them from others. Additionally, the profile is also partially maintained by our team for better visibility and citation. All associates get a dedicated page on the website with their biography.

Career

Credibility

Reputation

FUTURE WORK

GET DISCOUNTS ON THE FUTURE PUBLICATIONS

Associates receive discounts on the future publications with Global Journals up to 60%. Through our recommendation programs, members also receive discounts on publications made with OARS affiliated organizations.

Career

Financial



GJ ACCOUNT

UNLIMITED FORWARD OF EMAILS

Associates get secure and fast GJ work emails with unlimited storage of emails that they may use them as their primary email. For example, john [AT] globaljournals [DOT] org..

Career

Credibility

Reputation



PREMIUM TOOLS

ACCESS TO ALL THE PREMIUM TOOLS

To take future researches to the zenith, associates receive access to all the premium tools that Global Journals have to offer along with the partnership with some of the best marketing leading tools out there.

Financial

CONFERENCES & EVENTS

ORGANIZE SEMINAR/CONFERENCE

Associates are authorized to organize symposium/seminar/conference on behalf of Global Journal Incorporation (USA). They can also participate in the same organized by another institution as representative of Global Journal. In both the cases, it is mandatory for him to discuss with us and obtain our consent. Additionally, they get free research conferences (and others) alerts.

Career

Credibility

Financial

EARLY INVITATIONS

EARLY INVITATIONS TO ALL THE SYMPOSIUMS, SEMINARS, CONFERENCES

All associates receive the early invitations to all the symposiums, seminars, conferences and webinars hosted by Global Journals in their subject.

Exclusive





PUBLISHING ARTICLES & BOOKS

EARN 30-40% OF SALES PROCEEDS

Associates can publish articles (limited) without any fees. Also, they can earn up to 30-40% of sales proceeds from the sale of reference/review books/literature/publishing of research paper.

Exclusive

Financial

REVIEWERS

GET A REMUNERATION OF 15% OF AUTHOR FEES

Associate members are eligible to join as a paid peer reviewer at Global Journals Incorporation (USA) and can get a remuneration of 15% of author fees, taken from the author of a respective paper.

Financial

AND MUCH MORE

GET ACCESS TO SCIENTIFIC MUSEUMS AND OBSERVATORIES ACROSS THE GLOBE

All members get access to 2 selected scientific museums and observatories across the globe. All researches published with Global Journals will be kept under deep archival facilities across regions for future protections and disaster recovery. They get 5 GB free secure cloud access for storing research files.



ASSOCIATE	FELLOW	RESEARCH GROUP	BASIC
<p>\$4800 lifetime designation</p> <hr/> <p>Certificate, LoR and Momento 2 discounted publishing/year Gradation of Research 10 research contacts/day 1 GB Cloud Storage GJ Community Access</p>	<p>\$6800 lifetime designation</p> <hr/> <p>Certificate, LoR and Momento Unlimited discounted publishing/year Gradation of Research Unlimited research contacts/day 5 GB Cloud Storage Online Presense Assistance GJ Community Access</p>	<p>\$12500.00 organizational</p> <hr/> <p>Certificates, LoRs and Momentos Unlimited free publishing/year Gradation of Research Unlimited research contacts/day Unlimited Cloud Storage Online Presense Assistance GJ Community Access</p>	<p>APC per article</p> <hr/> <p>GJ Community Access</p>



PREFERRED AUTHOR GUIDELINES

We accept the manuscript submissions in any standard (generic) format.

We typeset manuscripts using advanced typesetting tools like Adobe In Design, CorelDraw, TeXnicCenter, and TeXStudio. We usually recommend authors submit their research using any standard format they are comfortable with, and let Global Journals do the rest.

Alternatively, you can download our basic template from <https://globaljournals.org/Template.zip>

Authors should submit their complete paper/article, including text illustrations, graphics, conclusions, artwork, and tables. Authors who are not able to submit manuscript using the form above can email the manuscript department at submit@globaljournals.org or get in touch with chiefeditor@globaljournals.org if they wish to send the abstract before submission.

BEFORE AND DURING SUBMISSION

Authors must ensure the information provided during the submission of a paper is authentic. Please go through the following checklist before submitting:

1. Authors must go through the complete author guideline and understand and *agree to Global Journals' ethics and code of conduct*, along with author responsibilities.
2. Authors must accept the privacy policy, terms, and conditions of Global Journals.
3. Ensure corresponding author's email address and postal address are accurate and reachable.
4. Manuscript to be submitted must include keywords, an abstract, a paper title, co-author(s) names and details (email address, name, phone number, and institution), figures and illustrations in vector format including appropriate captions, tables, including titles and footnotes, a conclusion, results, acknowledgments and references.
5. Authors should submit paper in a ZIP archive if any supplementary files are required along with the paper.
6. Proper permissions must be acquired for the use of any copyrighted material.
7. Manuscript submitted *must not have been submitted or published elsewhere* and all authors must be aware of the submission.

Declaration of Conflicts of Interest

It is required for authors to declare all financial, institutional, and personal relationships with other individuals and organizations that could influence (bias) their research.

POLICY ON PLAGIARISM

Plagiarism is not acceptable in Global Journals submissions at all.

Plagiarized content will not be considered for publication. We reserve the right to inform authors' institutions about plagiarism detected either before or after publication. If plagiarism is identified, we will follow COPE guidelines:

Authors are solely responsible for all the plagiarism that is found. The author must not fabricate, falsify or plagiarize existing research data. The following, if copied, will be considered plagiarism:

- Words (language)
- Ideas
- Findings
- Writings
- Diagrams
- Graphs
- Illustrations
- Lectures



- Printed material
- Graphic representations
- Computer programs
- Electronic material
- Any other original work

AUTHORSHIP POLICIES

Global Journals follows the definition of authorship set up by the Open Association of Research Society, USA. According to its guidelines, authorship criteria must be based on:

1. Substantial contributions to the conception and acquisition of data, analysis, and interpretation of findings.
2. Drafting the paper and revising it critically regarding important academic content.
3. Final approval of the version of the paper to be published.

Changes in Authorship

The corresponding author should mention the name and complete details of all co-authors during submission and in manuscript. We support addition, rearrangement, manipulation, and deletions in authors list till the early view publication of the journal. We expect that corresponding author will notify all co-authors of submission. We follow COPE guidelines for changes in authorship.

Copyright

During submission of the manuscript, the author is confirming an exclusive license agreement with Global Journals which gives Global Journals the authority to reproduce, reuse, and republish authors' research. We also believe in flexible copyright terms where copyright may remain with authors/employers/institutions as well. Contact your editor after acceptance to choose your copyright policy. You may follow this form for copyright transfers.

Appealing Decisions

Unless specified in the notification, the Editorial Board's decision on publication of the paper is final and cannot be appealed before making the major change in the manuscript.

Acknowledgments

Contributors to the research other than authors credited should be mentioned in Acknowledgments. The source of funding for the research can be included. Suppliers of resources may be mentioned along with their addresses.

Declaration of funding sources

Global Journals is in partnership with various universities, laboratories, and other institutions worldwide in the research domain. Authors are requested to disclose their source of funding during every stage of their research, such as making analysis, performing laboratory operations, computing data, and using institutional resources, from writing an article to its submission. This will also help authors to get reimbursements by requesting an open access publication letter from Global Journals and submitting to the respective funding source.

PREPARING YOUR MANUSCRIPT

Authors can submit papers and articles in an acceptable file format: MS Word (doc, docx), LaTeX (.tex, .zip or .rar including all of your files), Adobe PDF (.pdf), rich text format (.rtf), simple text document (.txt), Open Document Text (.odt), and Apple Pages (.pages). Our professional layout editors will format the entire paper according to our official guidelines. This is one of the highlights of publishing with Global Journals—authors should not be concerned about the formatting of their paper. Global Journals accepts articles and manuscripts in every major language, be it Spanish, Chinese, Japanese, Portuguese, Russian, French, German, Dutch, Italian, Greek, or any other national language, but the title, subtitle, and abstract should be in English. This will facilitate indexing and the pre-peer review process.

The following is the official style and template developed for publication of a research paper. Authors are not required to follow this style during the submission of the paper. It is just for reference purposes.



Manuscript Style Instruction (Optional)

- Microsoft Word Document Setting Instructions.
- Font type of all text should be Swis721 Lt BT.
- Page size: 8.27" x 11", left margin: 0.65, right margin: 0.65, bottom margin: 0.75.
- Paper title should be in one column of font size 24.
- Author name in font size of 11 in one column.
- Abstract: font size 9 with the word "Abstract" in bold italics.
- Main text: font size 10 with two justified columns.
- Two columns with equal column width of 3.38 and spacing of 0.2.
- First character must be three lines drop-capped.
- The paragraph before spacing of 1 pt and after of 0 pt.
- Line spacing of 1 pt.
- Large images must be in one column.
- The names of first main headings (Heading 1) must be in Roman font, capital letters, and font size of 10.
- The names of second main headings (Heading 2) must not include numbers and must be in italics with a font size of 10.

Structure and Format of Manuscript

The recommended size of an original research paper is under 15,000 words and review papers under 7,000 words. Research articles should be less than 10,000 words. Research papers are usually longer than review papers. Review papers are reports of significant research (typically less than 7,000 words, including tables, figures, and references)

A research paper must include:

- a) A title which should be relevant to the theme of the paper.
- b) A summary, known as an abstract (less than 150 words), containing the major results and conclusions.
- c) Up to 10 keywords that precisely identify the paper's subject, purpose, and focus.
- d) An introduction, giving fundamental background objectives.
- e) Resources and techniques with sufficient complete experimental details (wherever possible by reference) to permit repetition, sources of information must be given, and numerical methods must be specified by reference.
- f) Results which should be presented concisely by well-designed tables and figures.
- g) Suitable statistical data should also be given.
- h) All data must have been gathered with attention to numerical detail in the planning stage.

Design has been recognized to be essential to experiments for a considerable time, and the editor has decided that any paper that appears not to have adequate numerical treatments of the data will be returned unrefereed.

- i) Discussion should cover implications and consequences and not just recapitulate the results; conclusions should also be summarized.
- j) There should be brief acknowledgments.
- k) There ought to be references in the conventional format. Global Journals recommends APA format.

Authors should carefully consider the preparation of papers to ensure that they communicate effectively. Papers are much more likely to be accepted if they are carefully designed and laid out, contain few or no errors, are summarizing, and follow instructions. They will also be published with much fewer delays than those that require much technical and editorial correction.

The Editorial Board reserves the right to make literary corrections and suggestions to improve brevity.



FORMAT STRUCTURE

It is necessary that authors take care in submitting a manuscript that is written in simple language and adheres to published guidelines.

All manuscripts submitted to Global Journals should include:

Title

The title page must carry an informative title that reflects the content, a running title (less than 45 characters together with spaces), names of the authors and co-authors, and the place(s) where the work was carried out.

Author details

The full postal address of any related author(s) must be specified.

Abstract

The abstract is the foundation of the research paper. It should be clear and concise and must contain the objective of the paper and inferences drawn. It is advised to not include big mathematical equations or complicated jargon.

Many researchers searching for information online will use search engines such as Google, Yahoo or others. By optimizing your paper for search engines, you will amplify the chance of someone finding it. In turn, this will make it more likely to be viewed and cited in further works. Global Journals has compiled these guidelines to facilitate you to maximize the web-friendliness of the most public part of your paper.

Keywords

A major lynchpin of research work for the writing of research papers is the keyword search, which one will employ to find both library and internet resources. Up to eleven keywords or very brief phrases have to be given to help data retrieval, mining, and indexing.

One must be persistent and creative in using keywords. An effective keyword search requires a strategy: planning of a list of possible keywords and phrases to try.

Choice of the main keywords is the first tool of writing a research paper. Research paper writing is an art. Keyword search should be as strategic as possible.

One should start brainstorming lists of potential keywords before even beginning searching. Think about the most important concepts related to research work. Ask, "What words would a source have to include to be truly valuable in a research paper?" Then consider synonyms for the important words.

It may take the discovery of only one important paper to steer in the right keyword direction because, in most databases, the keywords under which a research paper is abstracted are listed with the paper.

Numerical Methods

Numerical methods used should be transparent and, where appropriate, supported by references.

Abbreviations

Authors must list all the abbreviations used in the paper at the end of the paper or in a separate table before using them.

Formulas and equations

Authors are advised to submit any mathematical equation using either MathJax, KaTeX, or LaTeX, or in a very high-quality image.

Tables, Figures, and Figure Legends

Tables: Tables should be cautiously designed, uncrowned, and include only essential data. Each must have an Arabic number, e.g., Table 4, a self-explanatory caption, and be on a separate sheet. Authors must submit tables in an editable format and not as images. References to these tables (if any) must be mentioned accurately.



Figures

Figures are supposed to be submitted as separate files. Always include a citation in the text for each figure using Arabic numbers, e.g., Fig. 4. Artwork must be submitted online in vector electronic form or by emailing it.

PREPARATION OF ELETRONIC FIGURES FOR PUBLICATION

Although low-quality images are sufficient for review purposes, print publication requires high-quality images to prevent the final product being blurred or fuzzy. Submit (possibly by e-mail) EPS (line art) or TIFF (halftone/ photographs) files only. MS PowerPoint and Word Graphics are unsuitable for printed pictures. Avoid using pixel-oriented software. Scans (TIFF only) should have a resolution of at least 350 dpi (halftone) or 700 to 1100 dpi (line drawings). Please give the data for figures in black and white or submit a Color Work Agreement form. EPS files must be saved with fonts embedded (and with a TIFF preview, if possible).

For scanned images, the scanning resolution at final image size ought to be as follows to ensure good reproduction: line art: >650 dpi; halftones (including gel photographs): >350 dpi; figures containing both halftone and line images: >650 dpi.

Color charges: Authors are advised to pay the full cost for the reproduction of their color artwork. Hence, please note that if there is color artwork in your manuscript when it is accepted for publication, we would require you to complete and return a Color Work Agreement form before your paper can be published. Also, you can email your editor to remove the color fee after acceptance of the paper.

TIPS FOR WRITING A GOOD QUALITY ENGINEERING RESEARCH PAPER

Techniques for writing a good quality engineering research paper:

1. Choosing the topic: In most cases, the topic is selected by the interests of the author, but it can also be suggested by the guides. You can have several topics, and then judge which you are most comfortable with. This may be done by asking several questions of yourself, like "Will I be able to carry out a search in this area? Will I find all necessary resources to accomplish the search? Will I be able to find all information in this field area?" If the answer to this type of question is "yes," then you ought to choose that topic. In most cases, you may have to conduct surveys and visit several places. Also, you might have to do a lot of work to find all the rises and falls of the various data on that subject. Sometimes, detailed information plays a vital role, instead of short information. Evaluators are human: The first thing to remember is that evaluators are also human beings. They are not only meant for rejecting a paper. They are here to evaluate your paper. So present your best aspect.

2. Think like evaluators: If you are in confusion or getting demotivated because your paper may not be accepted by the evaluators, then think, and try to evaluate your paper like an evaluator. Try to understand what an evaluator wants in your research paper, and you will automatically have your answer. Make blueprints of paper: The outline is the plan or framework that will help you to arrange your thoughts. It will make your paper logical. But remember that all points of your outline must be related to the topic you have chosen.

3. Ask your guides: If you are having any difficulty with your research, then do not hesitate to share your difficulty with your guide (if you have one). They will surely help you out and resolve your doubts. If you can't clarify what exactly you require for your work, then ask your supervisor to help you with an alternative. He or she might also provide you with a list of essential readings.

4. Use of computer is recommended: As you are doing research in the field of research engineering then this point is quite obvious. Use right software: Always use good quality software packages. If you are not capable of judging good software, then you can lose the quality of your paper unknowingly. There are various programs available to help you which you can get through the internet.

5. Use the internet for help: An excellent start for your paper is using Google. It is a wondrous search engine, where you can have your doubts resolved. You may also read some answers for the frequent question of how to write your research paper or find a model research paper. You can download books from the internet. If you have all the required books, place importance on reading, selecting, and analyzing the specified information. Then sketch out your research paper. Use big pictures: You may use encyclopedias like Wikipedia to get pictures with the best resolution. At Global Journals, you should strictly follow [here](#).



6. Bookmarks are useful: When you read any book or magazine, you generally use bookmarks, right? It is a good habit which helps to not lose your continuity. You should always use bookmarks while searching on the internet also, which will make your search easier.

7. Revise what you wrote: When you write anything, always read it, summarize it, and then finalize it.

8. Make every effort: Make every effort to mention what you are going to write in your paper. That means always have a good start. Try to mention everything in the introduction—what is the need for a particular research paper. Polish your work with good writing skills and always give an evaluator what he wants. Make backups: When you are going to do any important thing like making a research paper, you should always have backup copies of it either on your computer or on paper. This protects you from losing any portion of your important data.

9. Produce good diagrams of your own: Always try to include good charts or diagrams in your paper to improve quality. Using several unnecessary diagrams will degrade the quality of your paper by creating a hodgepodge. So always try to include diagrams which were made by you to improve the readability of your paper. Use of direct quotes: When you do research relevant to literature, history, or current affairs, then use of quotes becomes essential, but if the study is relevant to science, use of quotes is not preferable.

10. Use proper verb tense: Use proper verb tenses in your paper. Use past tense to present those events that have happened. Use present tense to indicate events that are going on. Use future tense to indicate events that will happen in the future. Use of wrong tenses will confuse the evaluator. Avoid sentences that are incomplete.

11. Pick a good study spot: Always try to pick a spot for your research which is quiet. Not every spot is good for studying.

12. Know what you know: Always try to know what you know by making objectives, otherwise you will be confused and unable to achieve your target.

13. Use good grammar: Always use good grammar and words that will have a positive impact on the evaluator; use of good vocabulary does not mean using tough words which the evaluator has to find in a dictionary. Do not fragment sentences. Eliminate one-word sentences. Do not ever use a big word when a smaller one would suffice.

Verbs have to be in agreement with their subjects. In a research paper, do not start sentences with conjunctions or finish them with prepositions. When writing formally, it is advisable to never split an infinitive because someone will (wrongly) complain. Avoid clichés like a disease. Always shun irritating alliteration. Use language which is simple and straightforward. Put together a neat summary.

14. Arrangement of information: Each section of the main body should start with an opening sentence, and there should be a changeover at the end of the section. Give only valid and powerful arguments for your topic. You may also maintain your arguments with records.

15. Never start at the last minute: Always allow enough time for research work. Leaving everything to the last minute will degrade your paper and spoil your work.

16. Multitasking in research is not good: Doing several things at the same time is a bad habit in the case of research activity. Research is an area where everything has a particular time slot. Divide your research work into parts, and do a particular part in a particular time slot.

17. Never copy others' work: Never copy others' work and give it your name because if the evaluator has seen it anywhere, you will be in trouble. Take proper rest and food: No matter how many hours you spend on your research activity, if you are not taking care of your health, then all your efforts will have been in vain. For quality research, take proper rest and food.

18. Go to seminars: Attend seminars if the topic is relevant to your research area. Utilize all your resources.

19. Refresh your mind after intervals: Try to give your mind a rest by listening to soft music or sleeping in intervals. This will also improve your memory. Acquire colleagues: Always try to acquire colleagues. No matter how sharp you are, if you acquire colleagues, they can give you ideas which will be helpful to your research.

20. Think technically: Always think technically. If anything happens, search for its reasons, benefits, and demerits. Think and then print: When you go to print your paper, check that tables are not split, headings are not detached from their descriptions, and page sequence is maintained.



21. Adding unnecessary information: Do not add unnecessary information like "I have used MS Excel to draw graphs." Irrelevant and inappropriate material is superfluous. Foreign terminology and phrases are not apropos. One should never take a broad view. Analogy is like feathers on a snake. Use words properly, regardless of how others use them. Remove quotations. Puns are for kids, not grunt readers. Never oversimplify: When adding material to your research paper, never go for oversimplification; this will definitely irritate the evaluator. Be specific. Never use rhythmic redundancies. Contractions shouldn't be used in a research paper. Comparisons are as terrible as clichés. Give up ampersands, abbreviations, and so on. Remove commas that are not necessary. Parenthetical words should be between brackets or commas. Understatement is always the best way to put forward earth-shaking thoughts. Give a detailed literary review.

22. Report concluded results: Use concluded results. From raw data, filter the results, and then conclude your studies based on measurements and observations taken. An appropriate number of decimal places should be used. Parenthetical remarks are prohibited here. Proofread carefully at the final stage. At the end, give an outline to your arguments. Spot perspectives of further study of the subject. Justify your conclusion at the bottom sufficiently, which will probably include examples.

23. Upon conclusion: Once you have concluded your research, the next most important step is to present your findings. Presentation is extremely important as it is the definite medium through which your research is going to be in print for the rest of the crowd. Care should be taken to categorize your thoughts well and present them in a logical and neat manner. A good quality research paper format is essential because it serves to highlight your research paper and bring to light all necessary aspects of your research.

INFORMAL GUIDELINES OF RESEARCH PAPER WRITING

Key points to remember:

- Submit all work in its final form.
- Write your paper in the form which is presented in the guidelines using the template.
- Please note the criteria peer reviewers will use for grading the final paper.

Final points:

One purpose of organizing a research paper is to let people interpret your efforts selectively. The journal requires the following sections, submitted in the order listed, with each section starting on a new page:

The introduction: This will be compiled from reference matter and reflect the design processes or outline of basis that directed you to make a study. As you carry out the process of study, the method and process section will be constructed like that. The results segment will show related statistics in nearly sequential order and direct reviewers to similar intellectual paths throughout the data that you gathered to carry out your study.

The discussion section:

This will provide understanding of the data and projections as to the implications of the results. The use of good quality references throughout the paper will give the effort trustworthiness by representing an alertness to prior workings.

Writing a research paper is not an easy job, no matter how trouble-free the actual research or concept. Practice, excellent preparation, and controlled record-keeping are the only means to make straightforward progression.

General style:

Specific editorial column necessities for compliance of a manuscript will always take over from directions in these general guidelines.

To make a paper clear: Adhere to recommended page limits.

Mistakes to avoid:

- Insertion of a title at the foot of a page with subsequent text on the next page.
- Separating a table, chart, or figure—confine each to a single page.
- Submitting a manuscript with pages out of sequence.
- In every section of your document, use standard writing style, including articles ("a" and "the").
- Keep paying attention to the topic of the paper.



- Use paragraphs to split each significant point (excluding the abstract).
- Align the primary line of each section.
- Present your points in sound order.
- Use present tense to report well-accepted matters.
- Use past tense to describe specific results.
- Do not use familiar wording; don't address the reviewer directly. Don't use slang or superlatives.
- Avoid use of extra pictures—include only those figures essential to presenting results.

Title page:

Choose a revealing title. It should be short and include the name(s) and address(es) of all authors. It should not have acronyms or abbreviations or exceed two printed lines.

Abstract: This summary should be two hundred words or less. It should clearly and briefly explain the key findings reported in the manuscript and must have precise statistics. It should not have acronyms or abbreviations. It should be logical in itself. Do not cite references at this point.

An abstract is a brief, distinct paragraph summary of finished work or work in development. In a minute or less, a reviewer can be taught the foundation behind the study, common approaches to the problem, relevant results, and significant conclusions or new questions.

Write your summary when your paper is completed because how can you write the summary of anything which is not yet written? Wealth of terminology is very essential in abstract. Use comprehensive sentences, and do not sacrifice readability for brevity; you can maintain it succinctly by phrasing sentences so that they provide more than a lone rationale. The author can at this moment go straight to shortening the outcome. Sum up the study with the subsequent elements in any summary. Try to limit the initial two items to no more than one line each.

Reason for writing the article—theory, overall issue, purpose.

- Fundamental goal.
- To-the-point depiction of the research.
- Consequences, including definite statistics—if the consequences are quantitative in nature, account for this; results of any numerical analysis should be reported. Significant conclusions or questions that emerge from the research.

Approach:

- Single section and succinct.
- An outline of the job done is always written in past tense.
- Concentrate on shortening results—limit background information to a verdict or two.
- Exact spelling, clarity of sentences and phrases, and appropriate reporting of quantities (proper units, important statistics) are just as significant in an abstract as they are anywhere else.

Introduction:

The introduction should "introduce" the manuscript. The reviewer should be presented with sufficient background information to be capable of comprehending and calculating the purpose of your study without having to refer to other works. The basis for the study should be offered. Give the most important references, but avoid making a comprehensive appraisal of the topic. Describe the problem visibly. If the problem is not acknowledged in a logical, reasonable way, the reviewer will give no attention to your results. Speak in common terms about techniques used to explain the problem, if needed, but do not present any particulars about the protocols here.

The following approach can create a valuable beginning:

- Explain the value (significance) of the study.
- Defend the model—why did you employ this particular system or method? What is its compensation? Remark upon its appropriateness from an abstract point of view as well as pointing out sensible reasons for using it.
- Present a justification. State your particular theory(-ies) or aim(s), and describe the logic that led you to choose them.
- Briefly explain the study's tentative purpose and how it meets the declared objectives.



Approach:

Use past tense except for when referring to recognized facts. After all, the manuscript will be submitted after the entire job is done. Sort out your thoughts; manufacture one key point for every section. If you make the four points listed above, you will need at least four paragraphs. Present surrounding information only when it is necessary to support a situation. The reviewer does not desire to read everything you know about a topic. Shape the theory specifically—do not take a broad view.

As always, give awareness to spelling, simplicity, and correctness of sentences and phrases.

Procedures (methods and materials):

This part is supposed to be the easiest to carve if you have good skills. A soundly written procedures segment allows a capable scientist to replicate your results. Present precise information about your supplies. The suppliers and clarity of reagents can be helpful bits of information. Present methods in sequential order, but linked methodologies can be grouped as a segment. Be concise when relating the protocols. Attempt to give the least amount of information that would permit another capable scientist to replicate your outcome, but be cautious that vital information is integrated. The use of subheadings is suggested and ought to be synchronized with the results section.

When a technique is used that has been well-described in another section, mention the specific item describing the way, but draw the basic principle while stating the situation. The purpose is to show all particular resources and broad procedures so that another person may use some or all of the methods in one more study or referee the scientific value of your work. It is not to be a step-by-step report of the whole thing you did, nor is a methods section a set of orders.

Materials:

Materials may be reported in part of a section or else they may be recognized along with your measures.

Methods:

- Report the method and not the particulars of each process that engaged the same methodology.
- Describe the method entirely.
- To be succinct, present methods under headings dedicated to specific dealings or groups of measures.
- Simplify—detail how procedures were completed, not how they were performed on a particular day.
- If well-known procedures were used, account for the procedure by name, possibly with a reference, and that's all.

Approach:

It is embarrassing to use vigorous voice when documenting methods without using first person, which would focus the reviewer's interest on the researcher rather than the job. As a result, when writing up the methods, most authors use third person passive voice.

Use standard style in this and every other part of the paper—avoid familiar lists, and use full sentences.

What to keep away from:

- Resources and methods are not a set of information.
- Skip all descriptive information and surroundings—save it for the argument.
- Leave out information that is immaterial to a third party.

Results:

The principle of a results segment is to present and demonstrate your conclusion. Create this part as entirely objective details of the outcome, and save all understanding for the discussion.

The page length of this segment is set by the sum and types of data to be reported. Use statistics and tables, if suitable, to present consequences most efficiently.

You must clearly differentiate material which would usually be incorporated in a study editorial from any unprocessed data or additional appendix matter that would not be available. In fact, such matters should not be submitted at all except if requested by the instructor.



Content:

- Sum up your conclusions in text and demonstrate them, if suitable, with figures and tables.
- In the manuscript, explain each of your consequences, and point the reader to remarks that are most appropriate.
- Present a background, such as by describing the question that was addressed by creation of an exacting study.
- Explain results of control experiments and give remarks that are not accessible in a prescribed figure or table, if appropriate.
- Examine your data, then prepare the analyzed (transformed) data in the form of a figure (graph), table, or manuscript.

What to stay away from:

- Do not discuss or infer your outcome, report surrounding information, or try to explain anything.
- Do not include raw data or intermediate calculations in a research manuscript.
- Do not present similar data more than once.
- A manuscript should complement any figures or tables, not duplicate information.
- Never confuse figures with tables—there is a difference.

Approach:

As always, use past tense when you submit your results, and put the whole thing in a reasonable order.

Put figures and tables, appropriately numbered, in order at the end of the report.

If you desire, you may place your figures and tables properly within the text of your results section.

Figures and tables:

If you put figures and tables at the end of some details, make certain that they are visibly distinguished from any attached appendix materials, such as raw facts. Whatever the position, each table must be titled, numbered one after the other, and include a heading. All figures and tables must be divided from the text.

Discussion:

The discussion is expected to be the trickiest segment to write. A lot of papers submitted to the journal are discarded based on problems with the discussion. There is no rule for how long an argument should be.

Position your understanding of the outcome visibly to lead the reviewer through your conclusions, and then finish the paper with a summing up of the implications of the study. The purpose here is to offer an understanding of your results and support all of your conclusions, using facts from your research and generally accepted information, if suitable. The implication of results should be fully described.

Infer your data in the conversation in suitable depth. This means that when you clarify an observable fact, you must explain mechanisms that may account for the observation. If your results vary from your prospect, make clear why that may have happened. If your results agree, then explain the theory that the proof supported. It is never suitable to just state that the data approved the prospect, and let it drop at that. Make a decision as to whether each premise is supported or discarded or if you cannot make a conclusion with assurance. Do not just dismiss a study or part of a study as "uncertain."

Research papers are not acknowledged if the work is imperfect. Draw what conclusions you can based upon the results that you have, and take care of the study as a finished work.

- You may propose future guidelines, such as how an experiment might be personalized to accomplish a new idea.
- Give details of all of your remarks as much as possible, focusing on mechanisms.
- Make a decision as to whether the tentative design sufficiently addressed the theory and whether or not it was correctly restricted. Try to present substitute explanations if they are sensible alternatives.
- One piece of research will not counter an overall question, so maintain the large picture in mind. Where do you go next? The best studies unlock new avenues of study. What questions remain?
- Recommendations for detailed papers will offer supplementary suggestions.



Approach:

When you refer to information, differentiate data generated by your own studies from other available information. Present work done by specific persons (including you) in past tense.

Describe generally acknowledged facts and main beliefs in present tense.

THE ADMINISTRATION RULES

Administration Rules to Be Strictly Followed before Submitting Your Research Paper to Global Journals Inc.

Please read the following rules and regulations carefully before submitting your research paper to Global Journals Inc. to avoid rejection.

Segment draft and final research paper: You have to strictly follow the template of a research paper, failing which your paper may get rejected. You are expected to write each part of the paper wholly on your own. The peer reviewers need to identify your own perspective of the concepts in your own terms. Please do not extract straight from any other source, and do not rephrase someone else's analysis. Do not allow anyone else to proofread your manuscript.

Written material: You may discuss this with your guides and key sources. Do not copy anyone else's paper, even if this is only imitation, otherwise it will be rejected on the grounds of plagiarism, which is illegal. Various methods to avoid plagiarism are strictly applied by us to every paper, and, if found guilty, you may be blacklisted, which could affect your career adversely. To guard yourself and others from possible illegal use, please do not permit anyone to use or even read your paper and file.



CRITERION FOR GRADING A RESEARCH PAPER (COMPILATION)
BY GLOBAL JOURNALS

Please note that following table is only a Grading of "Paper Compilation" and not on "Performed/Stated Research" whose grading solely depends on Individual Assigned Peer Reviewer and Editorial Board Member. These can be available only on request and after decision of Paper. This report will be the property of Global Journals.

Topics	Grades		
	A-B	C-D	E-F
<i>Abstract</i>	Clear and concise with appropriate content, Correct format. 200 words or below	Unclear summary and no specific data, Incorrect form Above 200 words	No specific data with ambiguous information Above 250 words
<i>Introduction</i>	Containing all background details with clear goal and appropriate details, flow specification, no grammar and spelling mistake, well organized sentence and paragraph, reference cited	Unclear and confusing data, appropriate format, grammar and spelling errors with unorganized matter	Out of place depth and content, hazy format
<i>Methods and Procedures</i>	Clear and to the point with well arranged paragraph, precision and accuracy of facts and figures, well organized subheads	Difficult to comprehend with embarrassed text, too much explanation but completed	Incorrect and unorganized structure with hazy meaning
<i>Result</i>	Well organized, Clear and specific, Correct units with precision, correct data, well structuring of paragraph, no grammar and spelling mistake	Complete and embarrassed text, difficult to comprehend	Irregular format with wrong facts and figures
<i>Discussion</i>	Well organized, meaningful specification, sound conclusion, logical and concise explanation, highly structured paragraph reference cited	Wordy, unclear conclusion, spurious	Conclusion is not cited, unorganized, difficult to comprehend
<i>References</i>	Complete and correct format, well organized	Beside the point, Incomplete	Wrong format and structuring



INDEX

A

Asteroid · 5, 16

B

Bisalloy · 7

C

Coaxially · 13
Contour · 35, 36, 37, 39, 40, 41, 42
Convex · 35, 37
Criterion · 4, 17
Cycloidal · 35, 36, 37, 39, 40, 42, 43

D

Dedendum · 17, 24, 27, 31, 32
Drexler · 68

E

Epigarmonic · 40

F

Flexures · 5, 6, 9

I

Inconspicuous · 30, 32
Intuitionistic · 27

O

Orifice · 1, 4, 7, 12

P

Pectratio · 9

R

Rotary · 35, 36, 38, 39, 43

S

Sinusoidal · 43
Sprocket · 13
Stratasys · 58, 61
Succinct · 27

T

Trapezium · 21, 22
Trapezoid · 35
Turbpiercer · 11

V

Vicinity · 37
Viscous · 28

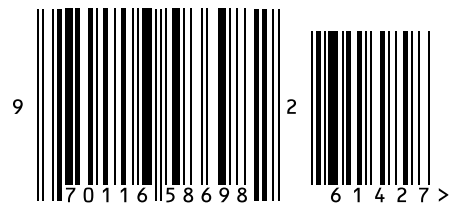


save our planet



Global Journal of Researches in Engineering

Visit us on the Web at www.GlobalJournals.org | www.EngineeringResearch.org
or email us at helpdesk@globaljournals.org



ISSN 9755861

© Global Journals